ANALYTICAL INVESTIGATION OF THE EFFECTS OF ALIGNED DOWEL BARS COATED WITH CORROSION PROTECTIVE SYSTEMS ON INITIAL DOWEL CONCRETE BOND STRESSES

Final Report

Submitted to
MICHIGAN DEPARTMENT OF TRANSPORTATION
Construction and Technology Division
Lansing, Michigan

by
Neeraj Buch (Principal Investigator)
Amit H. Varma (Co-Principal Investigator, Purdue University)
Milind L. Prabhu (Graduate Research Assistant)

Department of Civil and Environmental Engineering
Michigan State University
East Lansing, MI 48824-1226

February 2007

Technical Report Documentation Page

1. Report No. RC – 1488	2. Government Accession No.	3. Recipient's Catalog No.
4. Title and Subtitle Analytical investigation of the effects of aligned dowel bars coated with corrosion protective systems on initial dowel concrete bond stresses		5. Report Date February 2007
		6. Performing Organization Code
7. Author(s) Neeraj Buch, Amit H. Varma and Milind L. Prabhu		8. Performing Organization Report No.
9. Performing Organization Name Address Michigan State University Department of Civil and Environmental Engineering 3546 Engineering Building East Lansing, MI 48824		10. Work Unit No. (TRAIS)
		11. Contract or Grant No.
12. Sponsoring Agency Name and Address Michigan Department of Transportation. Construction and Technology Division Lansing, Michigan		13. Type of Report and Period Covered
		14. Sponsoring Agency Code
15. Supplementary Notes		

16. Abstract

This report presents an analytical investigation on the initial pullout bond stress of dowel bars with corrosion protection systems. The experimental pullout bond stress data on tectyl coated epoxy dowels, MMFX stainless steel and zinc clad dowel bars were provided by the Michigan Department of Transportation. The pullout bond stress for zinc clad dowel bars was the highest followed by the MMFX steel and the tectyl coated epoxy dowel bars. The three dimensional (3D) finite element (FE) models developed in the study titled "Experimental and analytical investigations of the mechanistic effects of Dowel Misalignment in Jointed Concrete Pavements" were used to validate the experimental results. The bond pullout force results from the 3DFE model compared favorably with the experimental results. The methodology of identifying events / material damage limit states that were developed in Phase I of this report was used. The results showed the formation of events / material damage limit states occurred during the dowel pullout behavior of zinc clad dowel bars. The results on the study of combined effects of load and different pullout bond stress data showed nominal stresses and strains forming around the dowel bar at a joint opening of 1/8 in. As wheel loads were applied, the bearing stresses in the concrete surrounding the dowel bar increased. The magnitude of the dowel pullout bond stress is a function of the dowel surface preparation and irregularities at the contact interface with the surrounding concrete. The results from the numerical (3D finite element) analysis indicate that if the dowel pullout bond stress is greater than 112 psi, then limit states B (onset of concrete material in-elasticity) or C (cracking stress exceeded) occur before dowel slip (limit state A). Thus, if the dowel pullout stress exceeds 112 psi, then there is potential for concrete cracking or inelasticity in the concrete at the dowel - concrete interface. This is not acceptable, because concrete cracking or inelasticity will lead to fatigue deterioration and eventual failure (functional or structural) of the joint with repeated cycles. The current MDOT specification of maximum pullout bond stress limited to 60 psi provides a resistance factor (or factor of safety) of approximately 1.87, which is reasonable. A detailed future study is recommended on the pullout bond stress using suitable MDOT approved bond breaking agents on the above mentioned dowel bars.

17. key Words Corrosion protection films, finite element analysis, rigid concrete pavements, dowel bars	18. Distribution Statement		
19. Security Classif. (of this report) Unclassified	20. Security Classif. (of this page) Unclassified	21. No of Pages 68	22. Price

Form DOT F 1700.7 (8-72) **Reproduction of completed page authorized**

ACKNOWLEDGMENTS

The research project was financially supported by the Michigan Department of Transportation. The project team would also like to acknowledge the technical support offered by the project technical assistance group (TAG).

DISCLAIMER

The contents of this report reflect the views of the authors. The contents do not necessarily reflect the views or policies of the Michigan Department of Transportation. This report does not constitute a standard, specification or regulation.

TABLE OF CONTENTS

LIST OF TABLES

LIST OF FIGURES

ABSTRACT

This report presents an analytical investigation on the initial pullout bond stress of dowel bars with corrosion protection systems. The experimental pullout bond stress data on tectyl coated epoxy steel dowels, MMFX stainless steel and zinc clad dowel bars were provided by the MDOT. The pullout bond stress for zinc clad dowel bars was the highest followed by the MMFX steel and the tectyl coated epoxy dowel bars. The three dimensional (3D) finite element (FE) models developed in the study titled "Experimental and analytical investigations of the mechanistic effects of Dowel Misalignment in Jointed Concrete Pavements" were used to validate the experimental results. The bond pullout force results from the 3DFE model compared favorably with the experimental results. The methodology of identifying events / material damage limit states that were developed in Phase I of this report was used. The results showed the formation of events / material damage limit states occurred during the dowel pullout behavior of zinc clad dowel bars. The results on the study of combined effects of load and different pullout bond stress data showed nominal stresses and strains forming around the dowel bar at a joint opening of 1/8 in. As wheel loads were applied, the bearing stresses in the concrete surrounding the dowel bar increased. The magnitude of the dowel pullout bond stress is a function of the dowel surface preparation and irregularities at the contact interface with the surrounding concrete. The results from the numerical (3D finite element) analysis indicate that if the dowel pullout bond stress exceeds 112 psi, then limit states B (concrete material inelasticity) or C (cracking stress) occur before dowel slip (limit state A). The current MDOT specification of maximum pullout bond stress limited to 60 psi provides a resistance factor (or factor of safety) of approximately 1.87, which is reasonable.

1.0 Introduction

This is the final report on the analytical study of effects on initial debonding stresses of aligned dowel bars with corrosion protection systems. The first part of this report summarizes the development of the finite element model calibrated for uncoated dowel bars using the data provided by MDOT and the results obtained from the analysis. Based on the results of the analysis a set of preliminary recommendations are presented. In the second part, the effects of initial debonding stresses in a jointed concrete pavement slab cross-section subjected to joint opening and axle loads is presented.

2.0 Objectives and Benefits of this Study

This analytical investigation is an extension of the ongoing dowel misalignment research project titled "A laboratory evaluation of alignment tolerances for dowel bars and their effect on joint opening behavior". The objectives of this analytical investigation are as follows:

1. Development of analytical models for predicting the opening behavior and stress states in concrete pavement joints with aligned dowel bars of different types (MMFX steel, zinc coated and tectyl coated epoxy dowel bars).
2. Analytical evaluation of the effects of different dowel bars and corresponding initial debonding stresses on the limit states in concrete pavements.
3. Analytical evaluation of the feasibility of using different dowel bars without causing significant distress or failure at a concrete pavement joints.

3.0 Research Plan

To achieve the objectives of this research study the following tasks were executed.

Task I: Development of Analytical Models: This task primarily focused on the development of the finite element models for pullout behavior of aligned dowel bars induced due to thermal expansion effects only. In this task (a) 3D finite element models were developed for aligned dowel bars (MMFX, Zinc coated, and tectyl coated epoxy), and (b) used to analytically predict the debonding stresses and limit states in the concrete pavement joints. The material inputs, geometry and dowel pullout load versus displacement experimental data necessary to develop the analytical models were provided by MDOT.

Task 2: Develop analytical models of realistic pavement joints with aligned dowel bars (of different types) subjected to traffic (tandem axle) loading and environmental (thermal expansion) effects.

Task I: Development of 3D Finite Element model for pullout behavior

The 3D finite element models were developed and analyzed using Abaqus *(1)*, which was selected due to the availability of a robust concrete damage plasticity and cracking model needed for this analysis. The concrete slabs and dowel bars were modeled using 3D first-order reduced-integration continuum elements (C3D8R-bricks). These elements are versatile in modeling simple linear and also complex nonlinear analyses involving contact, plasticity and large deformations. The concrete slab specimen is 24 in. x 24 in. x 10 in. and the dowel bar is a 1.25 in. diameter – 18 in. length embedded 9 in. into the concrete specimen placed at mid-height of the specimen.

I.1 Loading and Boundary conditions

The boundary and loading conditions were designed to simulate the experimental behavior of the tested specimens. The loads were applied in two steps. In the first step, the dead loads due to self weight of the concrete slab specimens and the portion of the dowel embedded in the concrete slab were applied as gravity loads, figure 1(a). This was important to develop contact pressures across the dowel concrete interface and activate the coulomb friction models. In the second step, a displacement control approach was used to pull the dowel bar from the concrete slab by 1.0 in as in the experiment, as shown in figure 1(b).

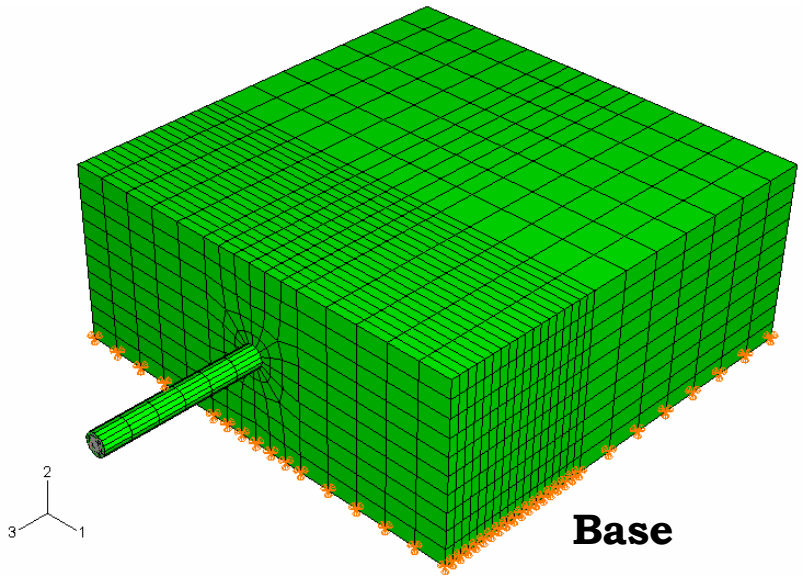

(a) Loading Step I: Application of Gravity Loading

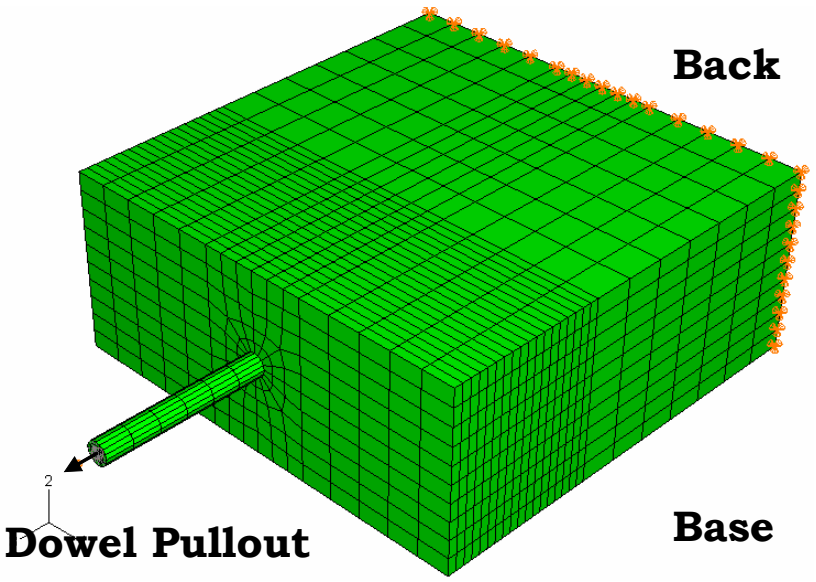

(b) Loading Step II: Displacement Boundary condition

Figure 1: Loading and Boundary condition for the 3D analytical models

I.2 Material Model

The concrete material was modeled using the concrete damage plasticity model developed by Lubliner et al *(2)*, modified by Lee and Fenves *(3)* and implemented in Abaqus. The steel dowel bar was modeled using an isotropic elastic material model.

To model the nonlinear inelastic behavior of concrete, the following input parameters were specified; the dilation angle, biaxial stress ratio, and the tensile-to-compressive meridian ratio were assumed to be equal to 15^{o}, 1.16, and 0.667, respectively, based on the recommendations by Chen and Han *(4)*. The uniaxial compression stress-strain curve was defined using the elastic modulus E_c and compressive strength f'_c and the modified Popovic's empirical stress-strain model recommended by Collins et al. *(5)*. The uniaxial tension stress-strain curve was defined using the direct tensile strength ($f'_t = 4\sqrt{f'_c}$) and a hypothetical tension stiffening stress-strain model developed by the authors, as shown in figure 2.

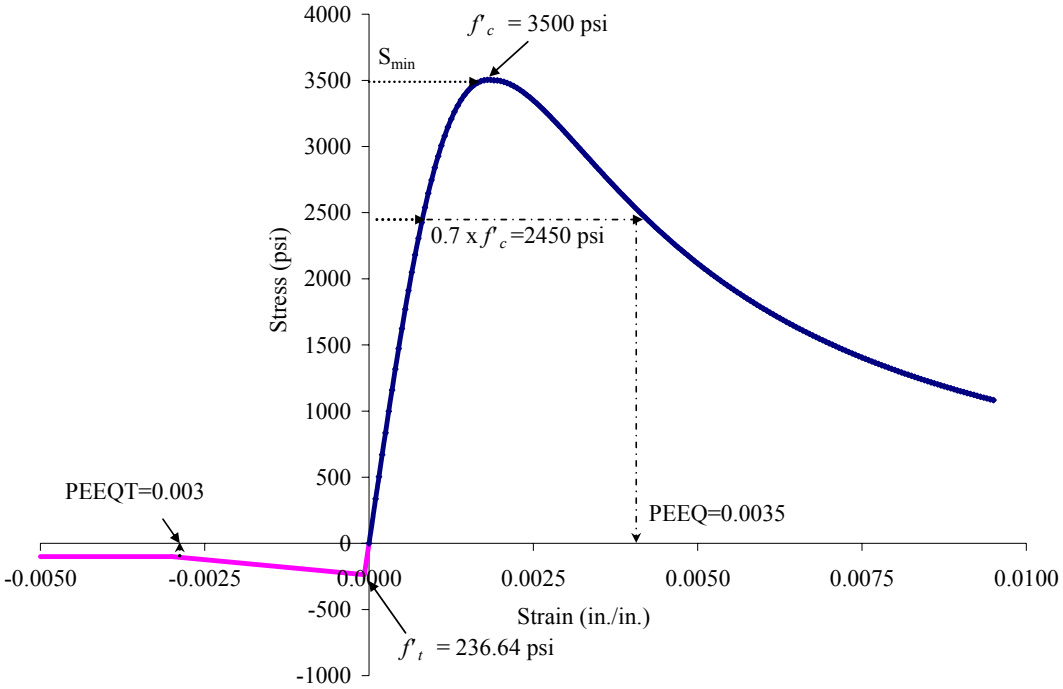

Figure 2: Uniaxial Compressive and Tension Stress-Strain curve for Concrete

The input property parameters for the dowel bars were the elastic modulus and poissons ratio equal to 29,000 ksi and 0.3 respectively for all the dowel bars. The same elastic modulus was used even though the yield and ultimate stresses for the MMFX steel dowel bar is twice as compared to the grade 60 billet steel dowel bar as confirmed with MDOT and test results from a research conducted at NC State *(6)*. The yield and ultimate stresses were not required because the dowel bar was assumed to remain elastic throughout the analysis.

I.3 Interaction between Dowel and Concrete

The longitudinal and transverse interactions between the dowel bars and the concrete slabs were modeled using two models: (a) the first model focused on the longitudinal

bond between the steel and concrete due to mechanical interlock and static friction and (b) the second model focused on the transverse interaction between the steel dowel and surrounding concrete resulting in large contact or bearing stresses and additional friction bond in the longitudinal direction due to the normal (bearing) stresses and coulomb friction coefficients.

The first model was calibrated using experimental results (dowel pullout force – displacement) from an MDOT report *(7)*. Nonlinear spring elements with nonlinear force-deformation relations in the longitudinal direction were used to model the longitudinal bond between the dowel bar and surrounding concrete nodes of the finite element model. The average bond stress, as given by MDOT experimental data, was converted to the force in the spring by assuming a tributary area at the point of connectivity. The spring elements were assigned between the coinciding nodes of the dowel bar and concrete. These coinciding nodes were oriented along four diametrically opposite lines. The initial slip in the grips of the MTS machine was accounted for in the calibration of the spring model. A typical nonlinear bond stress vs. displacement experimental data used for the analytical model is shown in figure 3.

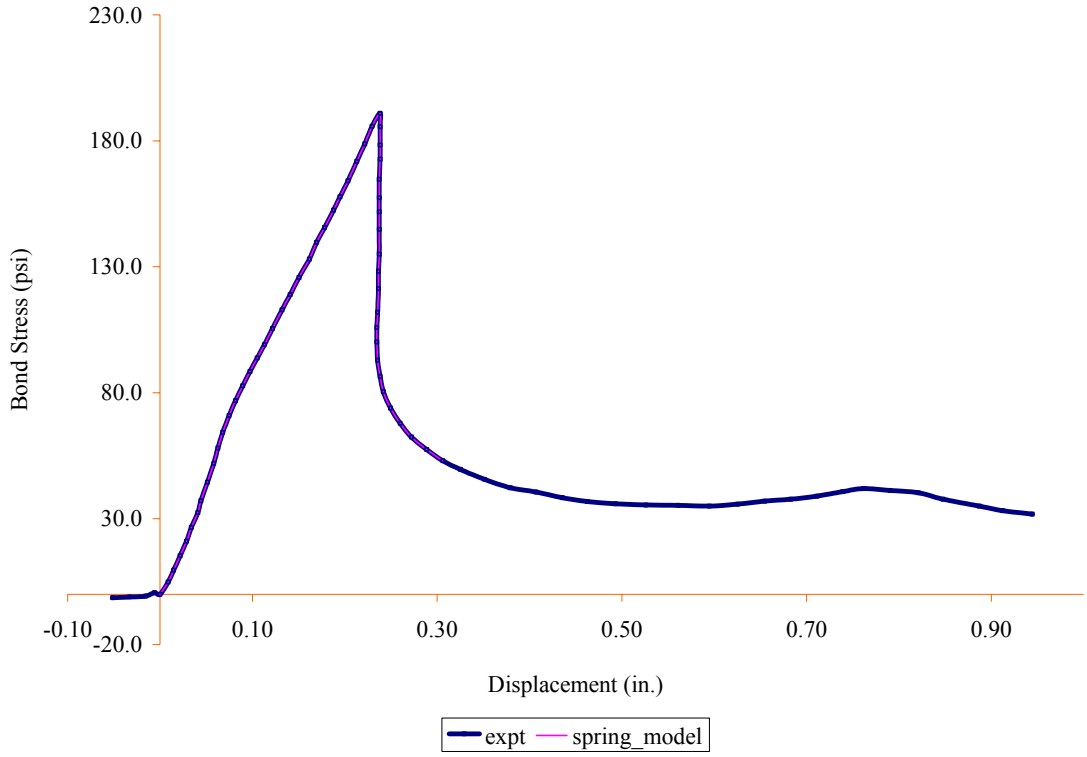

Figure 3: Typical Dowel Pullout Stress vs. Displacement experimental data from MDOT report (7)

From the results presented in Appendix A for each of the test specimens, it is clearly seen that the steep post failure debonding slope is accurately captured by the calibrated spring model.

The second model focuses on the transverse interactions between the steel dowel and the concrete slabs and the resulting frictional bond. The transverse interaction was modeled using special surface-to-surface contact elements. These elements model hard contact behavior with coulomb friction. The hard surface contact results in large bearing (normal) stresses at contact locations, and the coulomb friction model permits slip only if the applied shear is greater than the normal stress multiplied by the friction coefficient. A

coefficient of friction of 0.384 was assumed between the dowel bar and the surrounding concrete *(8)*.

I.4 Events / Material Damage Limit States

The following events / material damage limit states were identified based on the 3D stress state results from the on-going dowel bar research study and are again explained below:

(A) Debonding / initial slip state (τ_b)

(B) Onset of concrete inelasticity or cracking, PEEQ and PEEQT > 0

(C) Maximum principal stresses exceed the concrete tensile strength, i.e., $S_{max} > f'_t$

(D) Minimum principal stresses exceed the concrete compressive strength, i.e., $S_{min} > f'_c$

(E) Compressive crushing failure defined by equivalent compressive plastic strain limit (PEEQ) > 0.0035

(F) Tensile cracking failure defined by equivalent tensile plastic strain limit (PEEQT) > 0.003

These limit states are indicated on the analytically predicted pullout force-joint opening behaviors and are further explained below:

(A) Debonding / Initial slip state (τ_b) - The debonding / initial slip state (τ_b) is defined as the point where debonding occurs between the dowel and the concrete slab and the joint opening begins.

(C) and (D) Principal Stress States – In a multiaxial stress state, the principal stresses (S_{max} and S_{min}) can be determined from the analysis results. Event C indicated that the maximum principal stress exceeds the uniaxial tension strength (f'_t). This does not necessarily indicate cracking in a multiaxial state. Event D indicates that the

minimum principal stress exceeds the uniaxial compressive strength (f'_c), this does not necessarily mean crushing in a multiaxial state.

(B), (E) and (F) Plastic Strain States (PEEQ and PEEQT) - Two new parameters "Equivalent Compressive Plastic Strain" (PEEQ) and "Equivalent Tensile Plastic Strain" (PEEQT) states were identified in the finite element models. The concrete material model assumes two main failure mechanisms, tensile cracking and compressive crushing. PEEQ and PEEQT represent the effective plastic strains in compression and tension, respectively. They represent the total or lumped multiaxial inelastic strain, which is resolved into the directional plastic strain tensor according to the non-associated flow rule. These terms provide a measure of the lumped plasticity at a material point and are based on the uniaxial compression and tension inelastic stress-strain behavior. Figure 3, shows the stress-plastic strain curve for concrete under uniaxial compression. This curve is used to calibrate the multiaxial flow rule and the compressive plastic strain becomes PEEQ, the effective equivalent plastic strain. Thus in a multiaxial loading and stress state, PEEQ=0.0035 corresponds to the same lumped plasticity as uniaxial compressive plastic strain=0.0035. We have chosen PEEQ=0.0035 to define the crushing limit state of concrete to account for the materials inherent ductility, shown in figure 2. Similarly, to define the tensile cracking limit strain PEEQT is assumed=0.003, which is approximately ten times the strain at onset of cracking.

I.5 Results and Discussion

The analysis results showing the dowel pullout force vs. distance for the different types of aligned dowel bars is shown in Appendix A for tectyl coated epoxy, MMFX steel

dowels and zinc coated dowel bars. Specimens 7, 8 and 9 correspond to dowel bar with tectyl coated epoxy dowel bars. Specimens 10, 11 and 12 correspond to MMFX dowel bars and specimens 13, 14 and 15 correspond to zinc coated dowel bars. The results of the dowel pullout force vs. displacement between the finite element analyses compares favorably with the experimental data.

For the tectyl coated epoxy dowel bars, the average bond stress is approximately 70 psi. The limit state (A) is reached at the peak force of 1500 lbs, 2600 lbs and 3000 lbs at a dowel pullout distance of 0.078 in., 0.152 in. and 0.112 in. for samples 8, 7 and 9 respectively. A summary of the dowel pullout force vs. displacement (in.) is shown in figure 4.

In the case of MMFX steel dowel bars, the average bond stress was approximately 99 psi, shown in figure 5. In the analysis of samples 10, 11 and 12, only limit state (A) was observed at a peak force of 3440 lbs, 3510 lbs and 3126 lbs at a dowel pullout distance of 0.098 in., 0.102 in. and 0.093 in. respectively

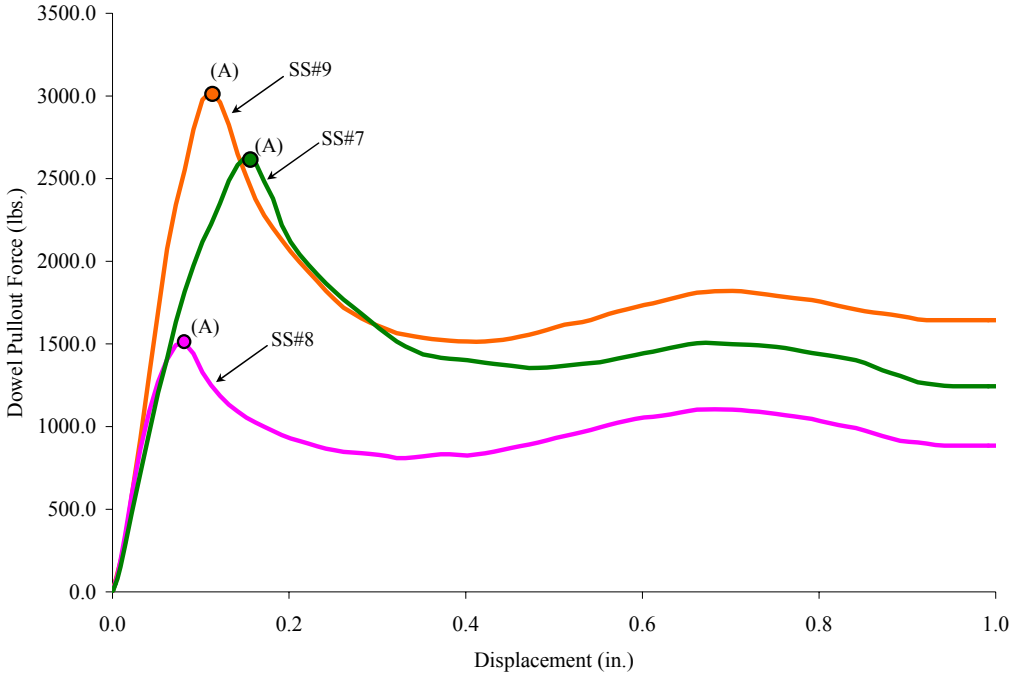

Figure 4: Dowel Pullout Force vs. displacement for tectyl coated epoxy dowel bar samples 7, 8 and 9

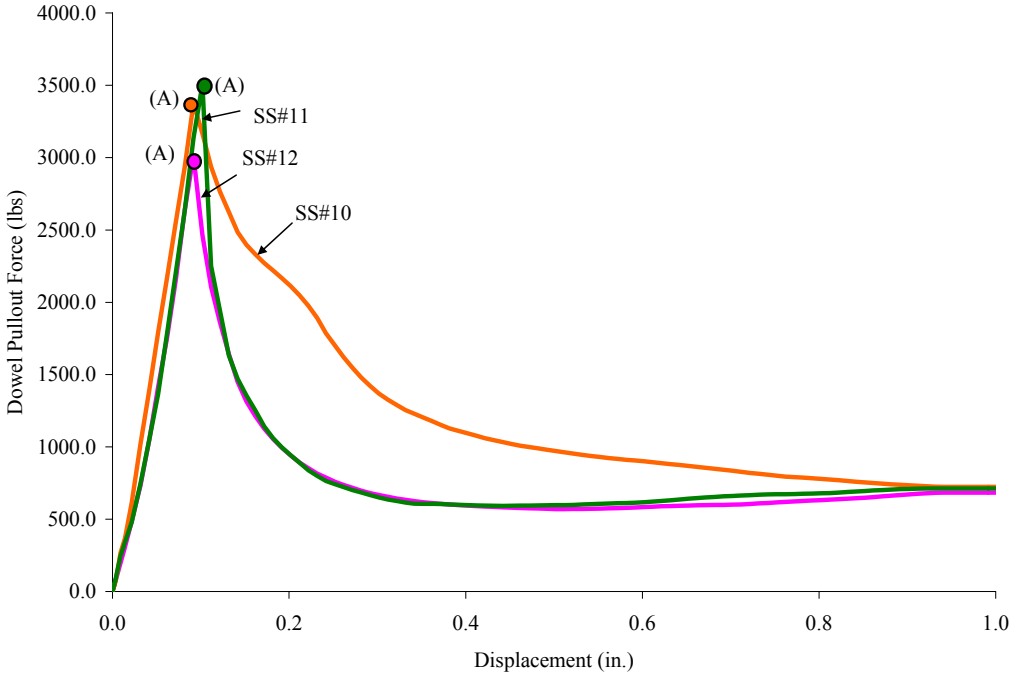

Figure 5: Dowel Pullout Force vs. displacement for MMFX Steel dowel bar samples 10, 11 and 12

The results of the finite element analysis of the zinc clad dowel bars showed that limit states (B) and (C) occurred before the debonding limit state (A). It means that the

material distresses occurred in the concrete surrounding the dowel bar before debonding actually occurred. The concrete material had started yielding in the multi axial state and it had reached the direct tensile strength. The dowel pullout force at which these limit states were observed to occur are presented in table 1. The average pullout bond stress for the zinc clad dowel specimen samples 13, 14 and 15 was 174 psi calculated at the peak force from the test data.

Table 1: Dowel pullout force and distance for limit states (B) and (C) in Zinc coated dowel bars

Specimen No.	Limit State	Dowel Pullout Force (lbs)	Distance (in)
13	B	4200	0.142
	C	4450	0.152
14	B	4170	0.142
	C	4460	0.152
15	B	3970	0.142
	C	4490	0.162

From the results of the finite element analysis, it is clearly seen that the zinc clad dowel bars had the highest average debonding stress of 174 psi followed by the MMFX steel and the tectyl coated epoxy bars with a debonding stress of 99 psi and 70 psi, respectively.

A recommended debonding strength is based on the following assumptions:

1) Debonding limit state occurs at the peak dowel pullout force

2) Only the debonding limit state (A) should be observed in the finite element analysis before the material undergoes any other distress / damage limit state

The spring model was calibrated using the dowel pullout force – displacement trend observed in sample 13 for zinc clad.

Considering the assumptions stated above, a peak dowel pullout force of 3960 lbs was considered in the calibration of the spring model. Figure 6, shows the dowel pullout

force vs. displacement curve that was used to calibrate the spring model in the finite element analysis.

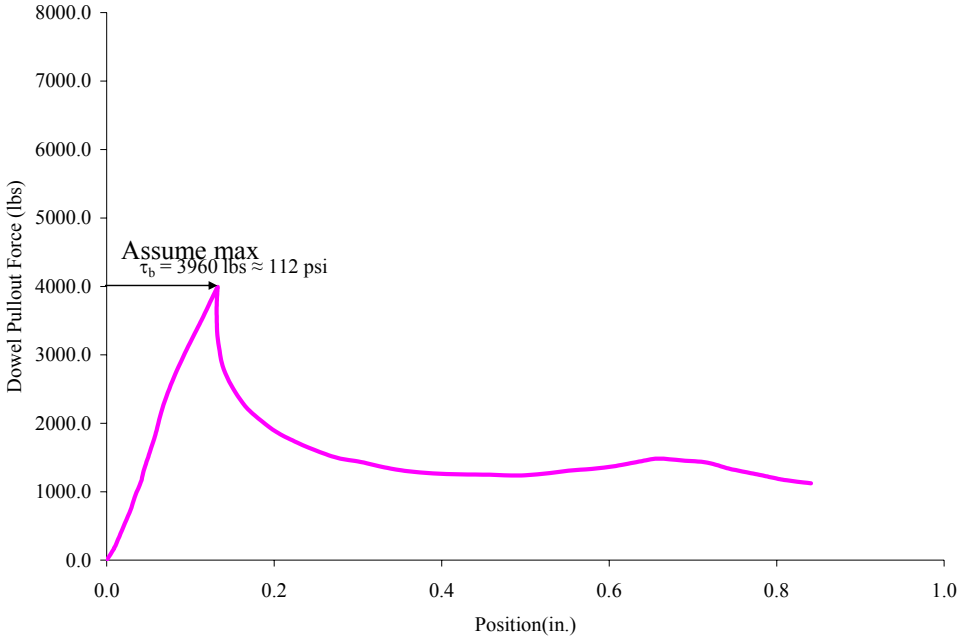

Figure 6: Dowel pullout force vs displacement behavior used for calibrating the spring model

The above pullout force of 3960 lbs corresponds to a pullout bond stress of 112.0 psi. Only limit state (A) was observed at the peak force and no other limit state stresses / strains occurred in the concrete surrounding the dowel bar, shown in figure 7.

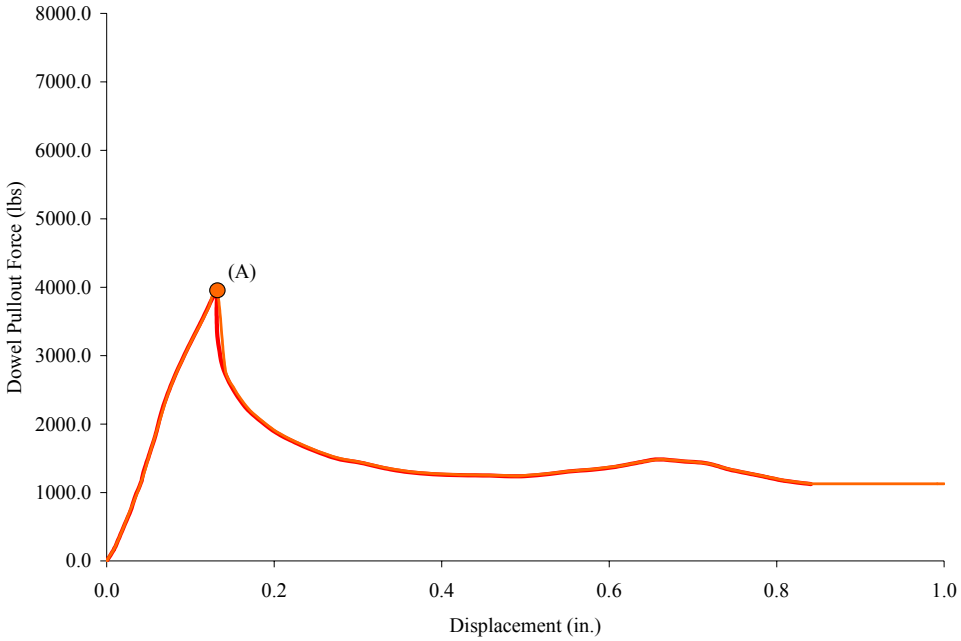

Figure 7: Dowel pullout force vs displacement for a recommended bond stress of 112.0 psi

I.6 Conclusions

The results obtained from the finite element analytical models showed that they compared favorably with the experimental results. The 3D FEM models were capable of capturing the steep post debonding failure slope from the experiments.

In the analysis of the zinc clad dowel bar specimens, material distress was observed from the analyses before debonding actually occurred due to dowel pullout.

In the next task, the development of the 3D nonlinear finite element model of the realistic pavement slab is presented. The dimensions, material model input, loading and boundary conditions and results are presented and discussed.

Task II: 3D Finite element models for aligned dowel bars of different types in a realistic pavement

This part of the report explains the development of the finite element model calibrated for different dowel bar specimens using the data provided by MDOT, the results obtained from the analysis and some initial recommendations. The analytical models of realistic pavement joints with aligned dowel bars (of different types) subjected to traffic (tandem axle) loading and environmental (thermal expansion) effects were developed.

II.1 Development of the 3D Finite Element model

The finite element models developed in this task were based on the Phase I study to investigate the effects of misaligned dowel bars combined with wheel loads. A three dimensional nonlinear finite element analysis was conducted using the nonlinear concrete damage plasticity model in Abaqus.

II.1.1 Nonlinear Material Model

The concrete material was modeled using the concrete damage plasticity model. The steel dowel bar was modeled using an isotropic elastic material model. To model the nonlinear inelastic behavior of concrete, the following input parameters were specified; the dilation angle, biaxial stress ratio, and the tensile-to-compressive meridian ratio were assumed to be equal to 15^{o}, 1.16, and 0.667, respectively. The uniaxial compression stress-strain curve was defined using the elastic modulus E_c and compressive strength f'_c and the modified Popovic's empirical stress-strain model recommended by Collins et al.*(5)* The

uniaxial tension stress-strain curve was defined using the direct tensile strength ($f'_t = 4\sqrt{f'_c}$) and a hypothetical tension stiffening stress-strain model developed by the authors, as shown in figure 8.

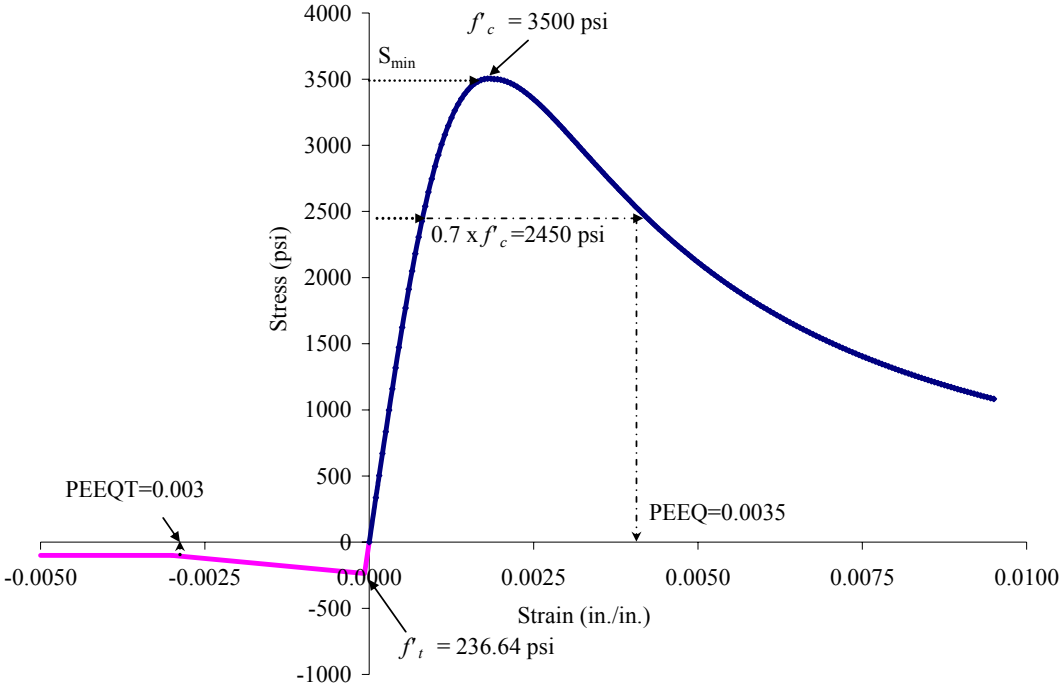

Figure 8: Uniaxial Compressive and Tension Stress-Strain curve for Concrete

The input property parameters for the dowel bars were the elastic modulus and poissons ratio equal to 29,000 ksi and 0.3 respectively for all the dowel bars. The same elastic modulus was used even though the yield and ultimate stresses for the MMFX steel dowel bar is twice as compared to the grade 60 billet steel dowel bar as confirmed with MDOT and test results from research conducted at NC State. The yield and ultimate stresses were not required because the dowel bar was assumed to remain elastic throughout the analysis.

II.1.2 Interaction between Dowel and Concrete

The longitudinal and transverse interactions between the dowel bars and the concrete slabs were modeled using two models: (a) the first model focused on the longitudinal bond between the steel and concrete due to mechanical interlock and static friction and (b) the second model focused on the transverse interaction between the steel dowel and surrounding concrete resulting in large contact or bearing stresses and additional friction bond in the longitudinal direction due to the normal (bearing) stresses and coulomb friction coefficients.

The first model was calibrated using experimental results (dowel pullout force – displacement) from an MDOT report. Nonlinear spring elements with nonlinear force-deformation relations in the longitudinal direction were used to model the longitudinal bond between the dowel bar and surrounding concrete nodes of the finite element model. The average bond stress, as given by MDOT experimental data, was converted to the force in the spring by assuming a tributary area at the point of connectivity. The spring elements were assigned between the coinciding nodes of the dowel bar and concrete. These coinciding nodes were oriented along four diametrically opposite lines. The initial slip in the grips of the MTS machine was accounted for in the calibration of the spring model. The data for the pullout behavior for tectyl coated epoxy, MMFX Steel and Zinc clad dowel bars were provided by MDOT. The pullout data from each test specimen was averaged out and used to calibrate the nonlinear force vs. displacement of the spring elements, shown in figure 9.

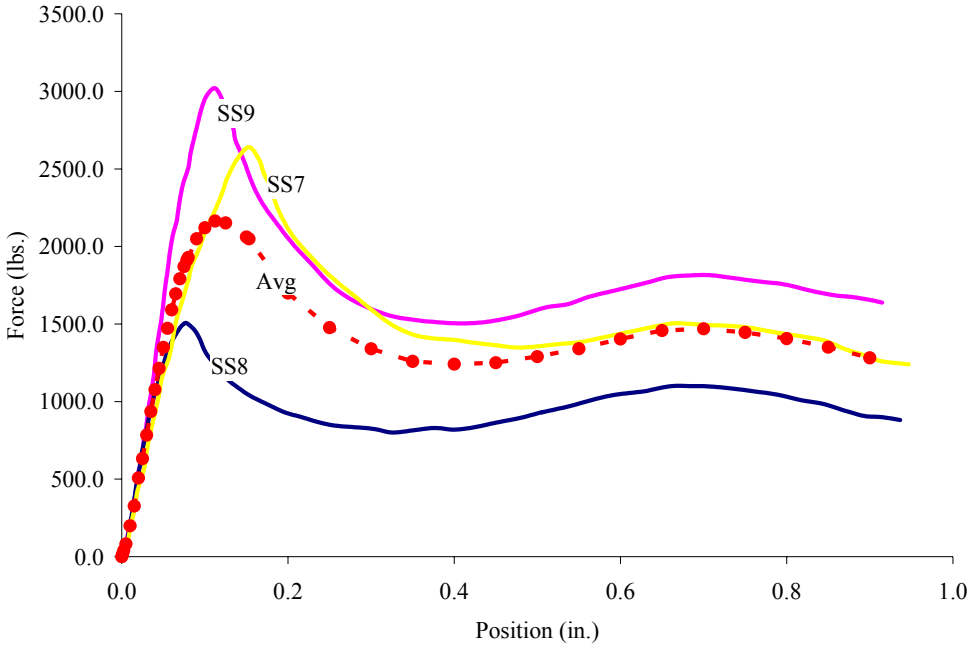

(a) Pullout data for tectyl coated epoxy bars (specimens 7, 8 and 9)

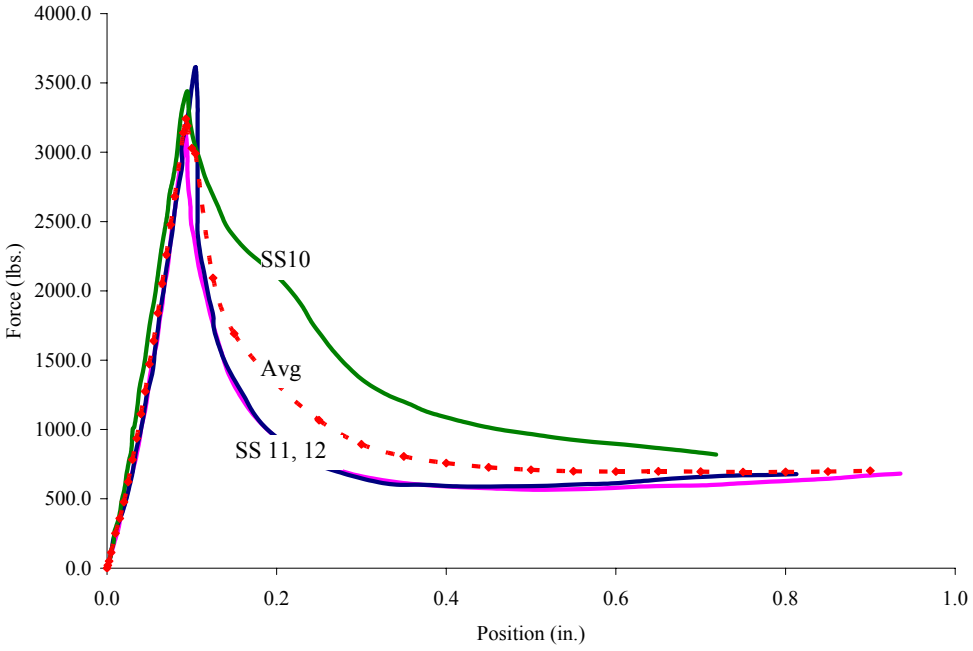

(b) Pullout data for MMFX Steel bars (specimens 10, 11 and 12)

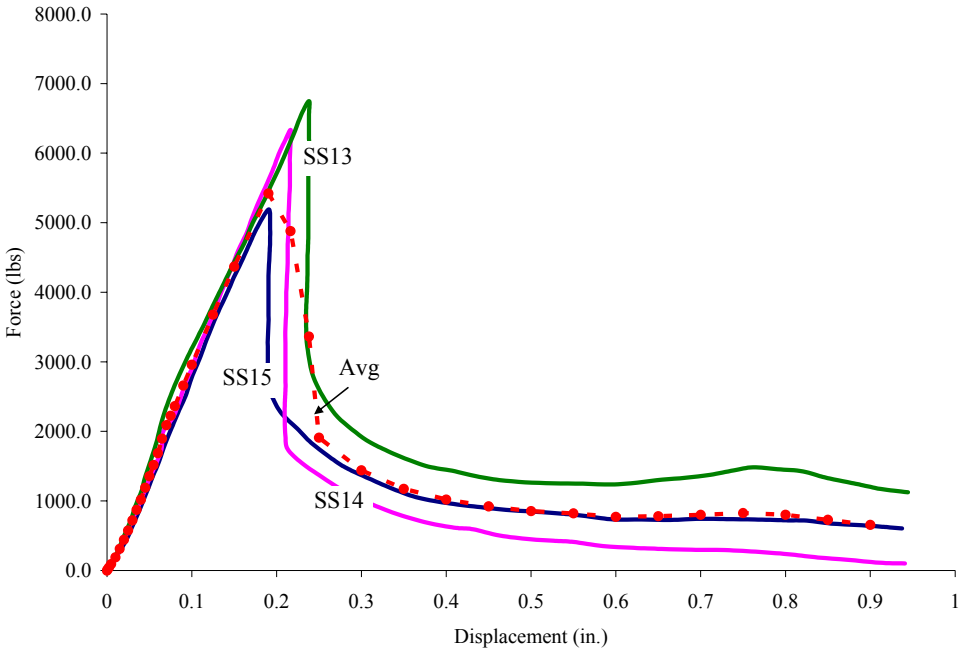

(c) Pullout data for Zinc Coated dowel bars (specimens 13, 14 and 15)

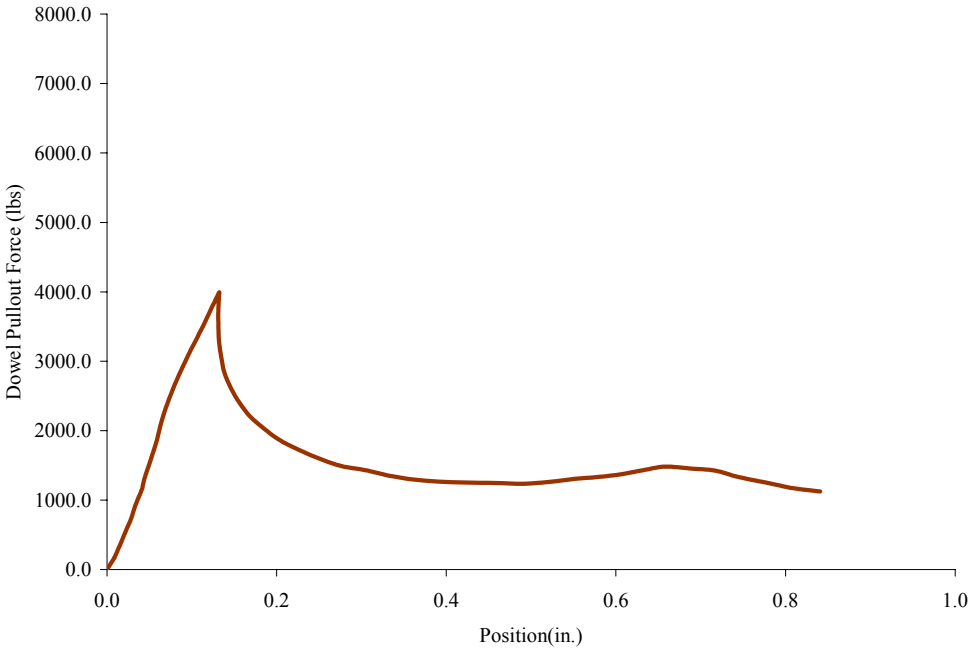

(d) Limiting dowel pullout data vs. displacement

Figure 9: Averaged pullout data vs. displacement for the three different dowel bar types and the limiting bond pullout – displacement data

The second model focuses on the transverse interactions between the steel dowel and the concrete slabs and the resulting frictional bond. The transverse interaction was modeled using special surface-to-surface contact elements. These elements model hard contact behavior with coulomb friction. The hard surface contact results in large bearing (normal) stresses at contact locations, and the coulomb friction model permits slip only if the applied shear is greater than the normal stress multiplied by the friction coefficient. A coefficient of friction of 0.076 was assumed between the dowel bar and the surrounding concrete. This low coefficient of friction was assumed as the MDOT data already incorporated the stiffness and transverse surface friction between the dowel and concrete. The constraint conditions between the various layers of the finite element model are shown in figure 10.

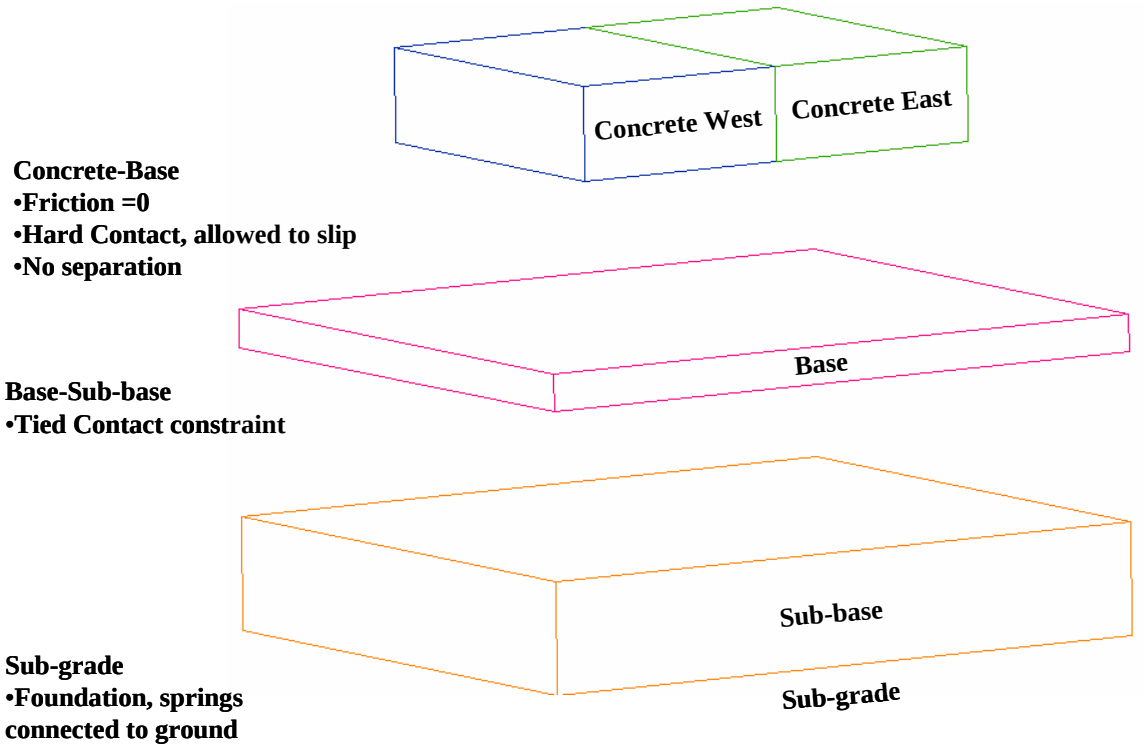

Figure 10: Typical constraint conditions used for the finite element model

II.1.2 Model, dimensions, loading and boundary conditions

Two aligned (single dowel – 1A and three dowels – 3A) three dimensional finite element models were developed in this study. The dimensions of the finite element models with a single and three dowel bars, cross section and loading dimensions are shown in figure 11.

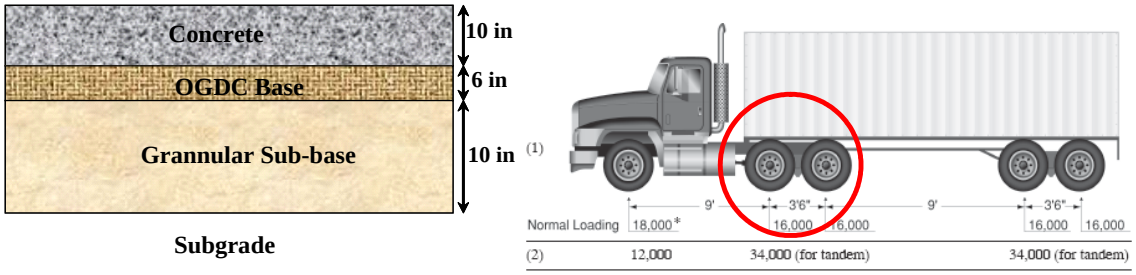

(a) Typical pavement cross section and truck loading

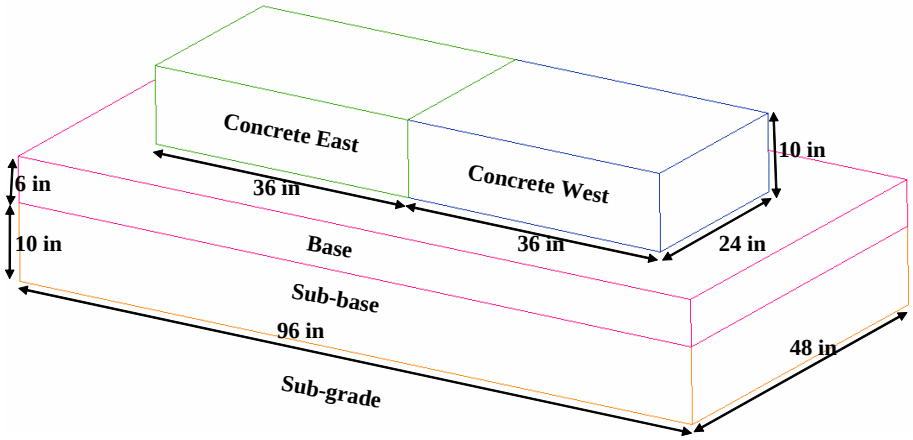

(b) Dimensions for a single dowel bar model

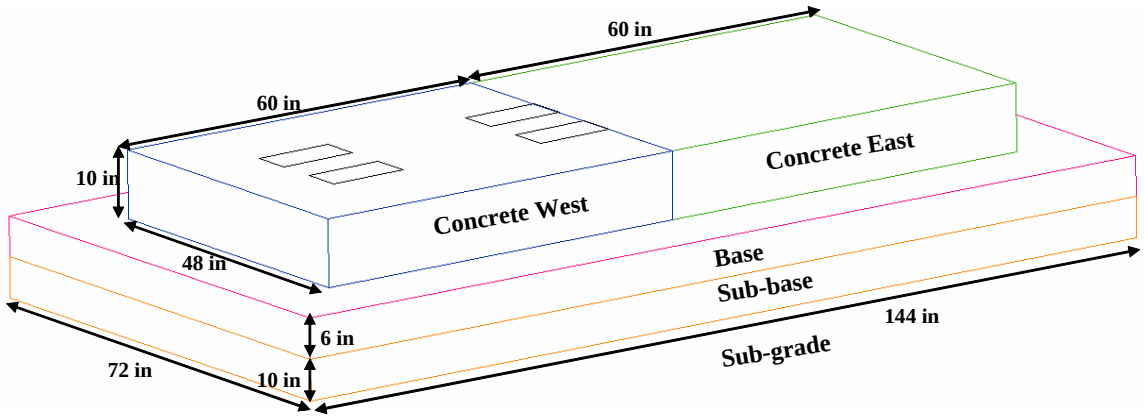

(c) Dimensions for three dowel bar model

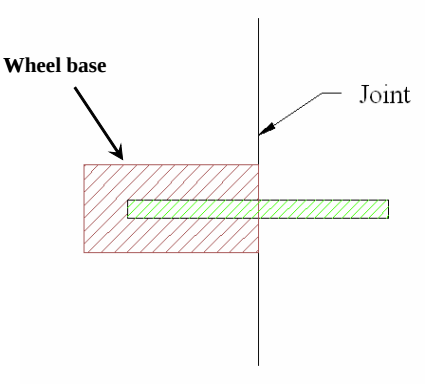

(d) Plan view of the location of wheel base for single dowel model

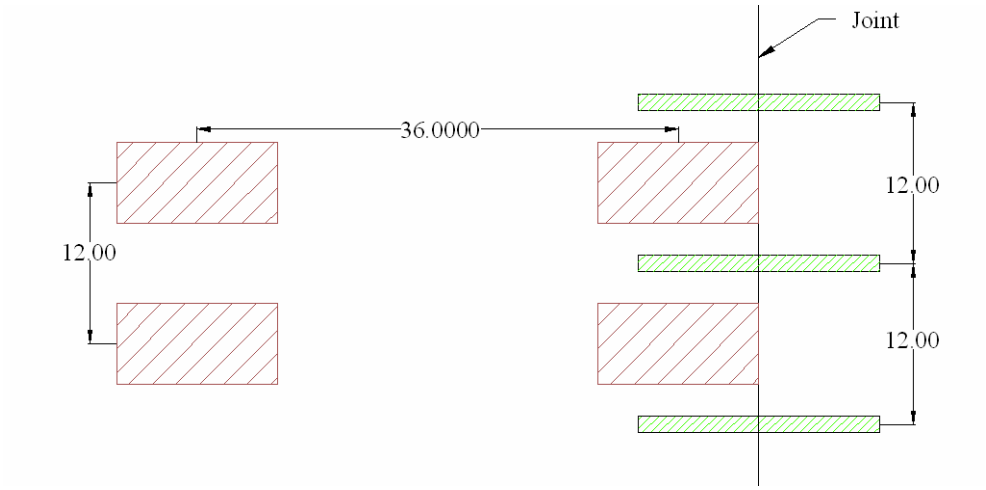

(e) Plan view of the position of wheel base of dual wheel tandem axle

Figure 11: Dimensions and location of various parts of the pavement slab and wheel base in the finite element model

Loading and boundary conditions used in the finite element analysis are shown in figure 12. The approximate joint opening was determined using the equation by Darter and Barenberg (1977),

$$\Delta L = C\ L\left(\alpha_t\ \Delta T + \varepsilon\right)$$

where, ΔL = joint opening caused by temperature change and drying shrinkage of concrete.

α_t = coefficient of thermal expansion of concrete (5 to 7 x 10^{-6} /^{o}F)

ε = drying shrinkage coefficient of concrete (0.5 to 2.5 x 10^{-4})

L = joint spacing or slab length = 15 ft.

ΔT = temperature range, i.e., temperature at placement minus lowest mean monthly temperature

C = adjustment factor due to slab-subbase friction, 0.8 for granular subbase

Finally, the wheel loads are applied close to the face of the joint on one side of the pavement slab. The sequence of boundary and loading conditions is shown in figure 12.

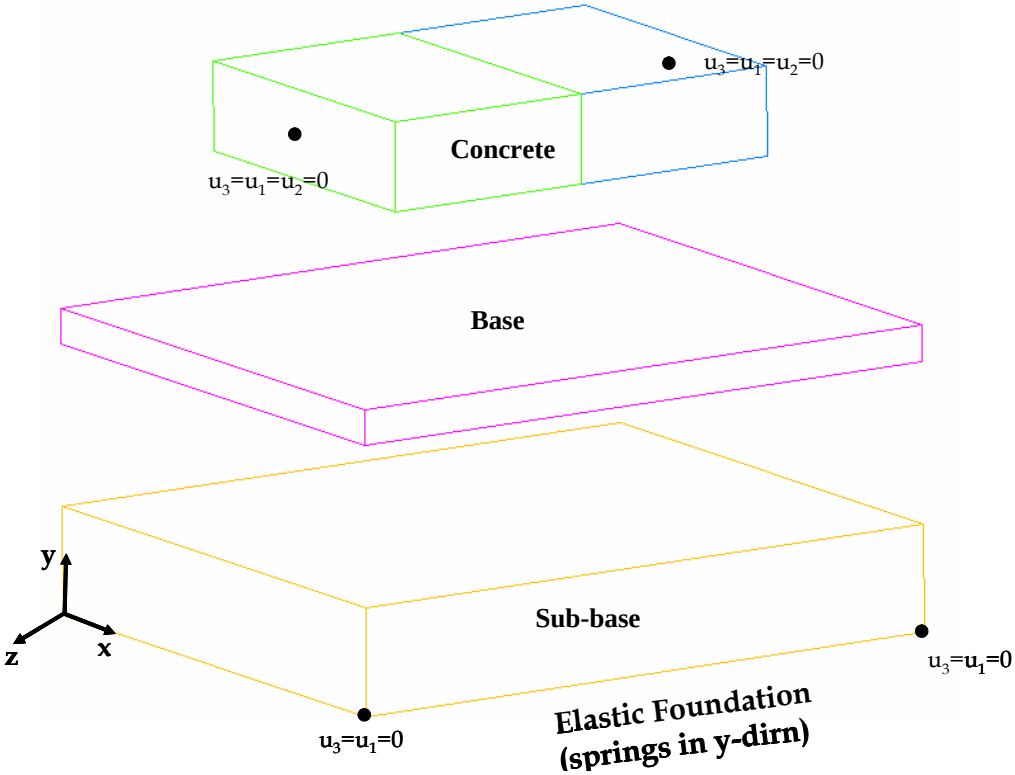

(a) Boundary Conditions for Step I of analysis (Gravity Loading)

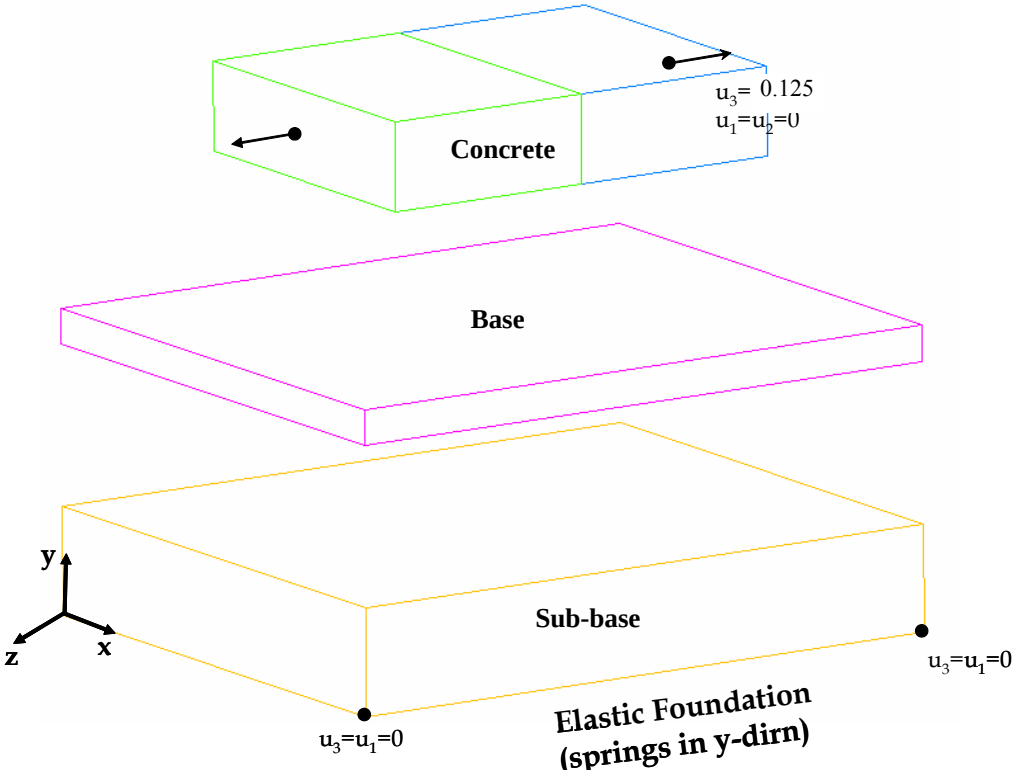

(b) Boundary Conditions for Step II (Joint Opening)

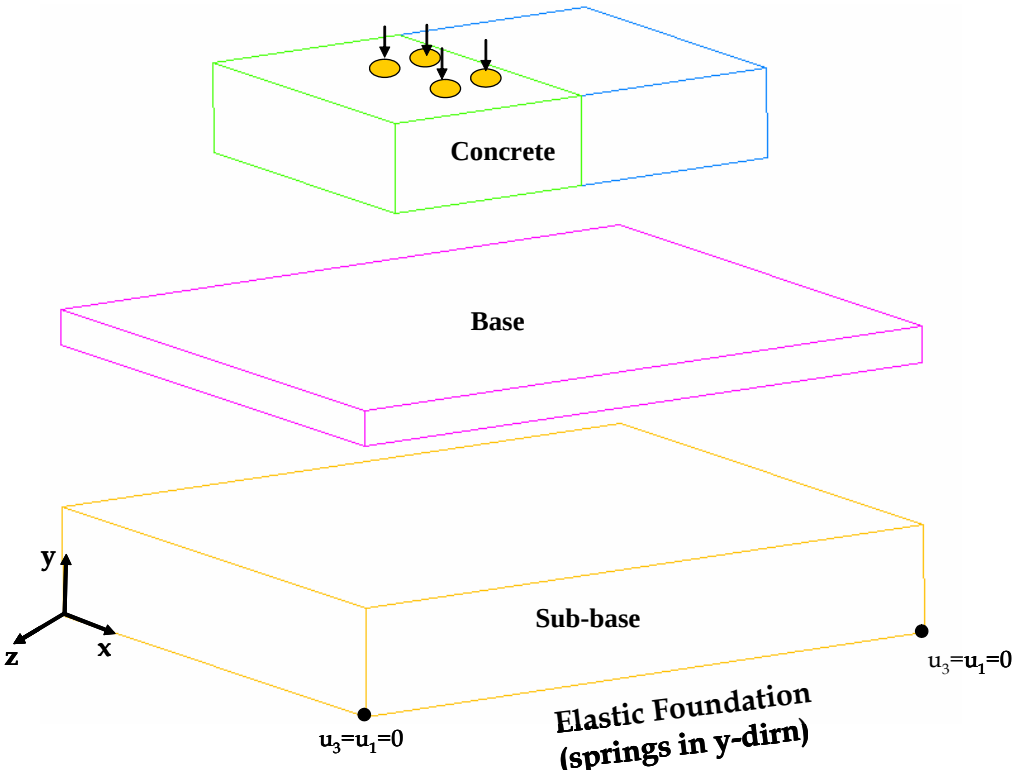

(c) Boundary Conditions for Step III (wheel loading)

Figure 12: Typical Boundary and Loading conditions on the pavement system

II.2 Results obtained from the analysis

Figures 13 and 14, illustrate the behavior of a single aligned dowel bar finite element model calibrated using the limiting bond pullout data vs. displacement, as shown in figure 9(d). The model is subjected first to joint opening and then a loading of 16 kips. Figures 15 and 16, illustrate the behavior of three aligned dowel bars calibrated using the same limiting bond pullout data vs. displacement and a joint opening of 1/8 in and loading of 8 kips. Tables 2(a) and (b) summarize the stresses and strains surrounding the dowel bar obtained at joint opening and after load application for a single aligned dowel bar model and three aligned dowel bar models.

Table 2(a): Summary of Results for single dowel bar with the limit bond – pullout behavior

	At Joint Opening		After Loading	
	Loaded side	Unloaded side	Loaded side	Unloaded side
S_{max} (psi)	204.80	204.60	219.50	235.80
S_{min} (psi)	302.70	295.60	2123.00	1261.00
PEEQ (in./in.)	0.00	0.00	3.99E-04	9.30E-05
PEEQT (in./in.)	0.00	0.00	6.14E-05	1.76E-04

Table 2(b): Summary of Results for three aligned dowel bar with limiting average bond – pullout behavior

	At Joint Opening		After Loading	
	Loaded side	Unloaded side	Loaded side	Unloaded side
S_{max} (psi)	204.50	201.30	176.60	140.50
S_{min} (psi)	239.00	238.90	883.90	306.00
PEEQ (in./in.)	0.00	0.00	5.23E-05	0.00
PEEQT (in./in.)	0.00	0.00	9.65E-06	0.00

In the single aligned dowel bar case, nominal tensile stresses (S_{max}) and compressive stresses (S_{min}) stresses are produced in the concrete due to the self weight of the concrete slabs and at a joint opening of 1/8 in, shown in figures 13(a) and (b). No

inelastic strains in tension (PEEQT) and compression (PEEQ) are produced as the stresses in the concrete are within the elastic range, shown in figures 13(c) and (d). With the application of the wheel loads on the concrete slab, a tremendous increase in the bearing stresses surrounding the dowel bar is observed, figure 14(a) and (b). Along with inelastic stresses and strains observed in the concrete, there is some uplift of the unloaded side (east) of the concrete slab.

In the three aligned dowel bars case, similar to the single aligned dowel bar case, nominal tensile stresses (S_{max}) and compressive stresses (S_{min}) were observed in the concrete. This is due to the self weight of the concrete slabs and at a joint opening of 1/8 in, shown in figures 15(a) and (b). No inelastic strains in tension (PEEQT) and compression (PEEQ) are produced as the stresses in the concrete are within the elastic range, shown in figures 15(c) and (d). With the application of the wheel loads (west side), some important observations were made in terms of the stresses and strains in the concrete slabs. As the load is applied, apart from an increase in the bearing stresses surrounding the dowel bar, stress redistribution is observed, figure 16(a) and (b). Figure 16(a), shows that the unloaded slab tries to uplift. The stresses shown in Table 2(b) are not the stresses surrounding the dowel bar but the stresses caused due to uplift of the concrete slab specimen after loading. Due to the placement of the wheel loads between the dowel bars, the center dowel was seen to carry higher stresses compared to the outer dowel bars. As a result of which, inelastic strains in tension and compression were observed only in the center dowel bar on the loaded side as shown in figure 16 (c) and (d).

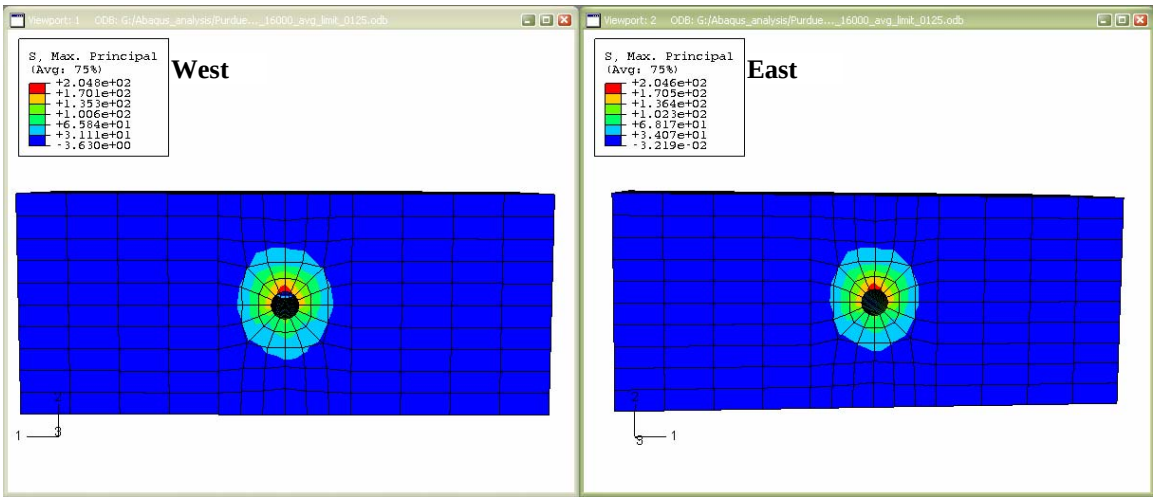

(a) Maximum Tensile Stress at Joint Opening (1/8 in.)

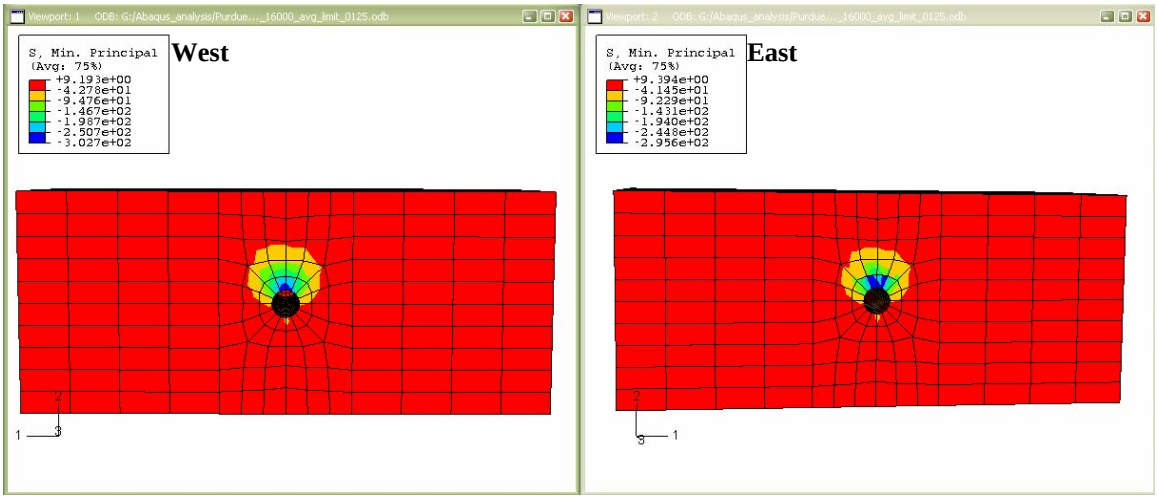

(b) Maximum Compressive Stress at Joint Opening (1/8 in.)

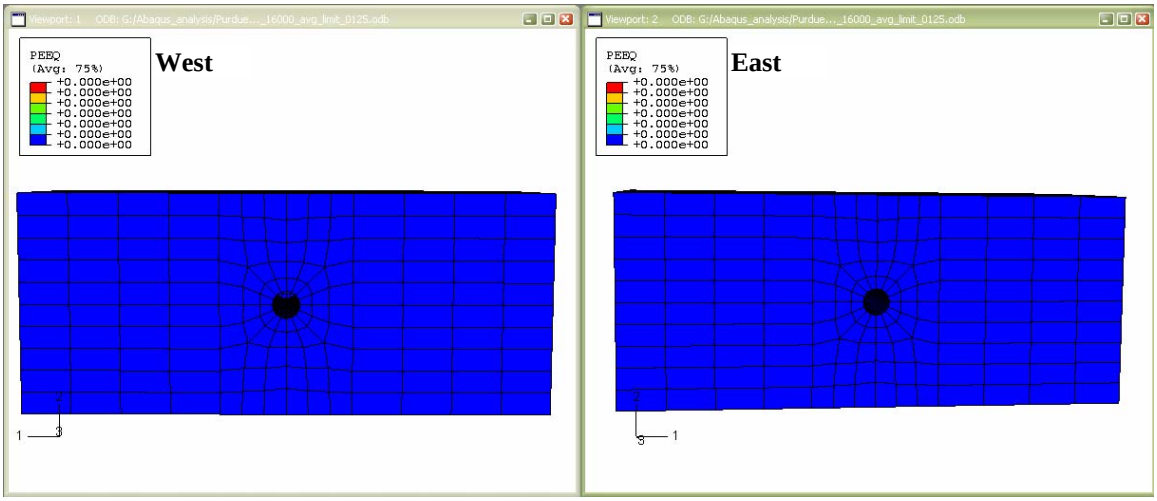

(c) Inelastic Compressive Strains at Joint Opening (1/8 in.)

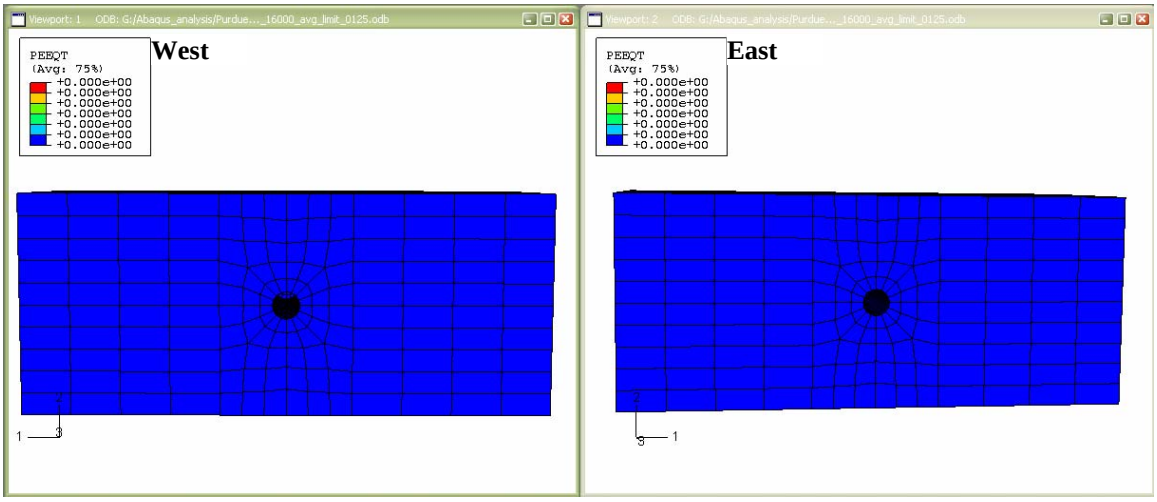

(d) Inelastic Tensile Strains at Joint Opening (1/8 in.)

Figure 13: Stresses and Strains for a single aligned dowel bar calibrated using the limiting bond – displacement behavior at 1/8 in joint opening

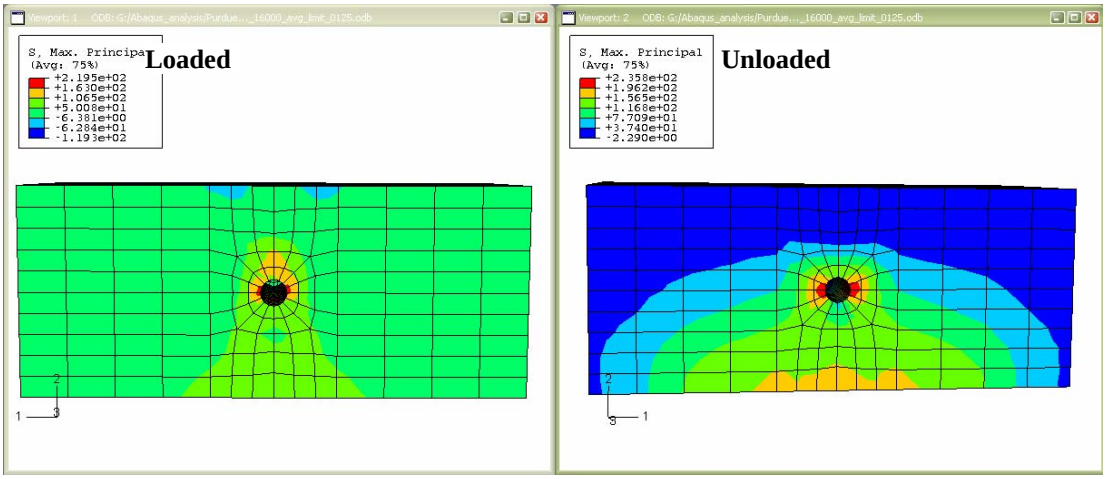

(a) Maximum Tensile Stresses at end of load application

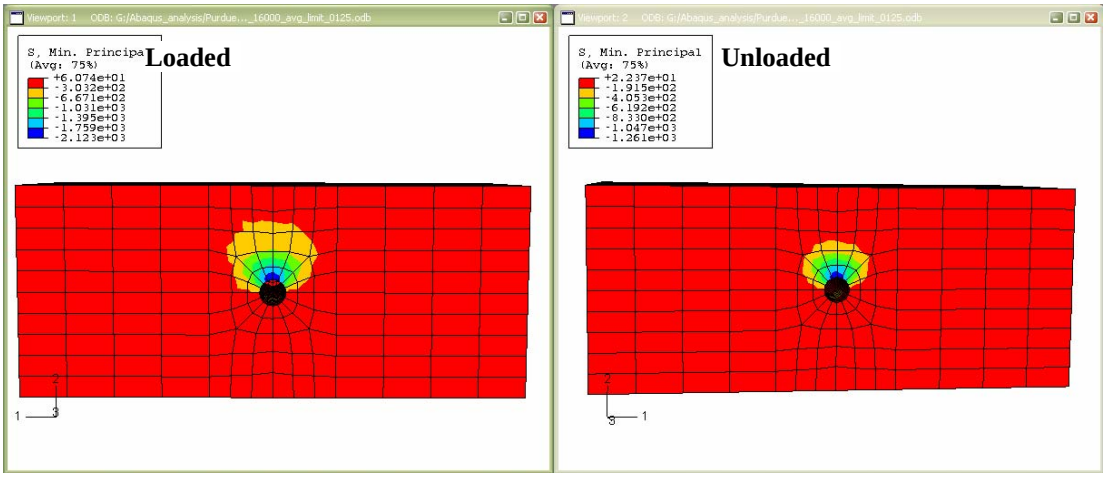

(b) Maximum Compressive Stresses at end of load application

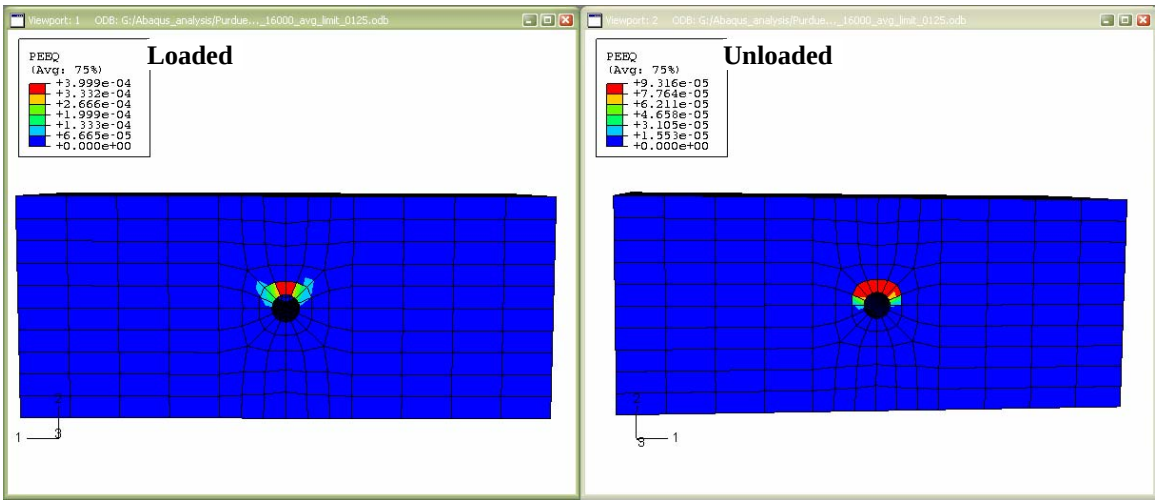

(c) Inelastic Compressive Strains at end of load application

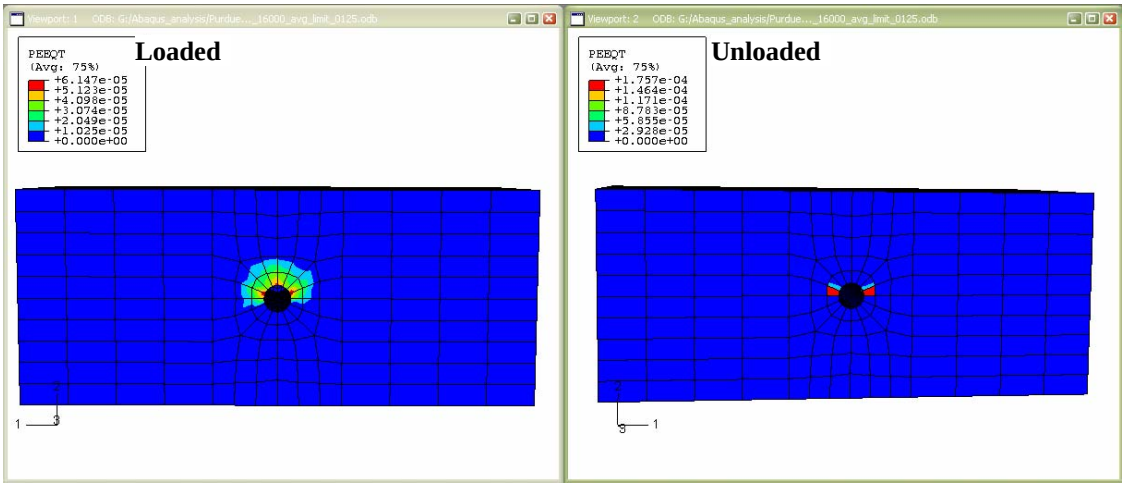

(d) Inelastic Tensile Strains at end of load application

Figure 14: Stresses and Strains for a single aligned dowel bar calibrated using the limiting bond – displacement behavior at end of load application

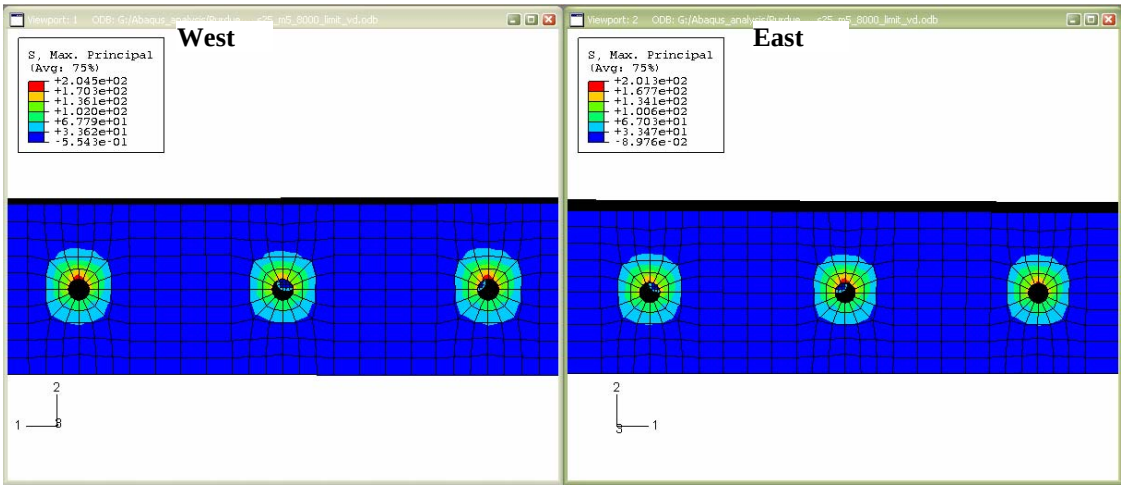

(a) Maximum Tensile Stress at Joint Opening (1/8 in.)

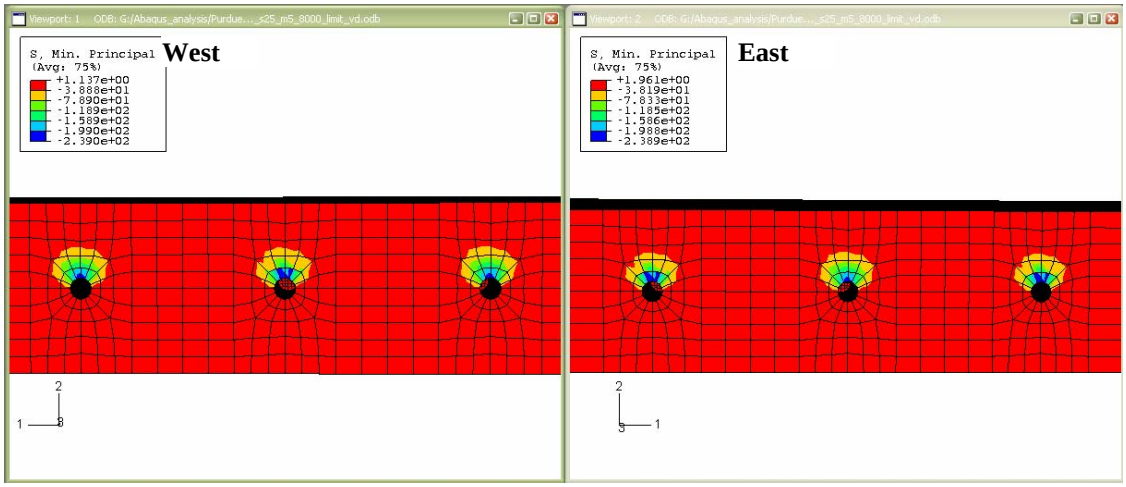

(b) Maximum Compressive Stress at Joint Opening (1/8 in.)

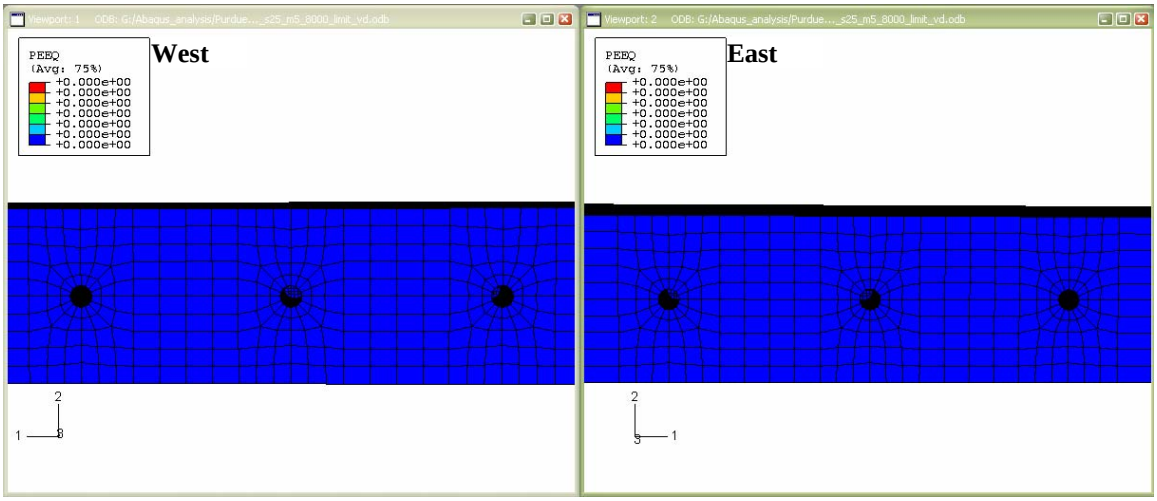

(c) Inelastic Compressive Strains at Joint Opening (1/8 in.)

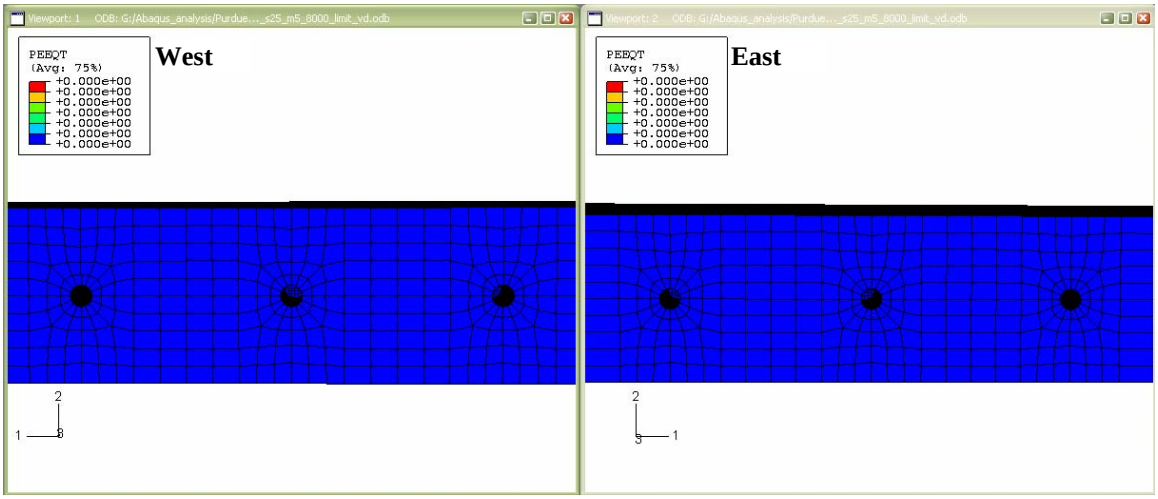

(d) Inelastic Tensile Strains at Joint Opening (1/8 in.)

Figure 15: Stresses and Strains for three aligned dowel bars calibrated using the limiting bond – displacement behavior at 1/8 in joint opening

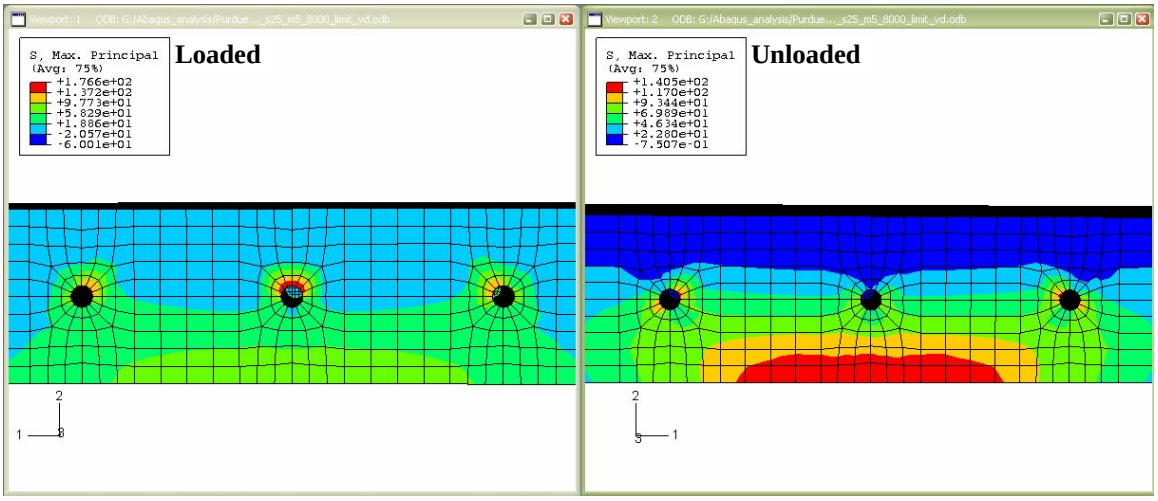

(a) Maximum Tensile Stresses at end of load application

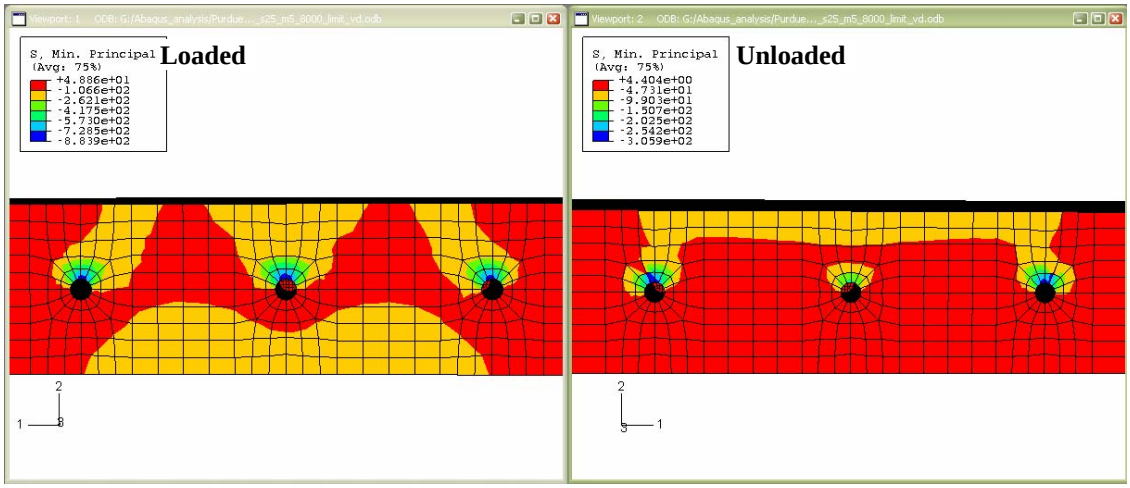

b) Maximum Compressive Stresses at end of load application

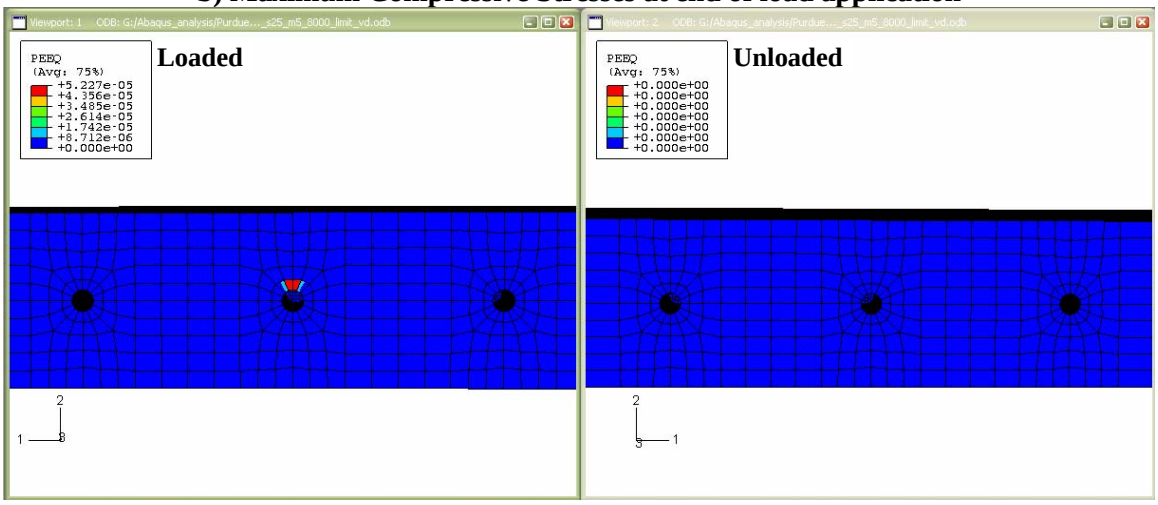

(c) Inelastic Compressive Strains at end of load application

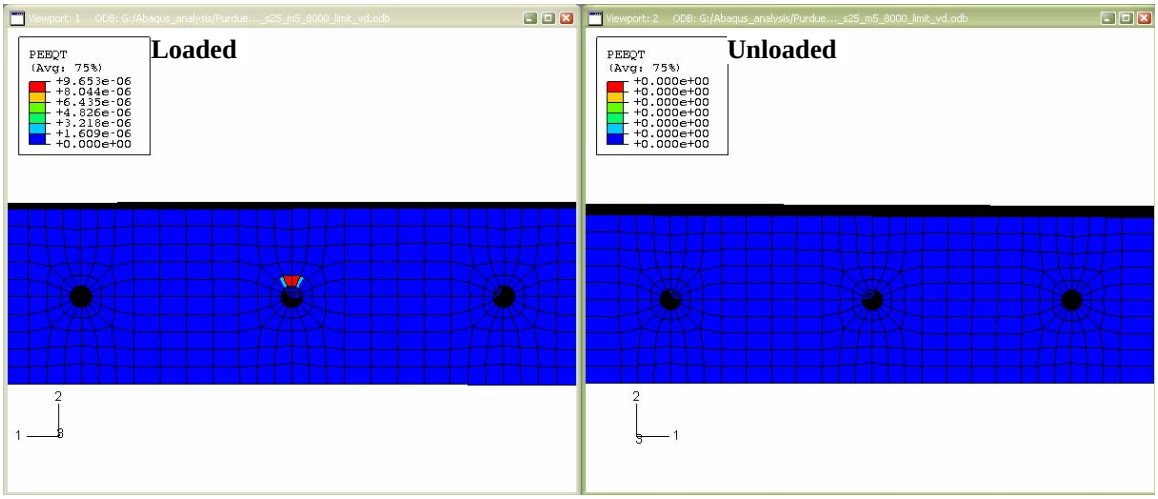

(d) Inelastic Tensile Strains at end of load application

Figure 16: Stresses and Strains for three aligned dowel bars calibrated using the limiting bond – displacement behavior at end of load application

The results for the single and three dowel bars before (at joint openings of 1/8 in.) and after load application for each of the dowel bar specimens are shown in the attached Appendix B.

II.3 Concluding remarks

The data on dowel pullout behavior vs. displacement provided by MDOT was used to calibrate the dowel-concrete bond interaction model. Behavior of three dowel specimens were investigated, namely, tectyl coated epoxy, MMFX Steel and Zinc Clad dowel bars. The single and three aligned dowel bar finite element models simulating the realistic concrete pavement joint and cross section from Phase I study was used. The preliminary conclusions derived from this study are as follows:

- In the single and multiple dowel bar analyses, at a joint opening of 1/8 in, nominal stresses were observed in the concrete surrounding the dowel bar. These stresses were produced due to the self weight of the concrete slabs.

- As the wheel loads were applied on the concrete slabs, the bearing stresses produced added to the stresses produced at joint opening. Inelastic tensile and compressive strains due to loading were observed around the central dowel bar in the multiple dowel bar models.

The magnitude of the dowel pullout bond stress is a function of the dowel surface preparation and irregularities at the contact interface with the surrounding concrete. The results from the numerical (3D finite element) analysis indicate that if the dowel pullout bond stress is greater than 112 psi, then limit states B (onset of concrete material inelasticity) or C (cracking stress exceeded) occur before dowel slip (limit state A).

Thus, if the dowel pullout stress exceeds 112 psi, then there is potential for concrete cracking or inelasticity in the concrete at the dowel - concrete interface. This is not acceptable, because concrete cracking or inelasticity will lead to fatigue deterioration and eventual failure (functional or structural) of the joint with repeated cycles. The current MDOT specification of maximum pullout bond stress limited to 60 psi provides a resistance factor (or factor of safety) of approximately 1.87, which is reasonable.

4.0 References

1. Abaqus User Manual, Abaqus Inc., Providence, RI, USA, 2005
2. Lubliner, J., J. Oliver, S. Oller, and E. Oñate. A Plastic-Damage Model for Concrete, International Journal of Solids and Structures, Vol. 25, 1989, pp. 299–329.
3. Lee, J., and G. L. Fenves, Plastic-Damage Model for Cyclic Loading of Concrete Structures, Journal of Engineering Mechanics, Vol. 124, no.8, 1998, pp. 892–900.
4. Chen, W. F., and Han, D. J. , Plasticity for Structural Engineers, Spring-Verlag, October, 1988.
5. Collins, M., Mitchell, D. and MacGregor, J. Structural Design Considerations for high strength concrete, Network of centers of Excellence on High Performance Concrete, Toronto, 1992
6. E-Hacha, R and Rizkalla, S. H., Fundamental Mechanical Properties of MMFX Steel rebars, a report submitted to MMFX Steel Corporation of America, NC State University, July 2002
7. Bennett, A, An Internal Report on Michigan Test Method for Bond Release Agents for Epoxy Coated Dowel bars, Michigan Department of Transportation, Lansing, MI.
8. Shoukry, S. N., Effect of Bonding Force on Stresses in Concrete Slabs, draft final report, West Virginia Department of Transportation, July 2003.

Appendix A

DOWEL PULLOUT FORCE - DISPLACEMENT BEHAVIOR FOR VARIOUS DOWEL SPECIMENS

TECTYL COATED EPOXY DOWEL BARS

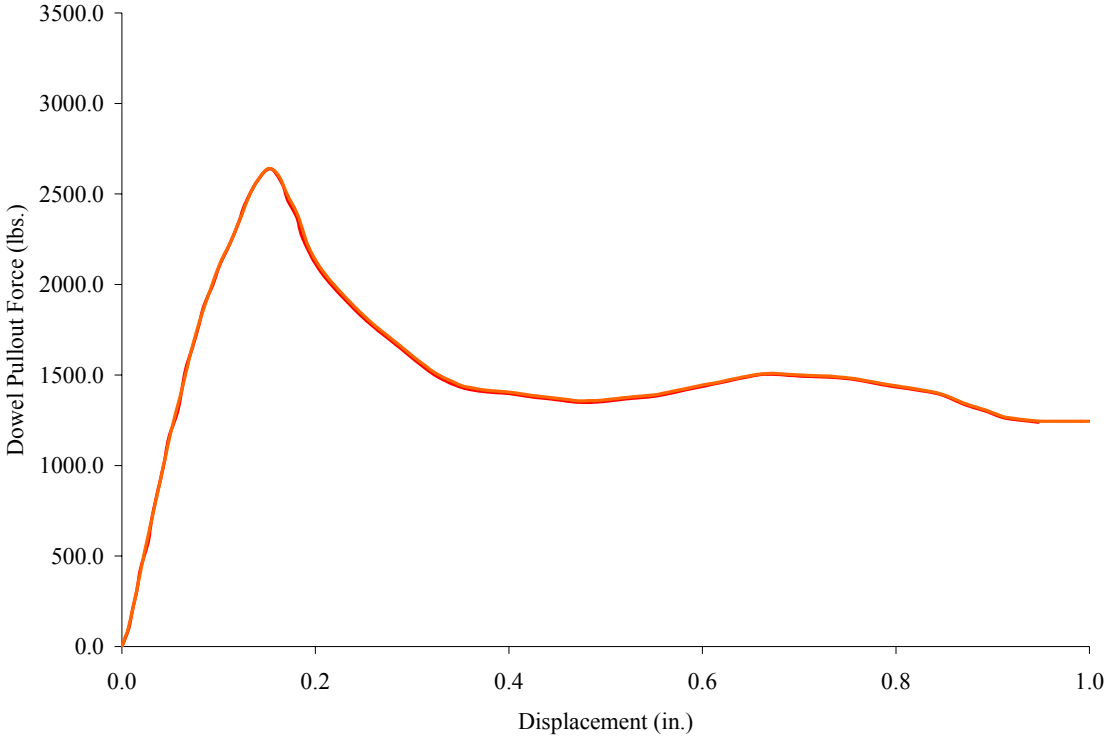

Figure A.1: Dowel Pullout Force vs. displacement for Sample 7

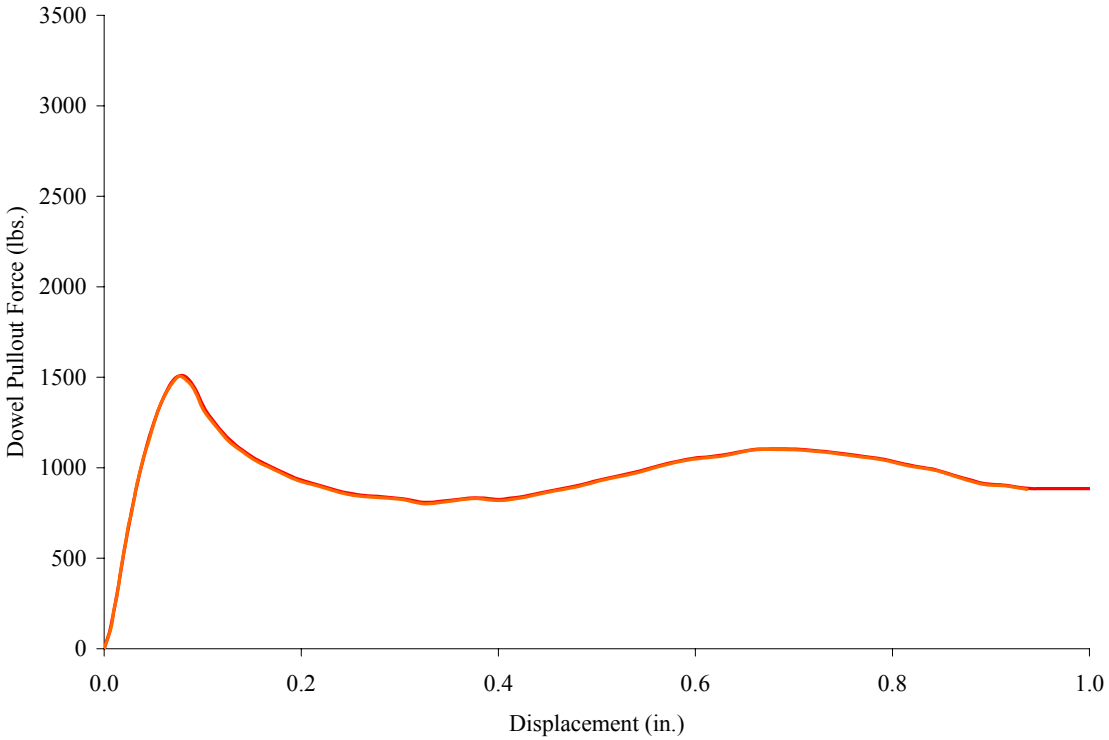

Figure A.2: Dowel Pullout Force vs. displacement for Sample 8

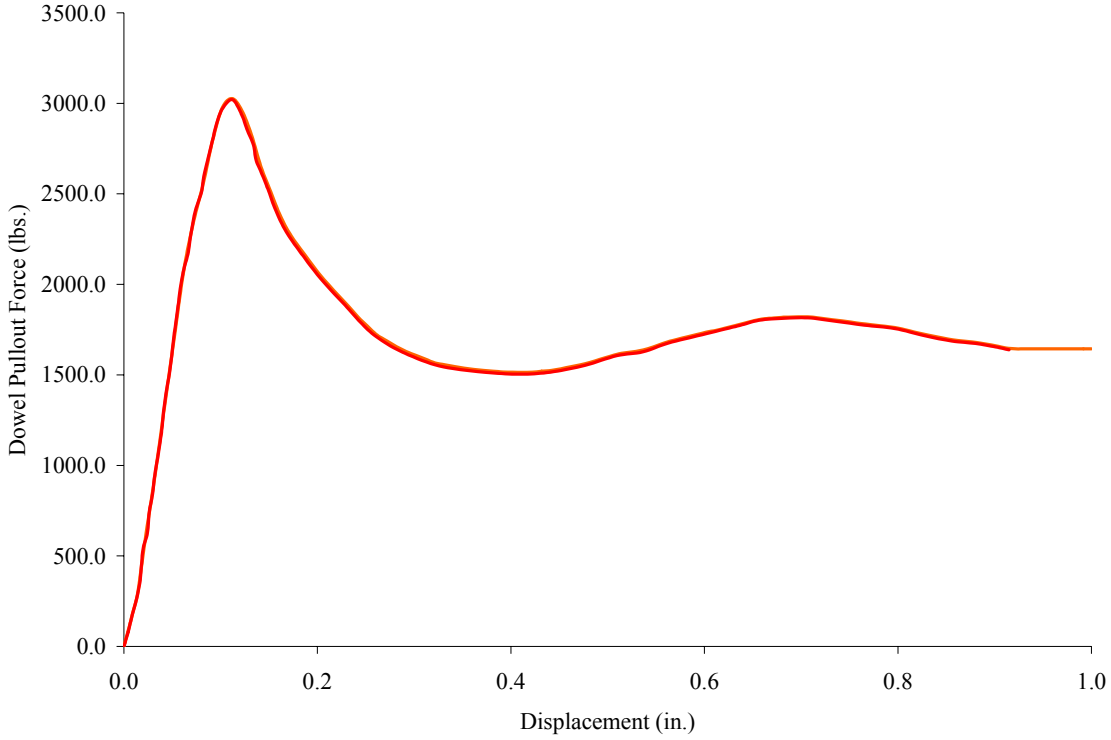

Figure A.3: Dowel Pullout Force vs. displacement for Sample 9

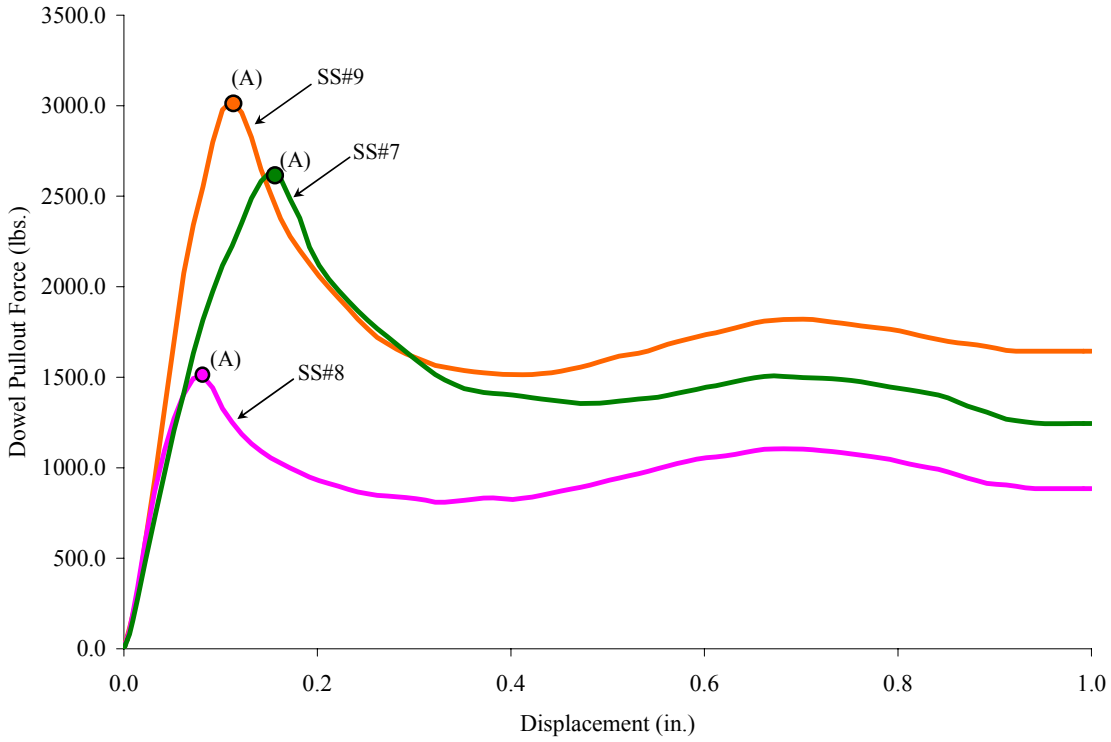

Figure A.4: Dowel Pullout Force vs. displacement for Samples 7, 8 and 9

MMFX STEEL DOWEL BARS

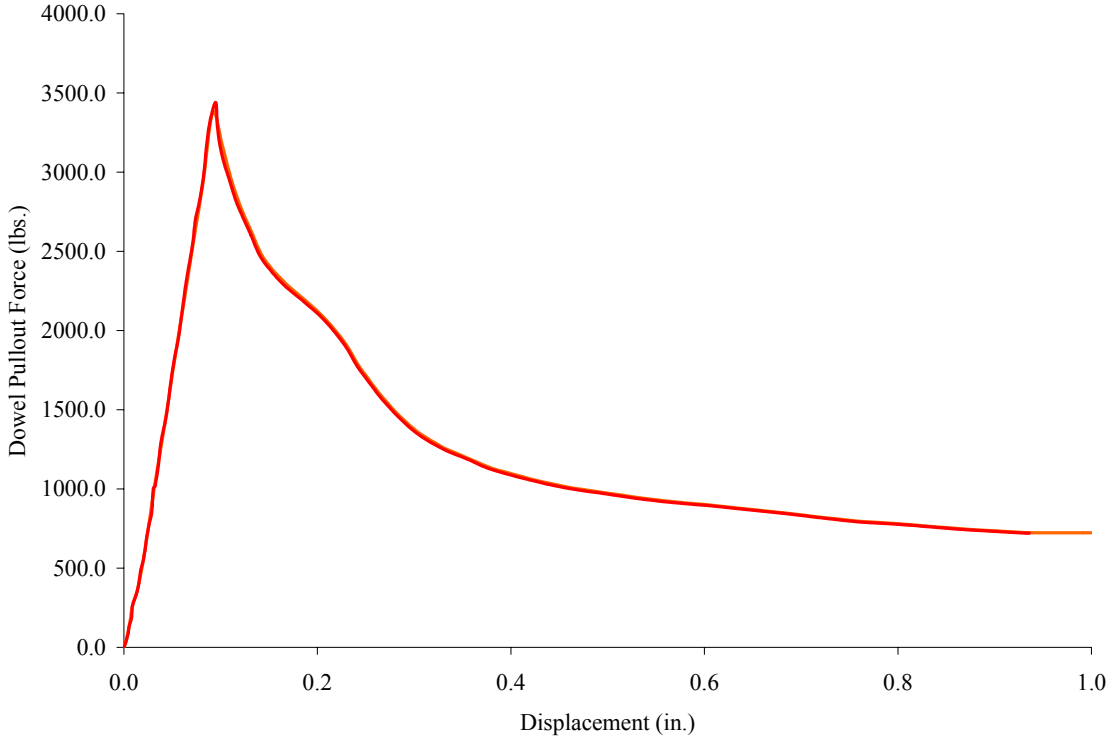

Figure A.5: Dowel Pullout Force vs. displacement for Sample 10

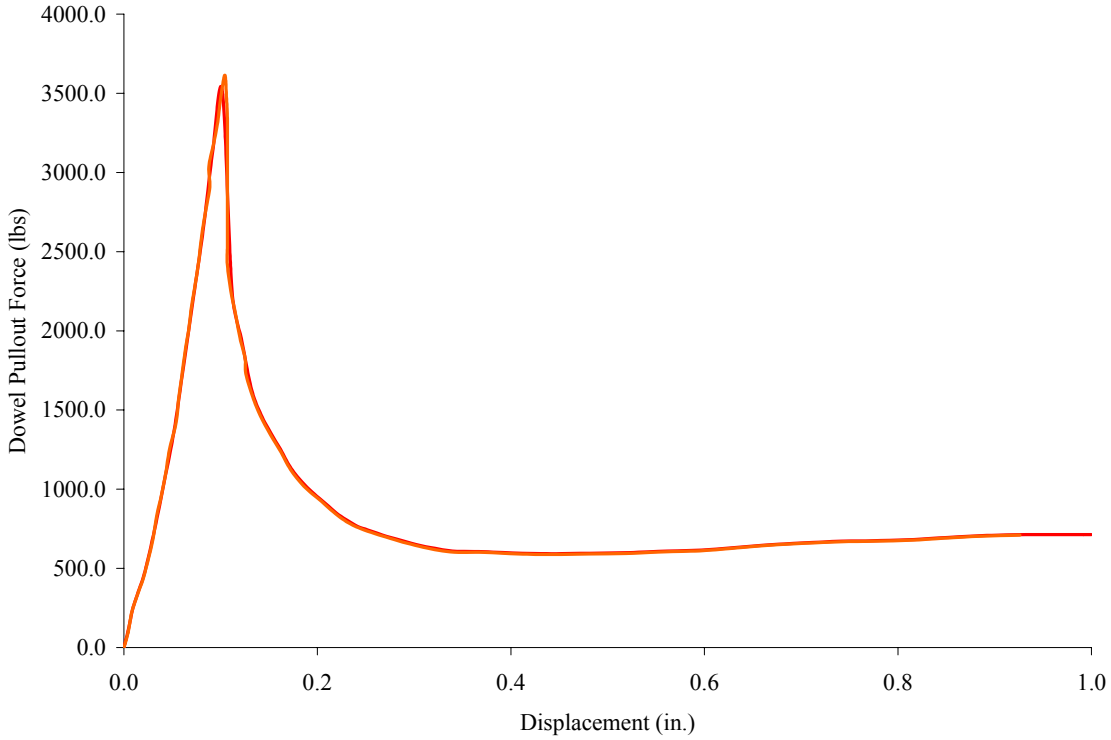

Figure A.6: Dowel Pullout Force vs. displacement for Sample 11

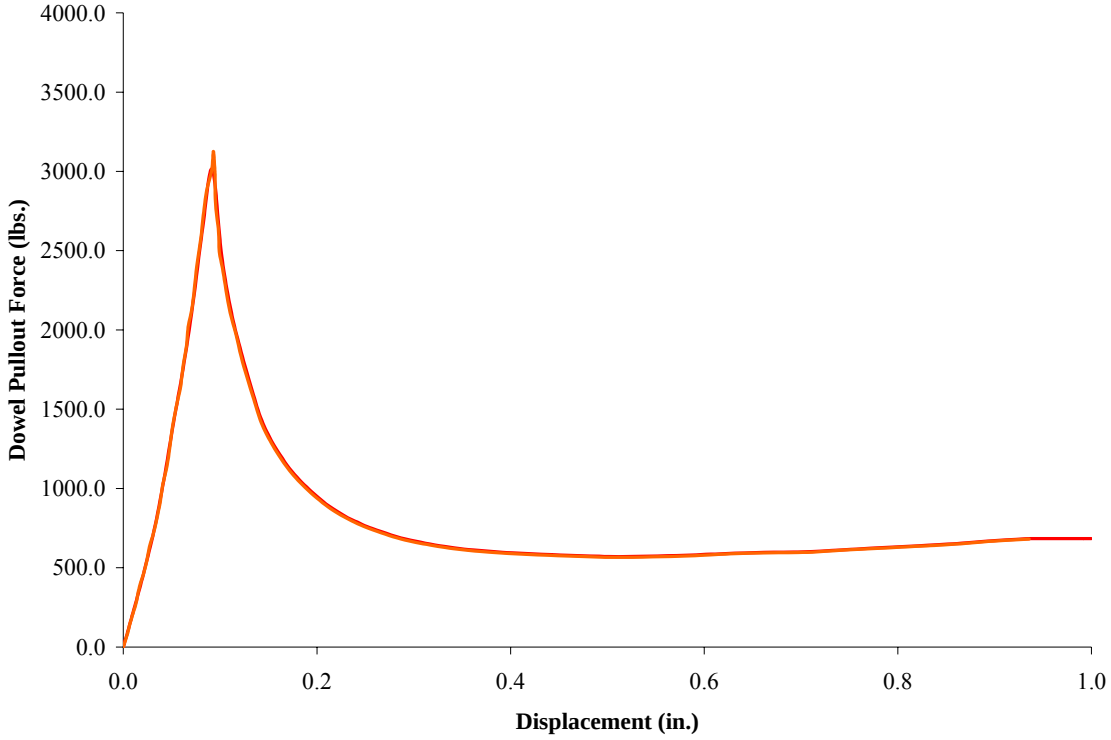

Figure A.7: Dowel Pullout Force vs. displacement for Sample 12

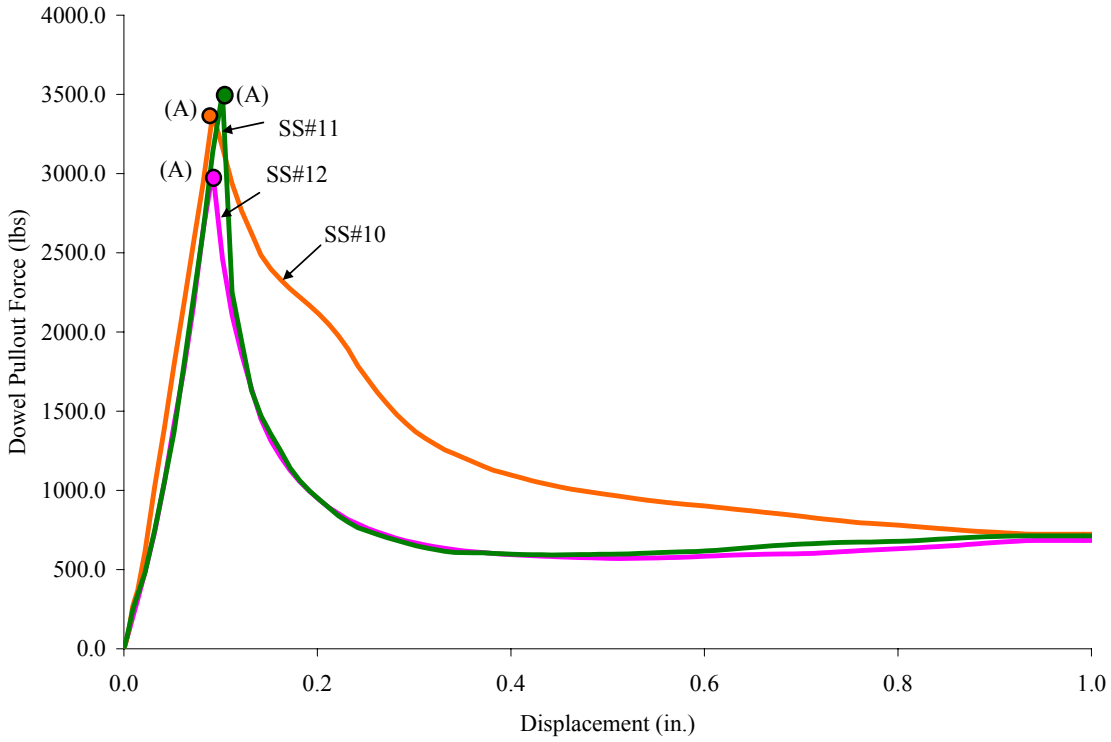

Figure A.8: Dowel Pullout Force vs. displacement for Samples 10, 11 and 12

ZINC CLAD DOWEL BARS

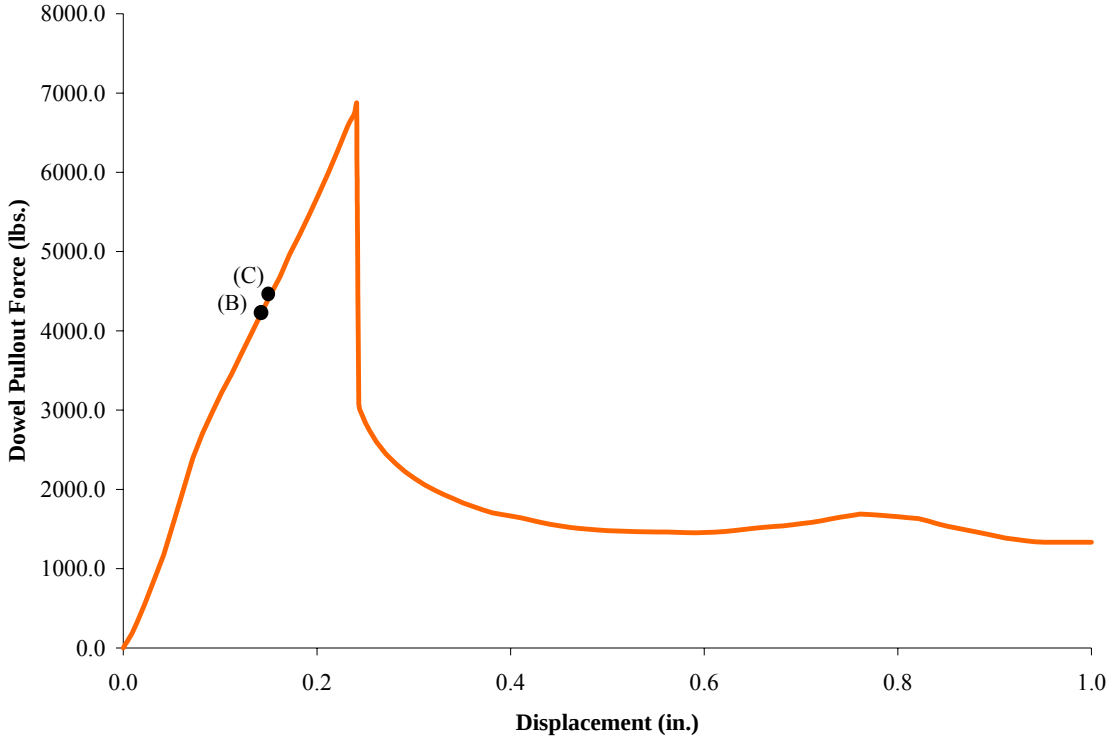

Figure A.9: Dowel Pullout Force vs. displacement for Sample 13

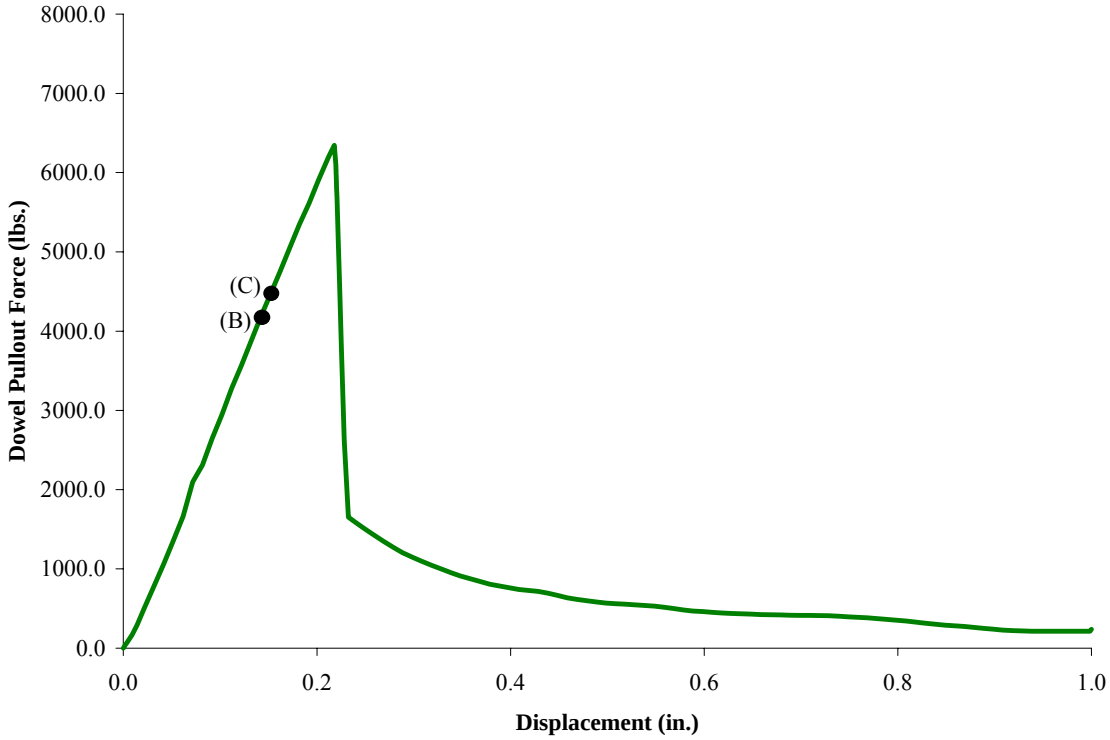

Figure A.10: Dowel Pullout Force vs. displacement for Sample 14

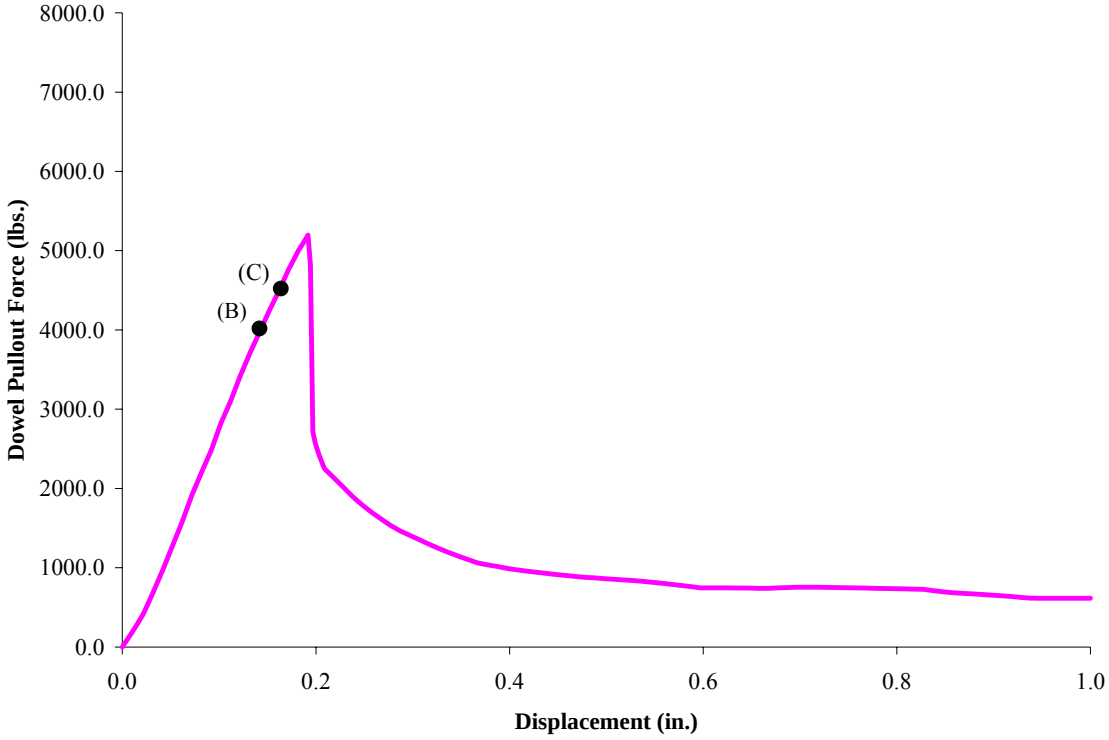

Figure A.11: Dowel Pullout Force vs. displacement for Sample 15

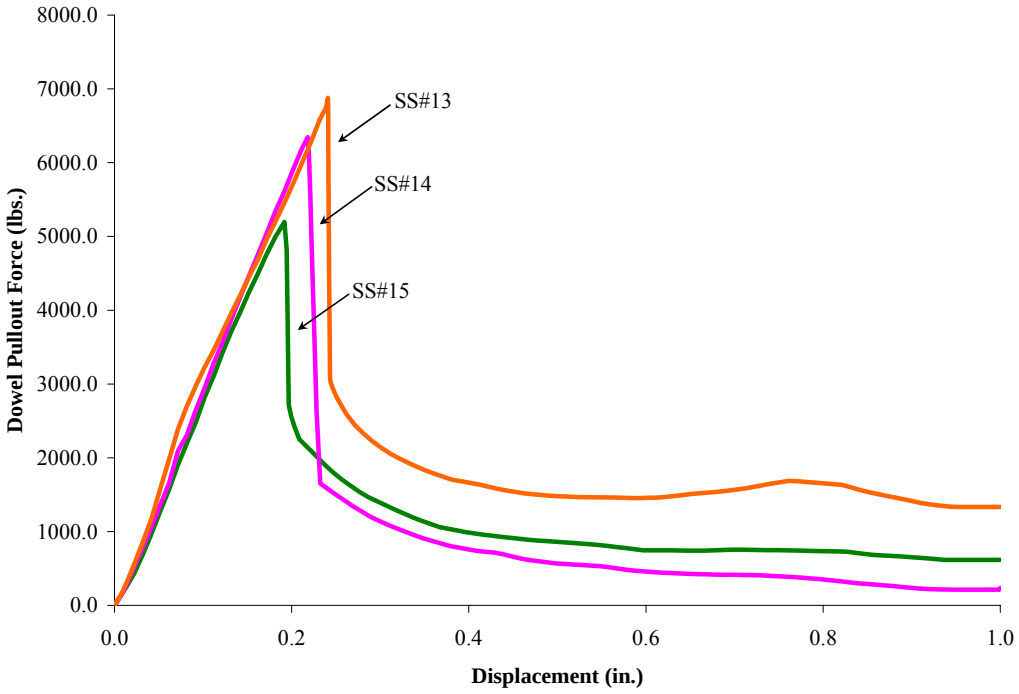

Figure A.12: Dowel Pullout Force vs. displacement for Samples 13, 14 and 15

Note: The material failure / limit states are not shown in Figure C.4 as they overlap each other.

Appendix B

BEHAVIOR OF DIFFERENT DOWEL SPECIMENS

BEHAVIOR OF TECTYL COATED EPOXY SPECIMENS

Table B1: Summary of Results for single aligned dowel bar with average bond – pullout behavior of tectyl coated epoxy specimens 7, 8 and 9

ss7_8_9	At Joint Opening		After Loading	
	Loaded side	Unloaded side	Loaded side	Unloaded side
Smax	188.40	187.70	219.50	235.80
Smin	304.40	297.10	2123.00	1261.00
PEEQ	0.00	0.00	4.01E-04	9.37E-05
PEEQT	0.00	0.00	6.15E-05	1.75E-04

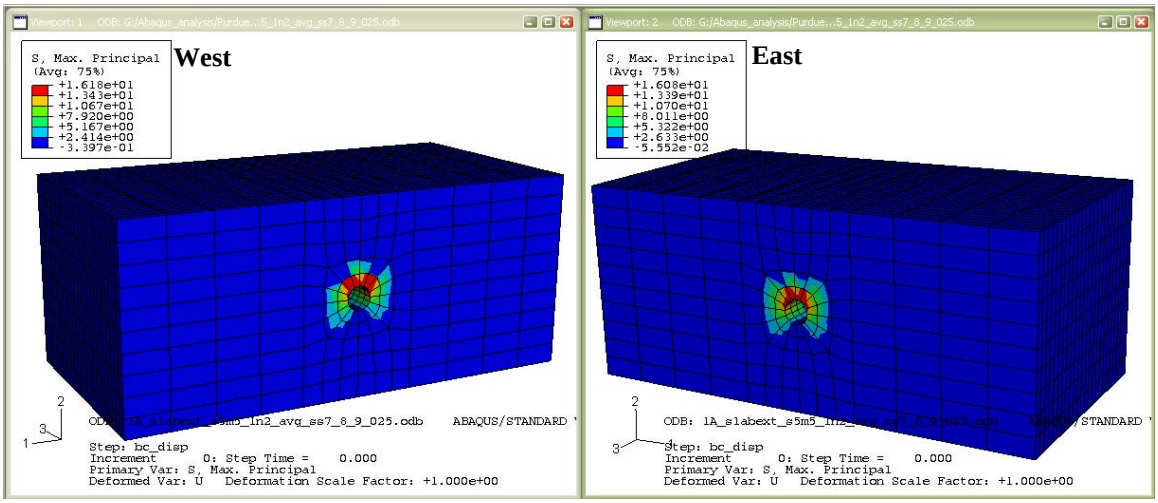

(a) Maximum Tensile Stress at Joint Opening (1/8 in.)

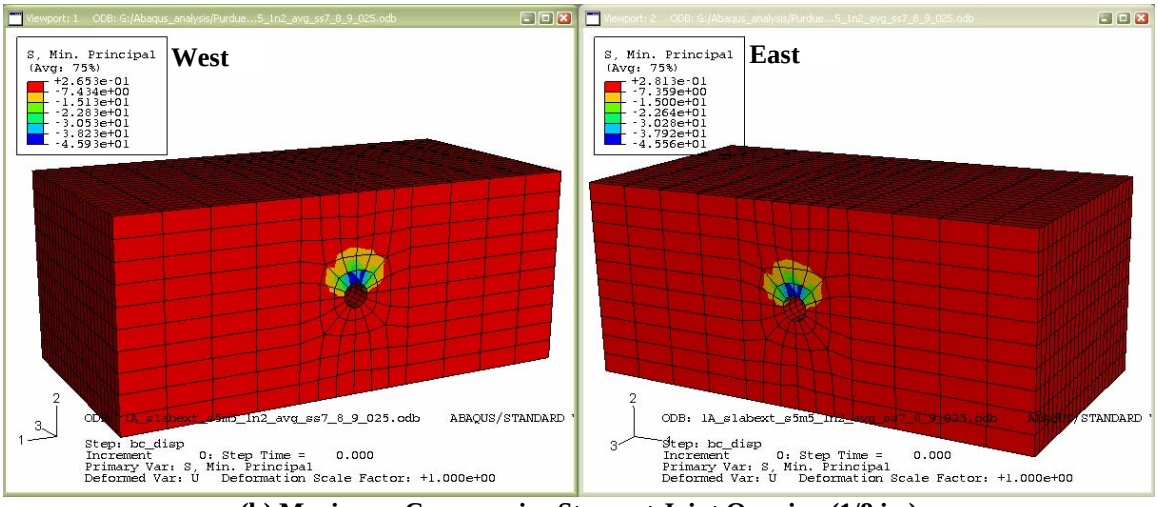

(b) Maximum Compressive Stress at Joint Opening (1/8 in.)

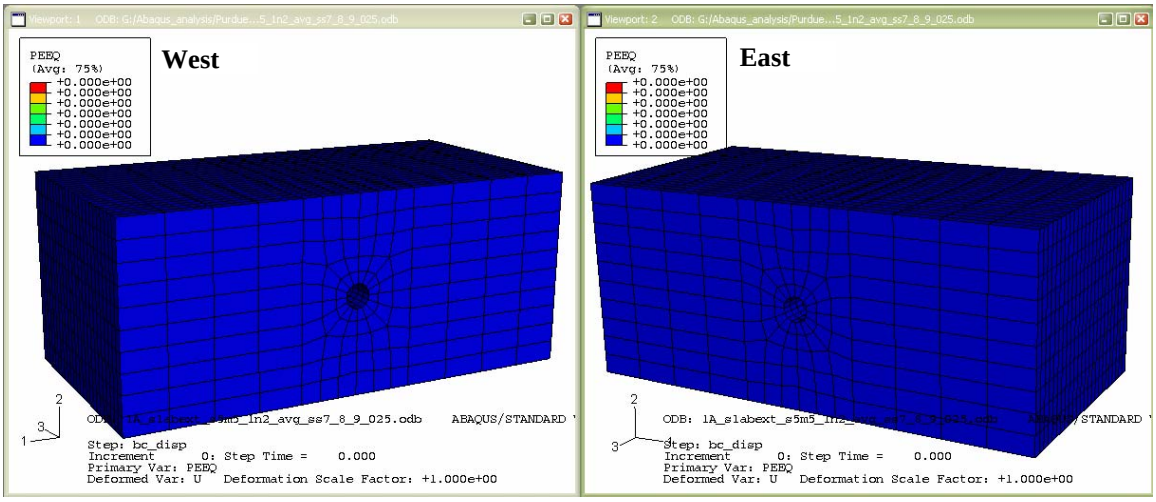

(c) Inelastic Compressive Strains at Joint Opening (1/8 in.)

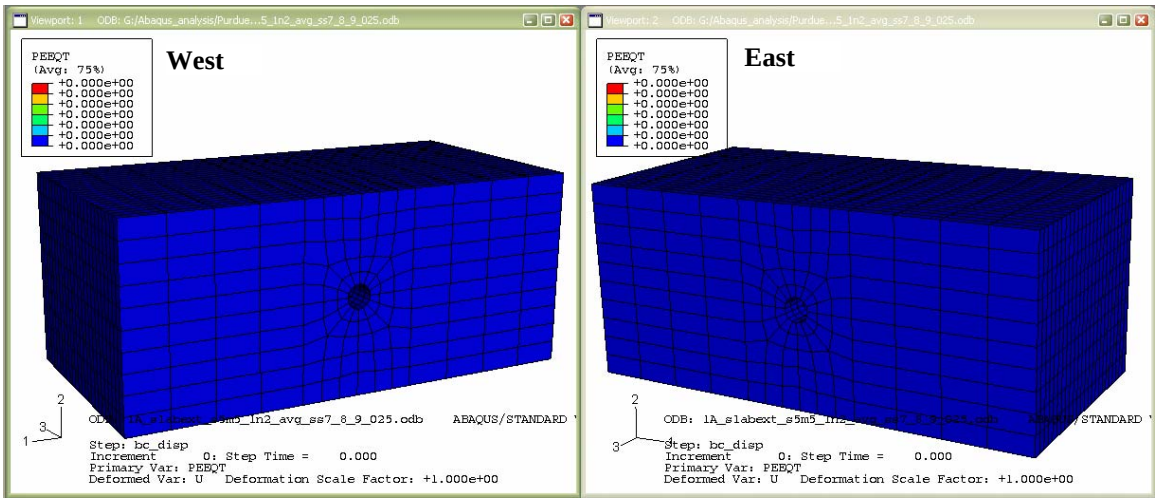

(d) Inelastic Tensile Strains at Joint Opening (1/8 in.)

Figure B1: Stresses and Strains for a single aligned dowel bar calibrated using the average bond – displacement behavior of specimens 7, 8 and 9 at 1/8 in joint opening

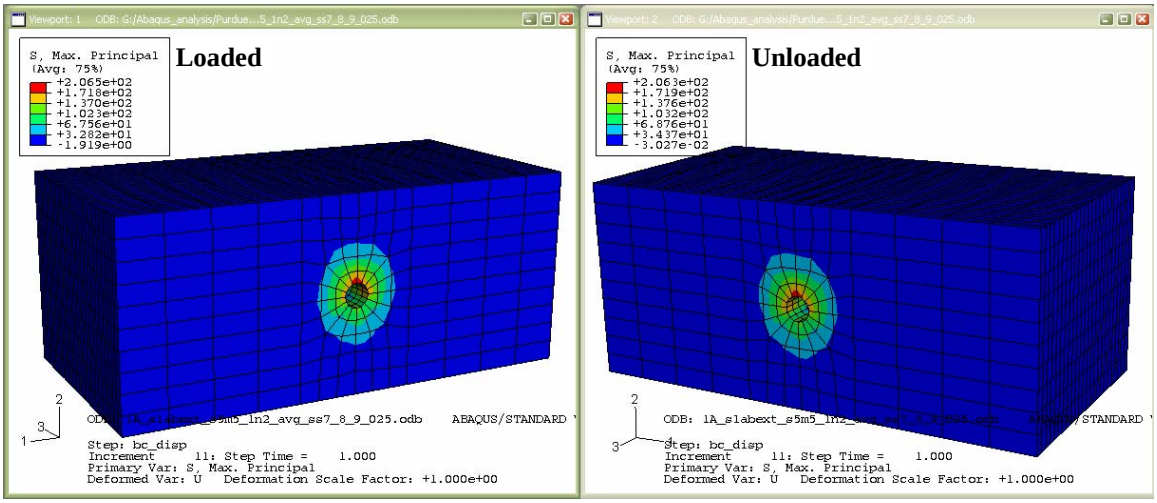

(a) Maximum Tensile Stresses at end of load application

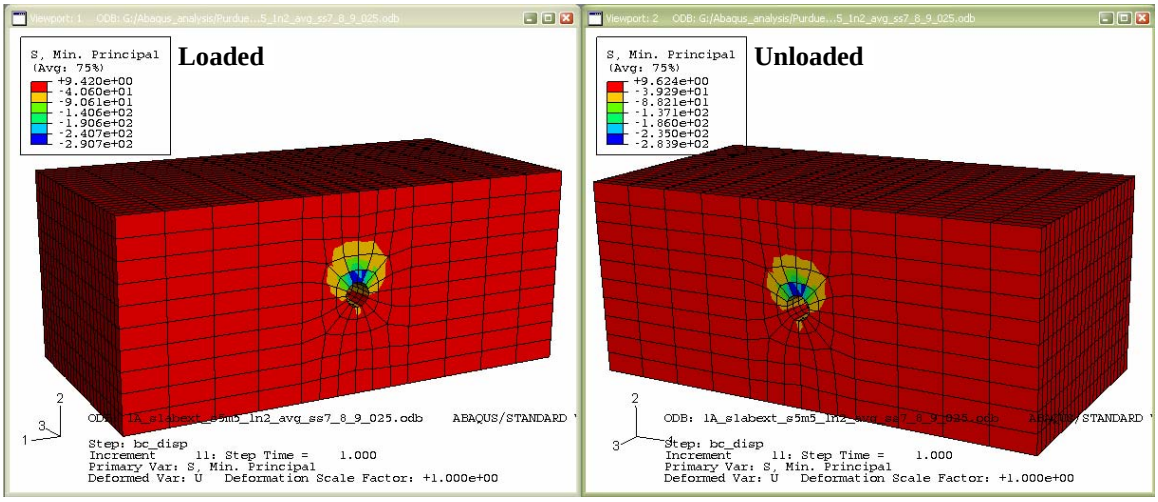

(b) Maximum Compressive Stresses at end of load application

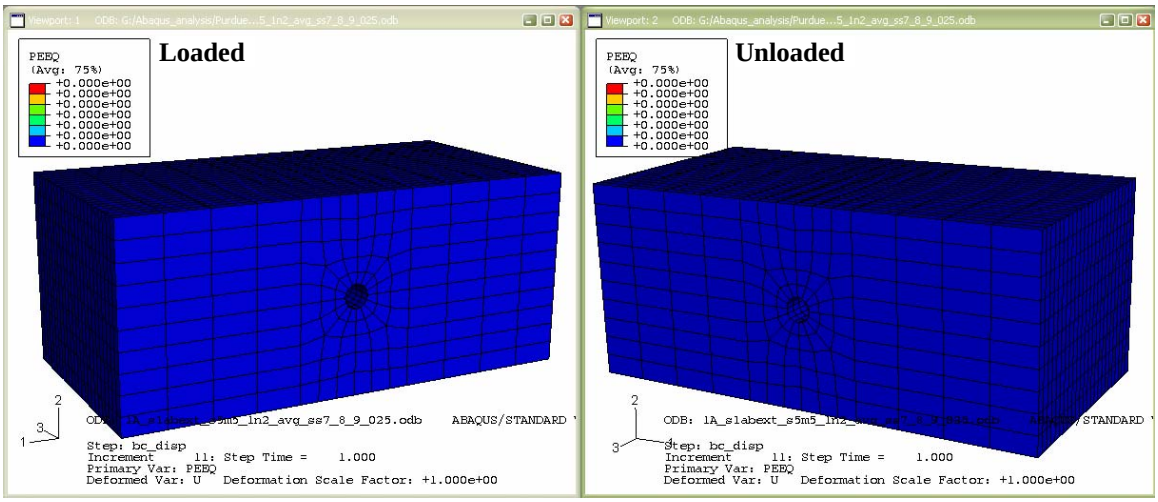

(c) Inelastic Compressive Strains at end of load application

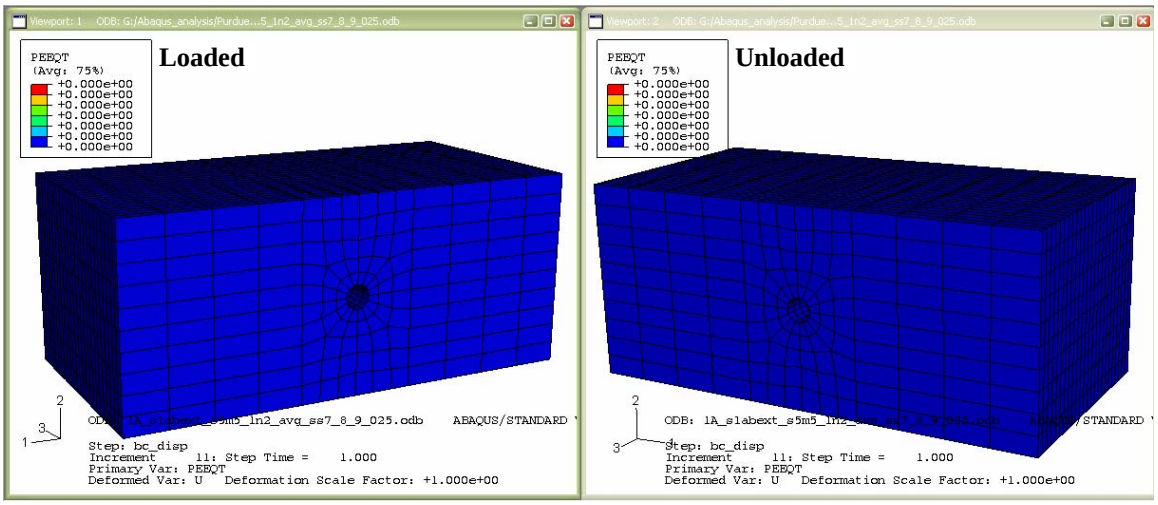

(d) Inelastic Tensile Strains at end of load application

Figure B2: Stresses and Strains for a single aligned dowel bar calibrated using the average bond – displacement behavior of specimens 7, 8 and 9 at end of load application

Table B2: Summary of Results for three aligned dowel bar with average bond – pullout behavior of tectyl coated epoxy specimens 7, 8 and 9

ss7_8_9	At Joint Opening		After Loading	
	Loaded side	Unloaded side	Loaded side	Unloaded side
Smax	189.70	186.20	176.20	140.20
Smin	244.90	244.30	883.80	284.80
PEEQ	0.00	0.00	5.23E-05	0.00E+00
PEEQT	0.00	0.00	9.65E-06	0.00E+00

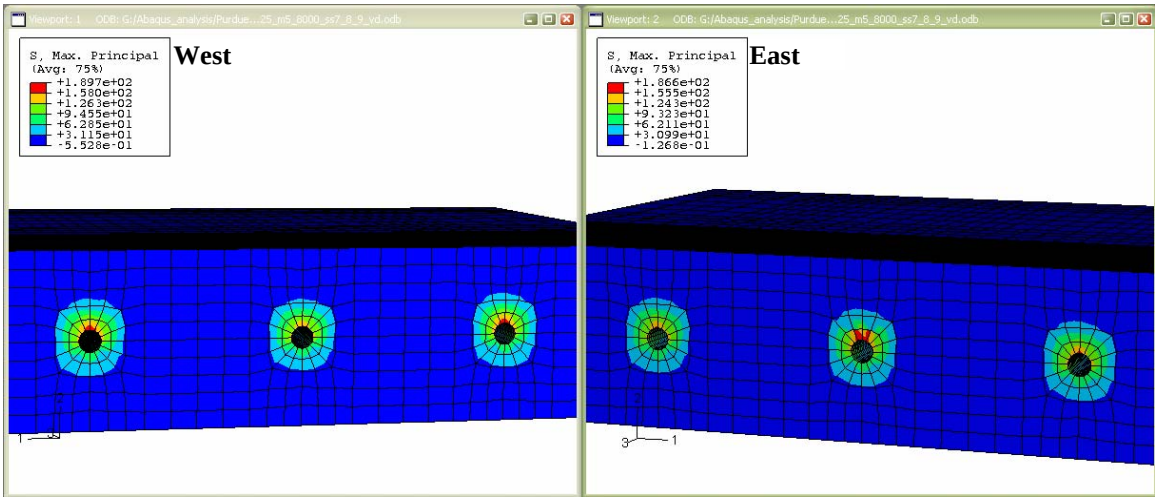

(a) Maximum Tensile Stress at Joint Opening (1/8 in.)

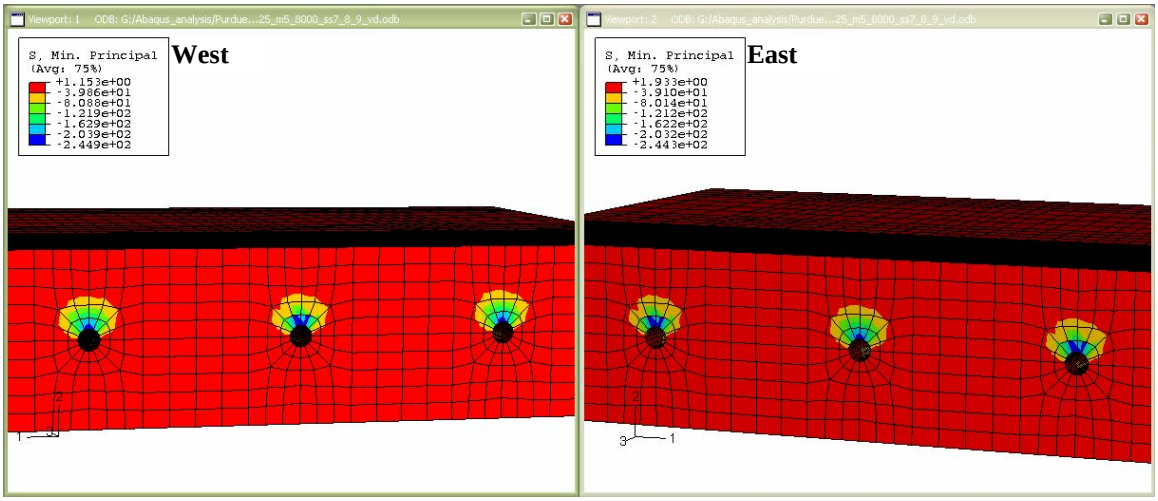

(b) Maximum Compressive Stress at Joint Opening (1/8 in.)

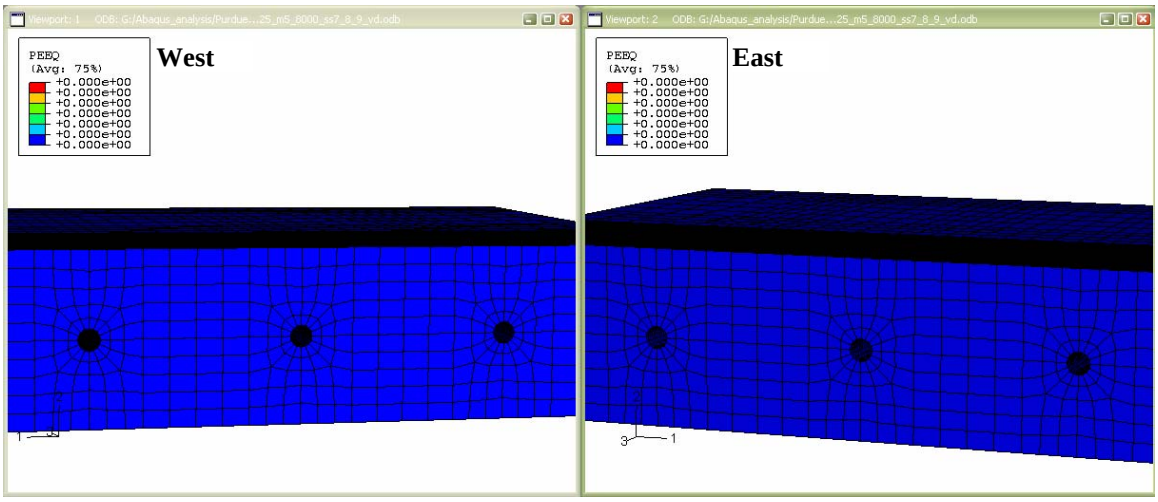

(c) Inelastic Compressive Strains at Joint Opening (1/8 in.)

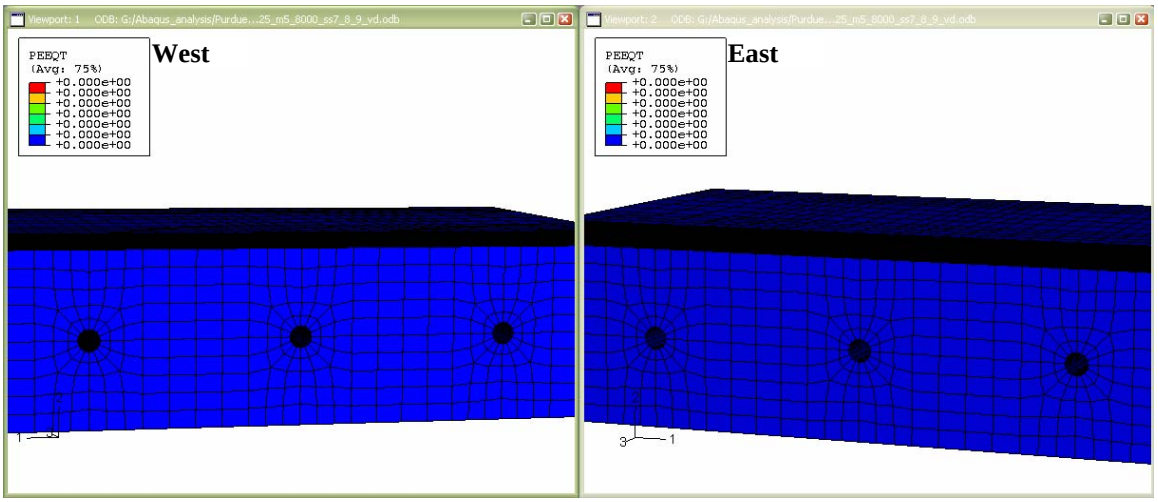

(d) Inelastic Tensile Strains at Joint Opening (1/8 in.)

Figure B3: Stresses and Strains for three aligned dowel bars calibrated using the average bond – displacement behavior of specimens 7, 8 and 9 at 1/8 in joint opening

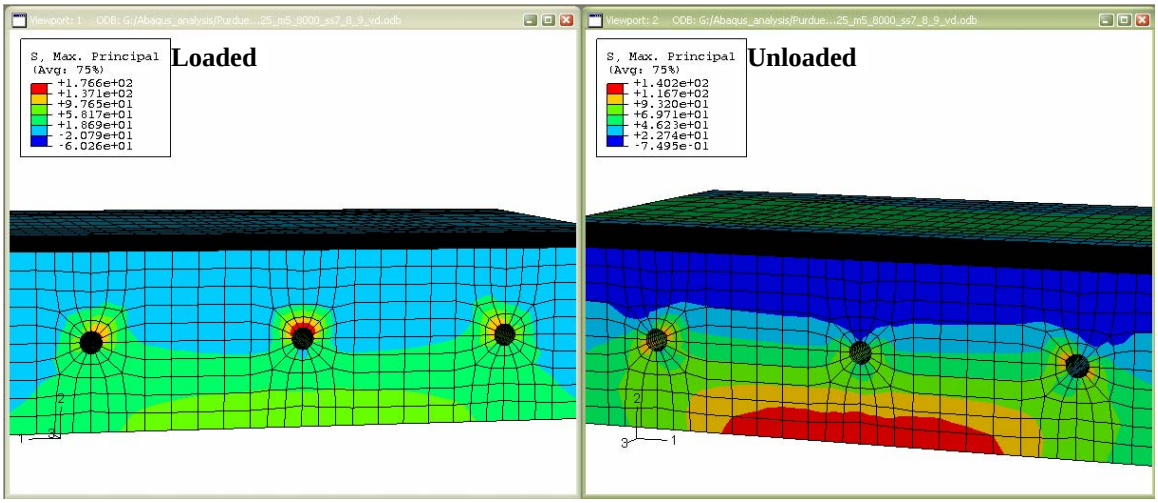

(a) Maximum Tensile Stresses at end of load application

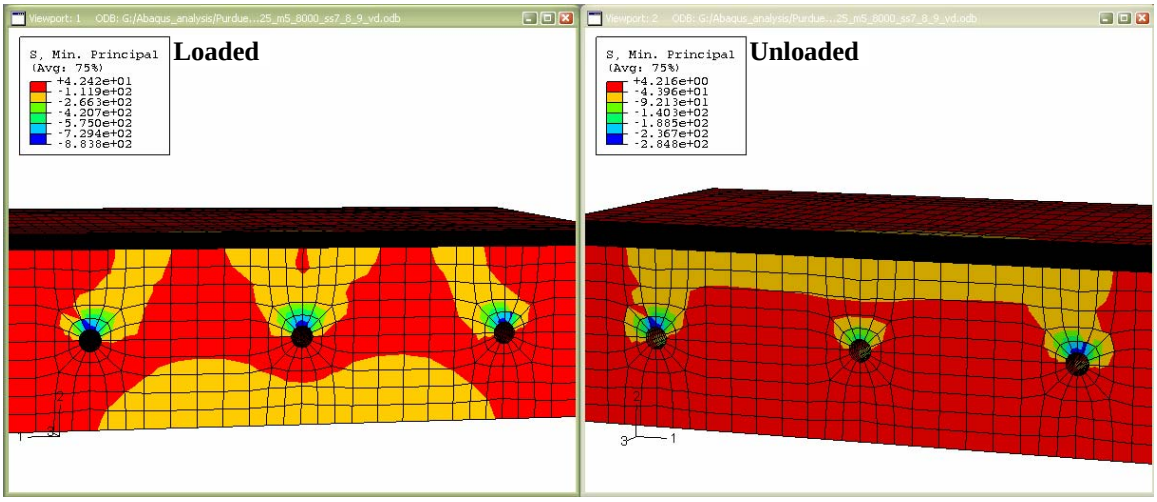

(b) Maximum Compressive Stresses at end of load application

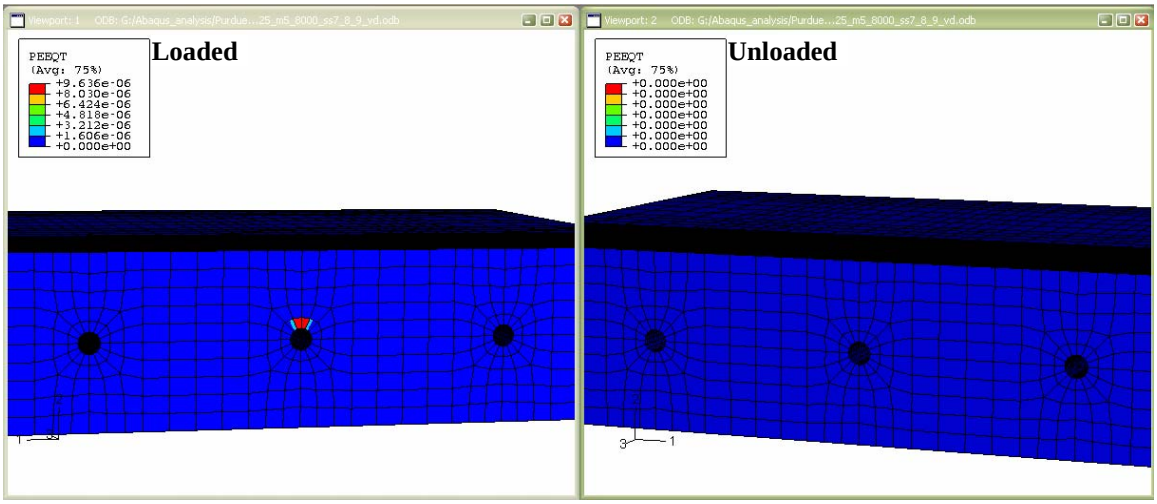

(c) Inelastic Compressive Strains at end of load application

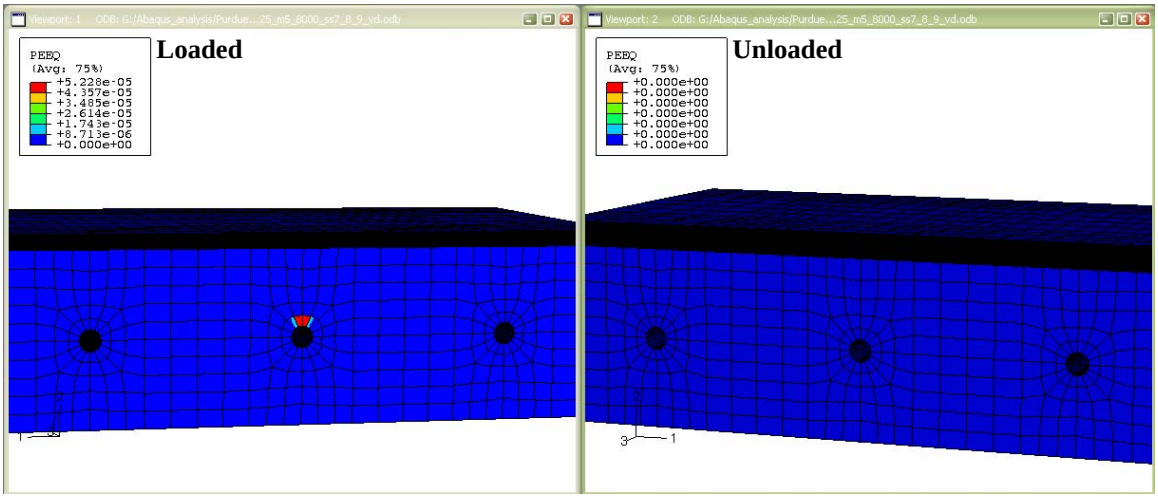

(d) Inelastic Tensile Strains at end of load application

Figure B4: Stresses and Strains for a single aligned dowel bar calibrated using the average bond – displacement behavior of specimens 7, 8 and 9 at end of load application

BEHAVIOR OF MMFX STEEL SPECIMENS

Table B3: Summary of Results for single dowel bar with average bond – pullout behavior of MMFX steel specimens 10, 11 and 12

ss10_11_12	At Joint Opening		After Loading	
	Loaded side	Unloaded side	Loaded side	Unloaded side
Smax	200.70	200.40	219.50	235.90
Smin	303.00	296.00	2123.00	1261.00
PEEQ	0.00	0.00	4.00E-04	9.32E-05
PEEQT	0.00	0.00	6.14E-05	1.75E-04

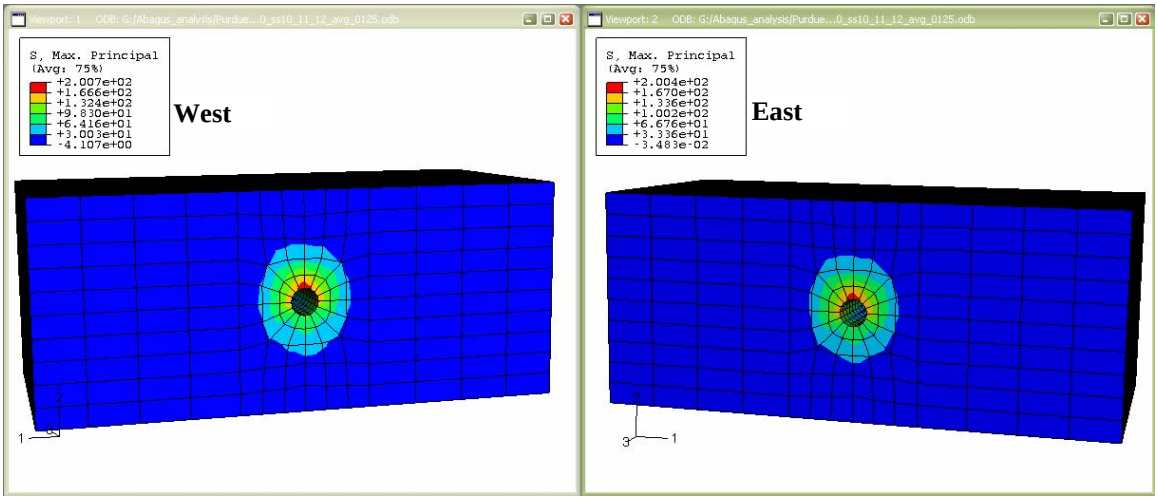

(a) Maximum Tensile Stress at Joint Opening (1/8 in.)

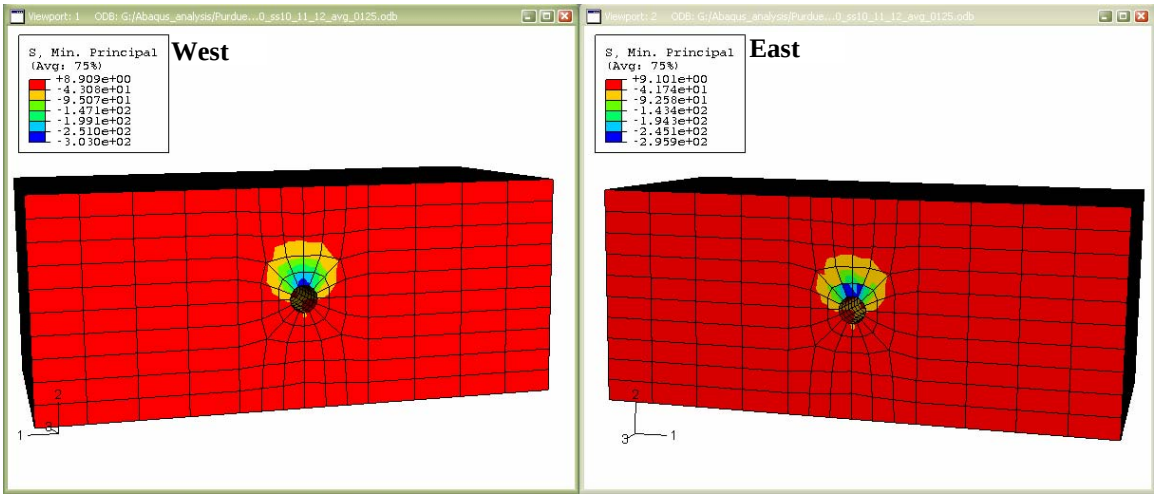

(b) Maximum Compressive Stress at Joint Opening (1/8 in.)

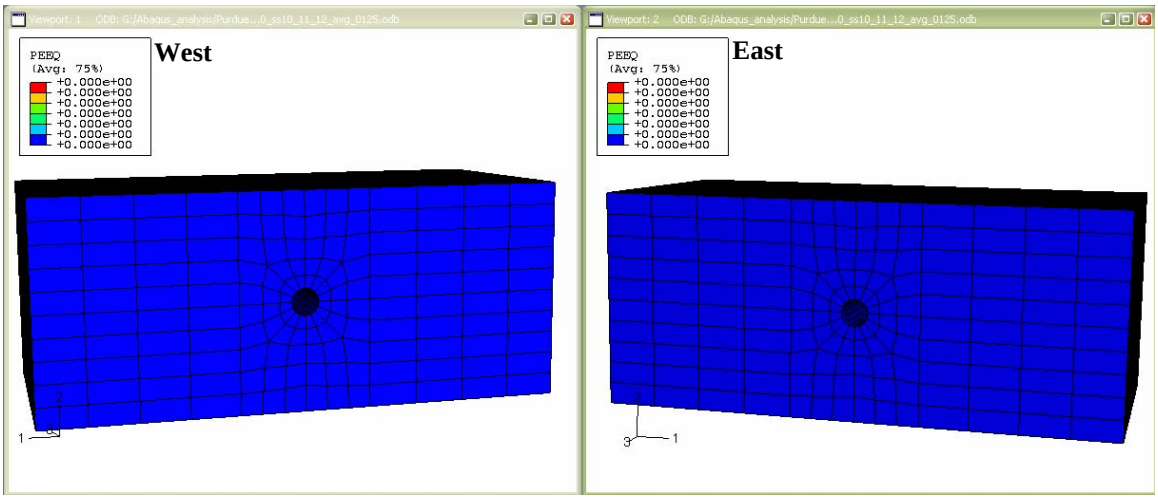

(c) Inelastic Compressive Strains at Joint Opening (1/8 in.)

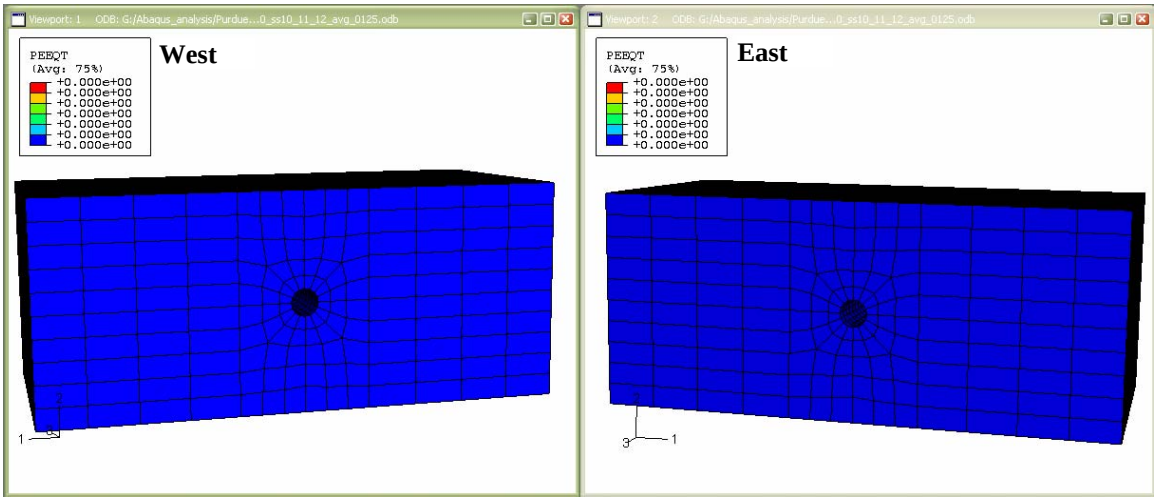

(d) Inelastic Tensile Strains at Joint Opening (1/8 in.)

Figure B5: Stresses and Strains for a single aligned dowel bar calibrated using the average bond – displacement behavior of specimens 10, 11 and 12 at 1/8 in joint opening

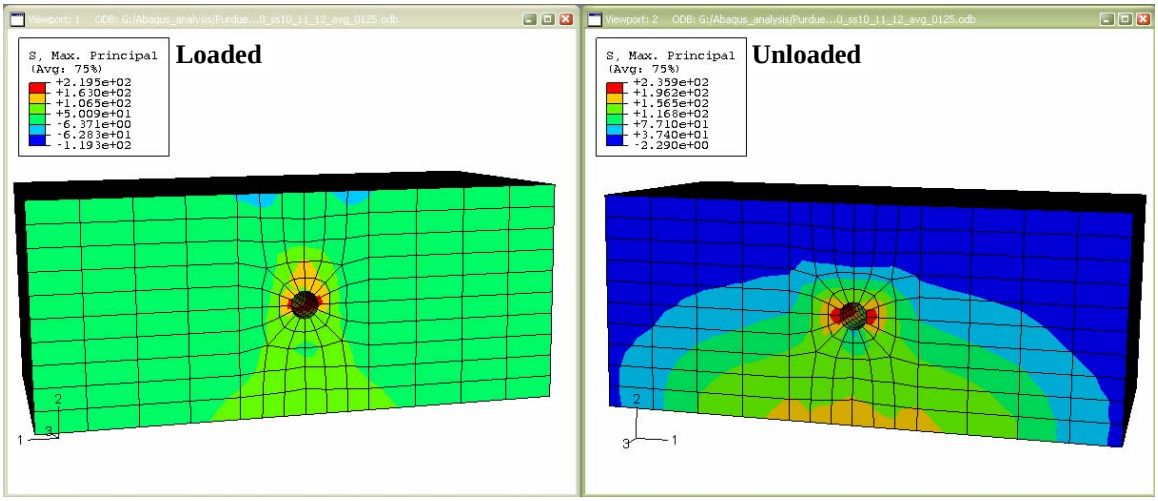

(a) Maximum Tensile Stresses at end of load application

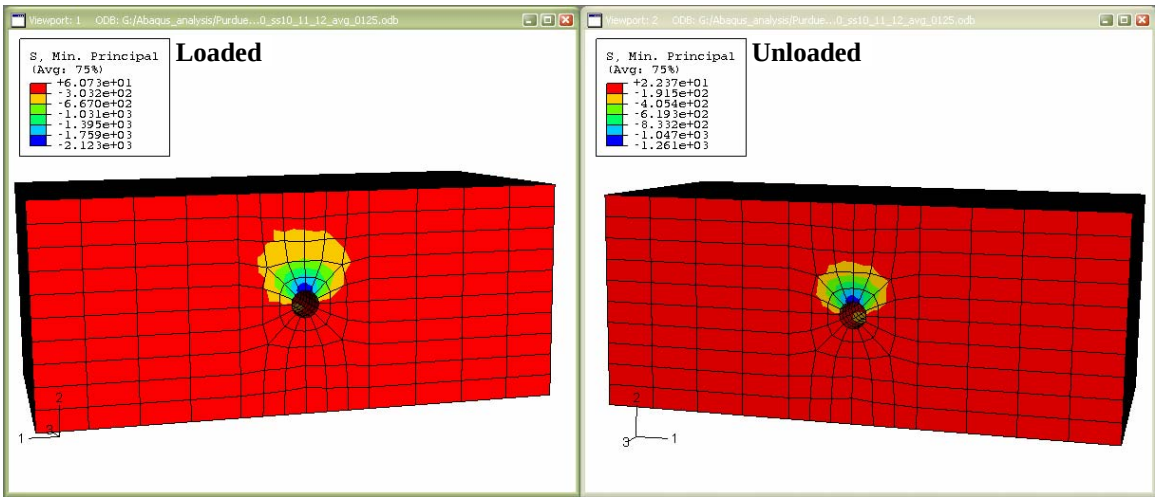

(b) Maximum Compressive Stresses at end of load application

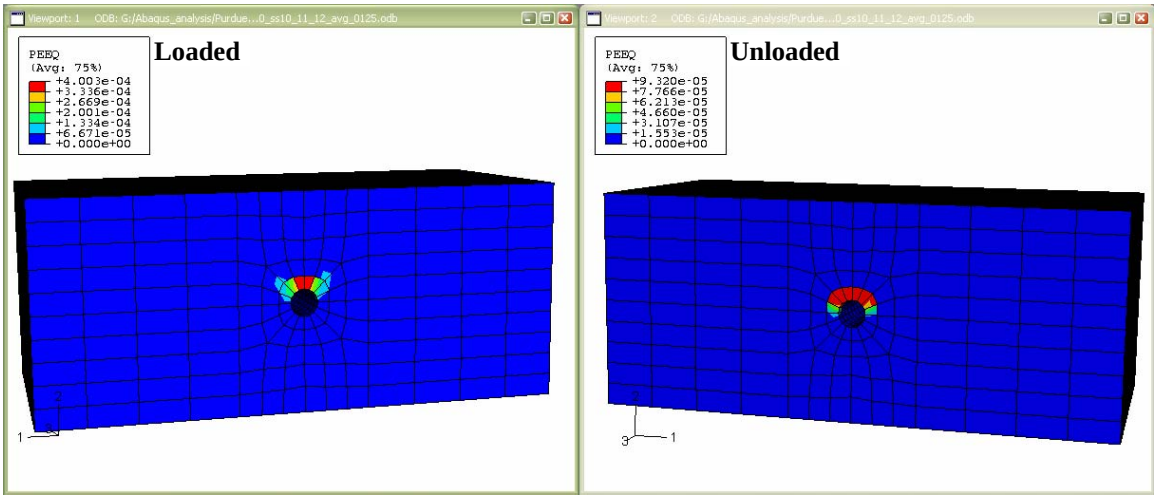

(c) Inelastic Compressive Strains at end of load application

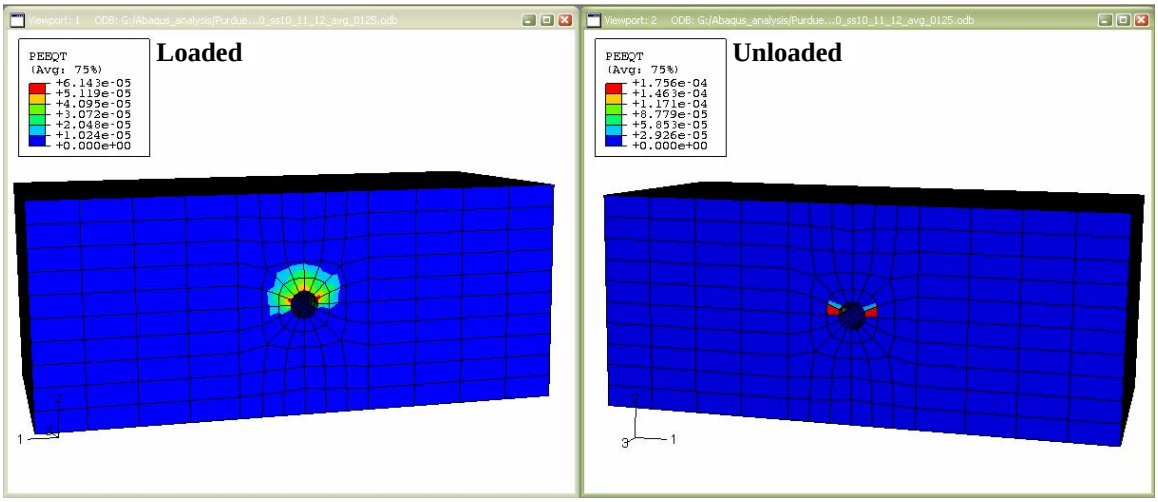

(d) Inelastic Tensile Strains at end of load application

Figure B6: Stresses and Strains for a single aligned dowel bar calibrated using the average bond – displacement behavior of specimens 10, 11 and 12 at end of load application

Table B4: Summary of Results for three aligned dowel bar with average bond – pullout behavior of MMFX Steel specimens 10, 11 and 12

ss10_11_12	At Joint Opening		After Loading	
	Loaded side	Unloaded side	Loaded side	Unloaded side
Smax	200.90	197.80	176.60	140.40
Smin	240.40	240.10	884.00	306.00
PEEQ	0.00	0.00	5.23E-05	0.00E+00
PEEQT	0.00	0.00	9.65E-06	0.00E+00

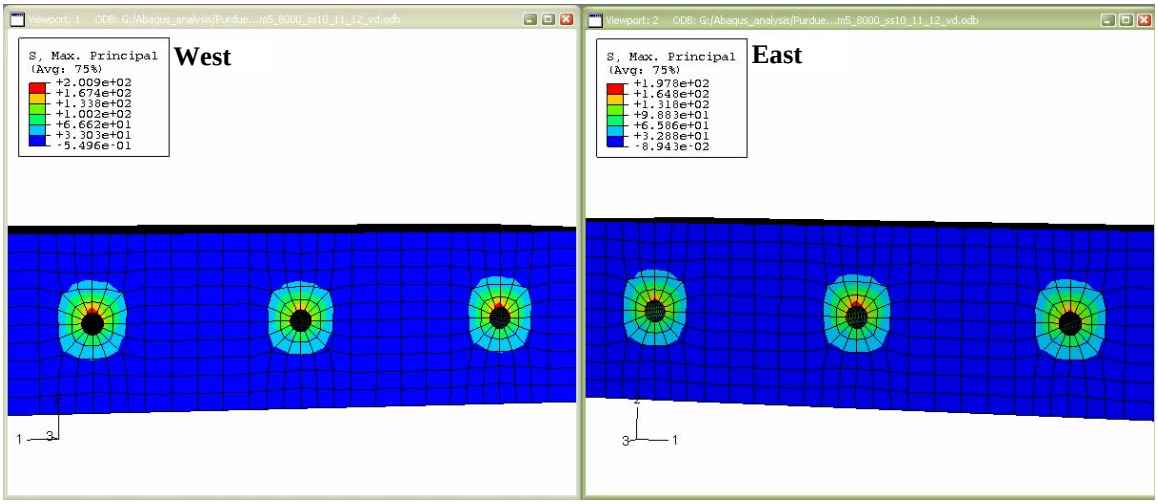

(a) Maximum Tensile Stress at Joint Opening (1/8 in.)

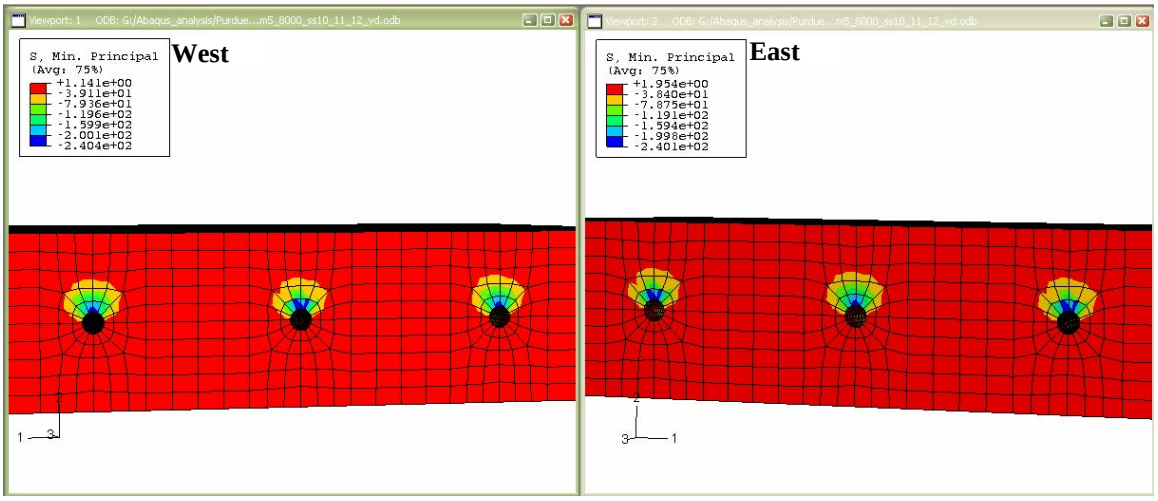

(b) Maximum Compressive Stress at Joint Opening (1/8 in.)

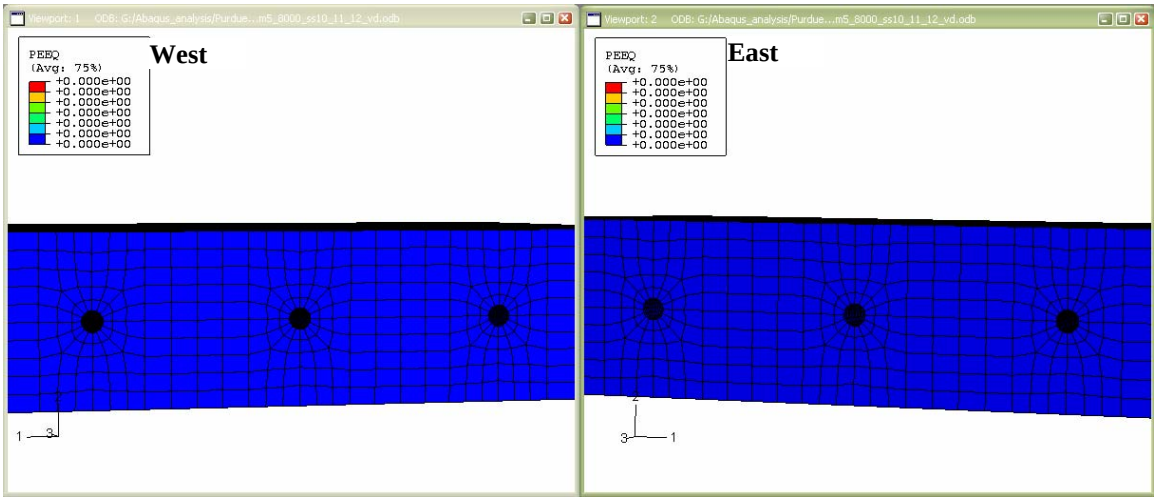

(c) Inelastic Compressive Strains at Joint Opening (1/8 in.)

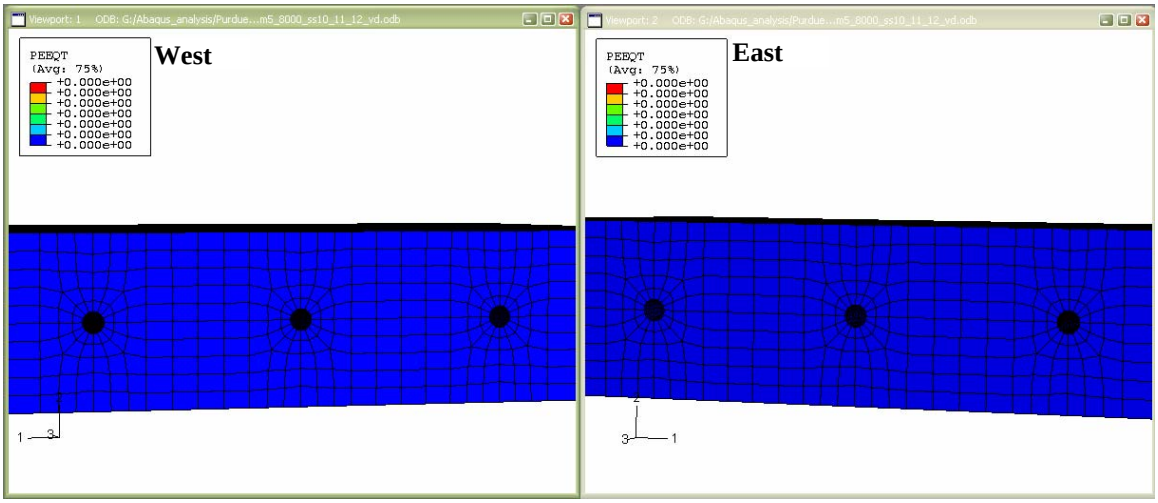

(d) Inelastic Tensile Strains at Joint Opening (1/8 in.)

Figure B7: Stresses and Strains for three aligned dowel bars calibrated using the average bond – displacement behavior of specimens 10, 11 and 12 at 1/8 in joint opening

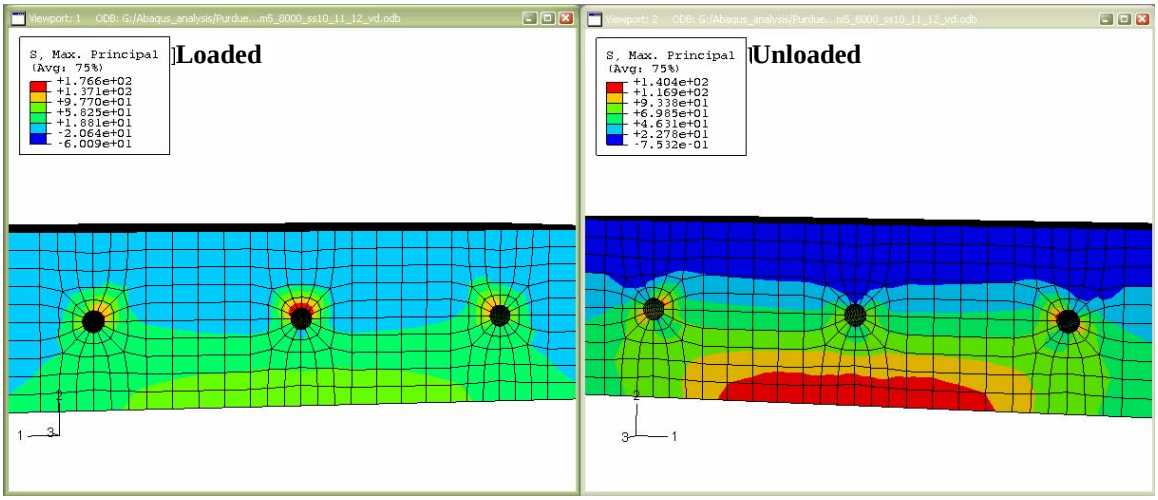

(a) Maximum Tensile Stresses at end of load application

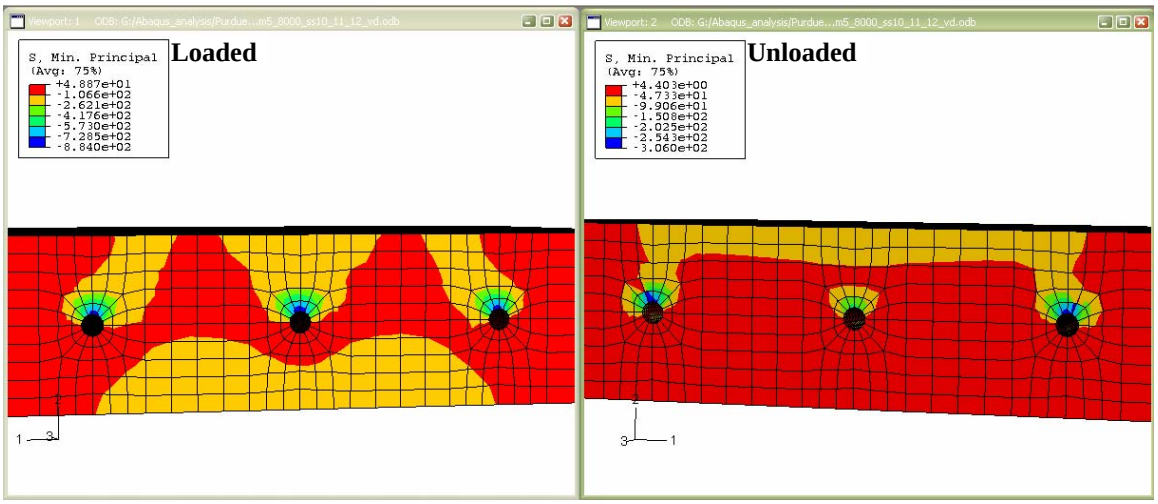

(b) Maximum Compressive Stresses at end of load application

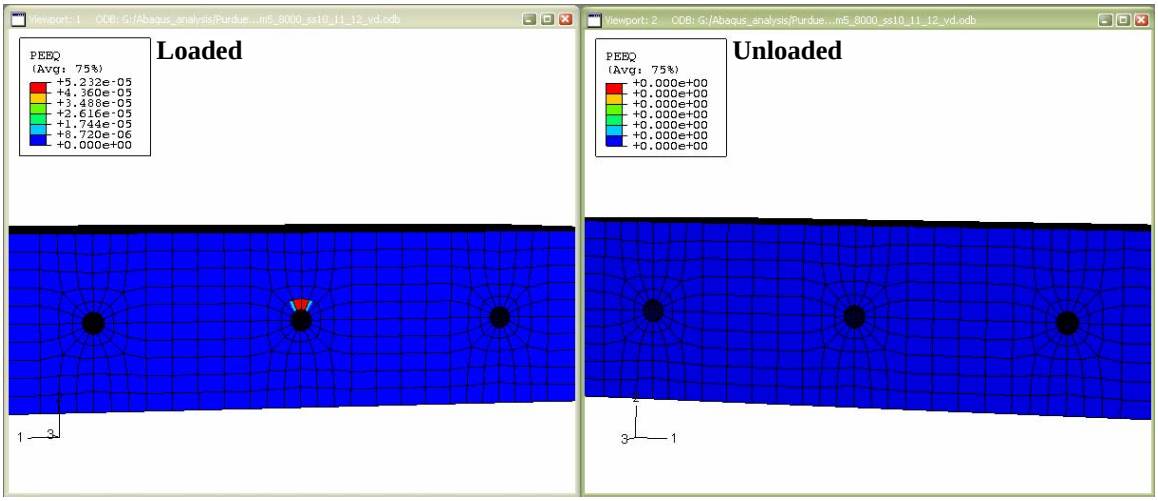

(c) Inelastic Compressive Strains at end of load application

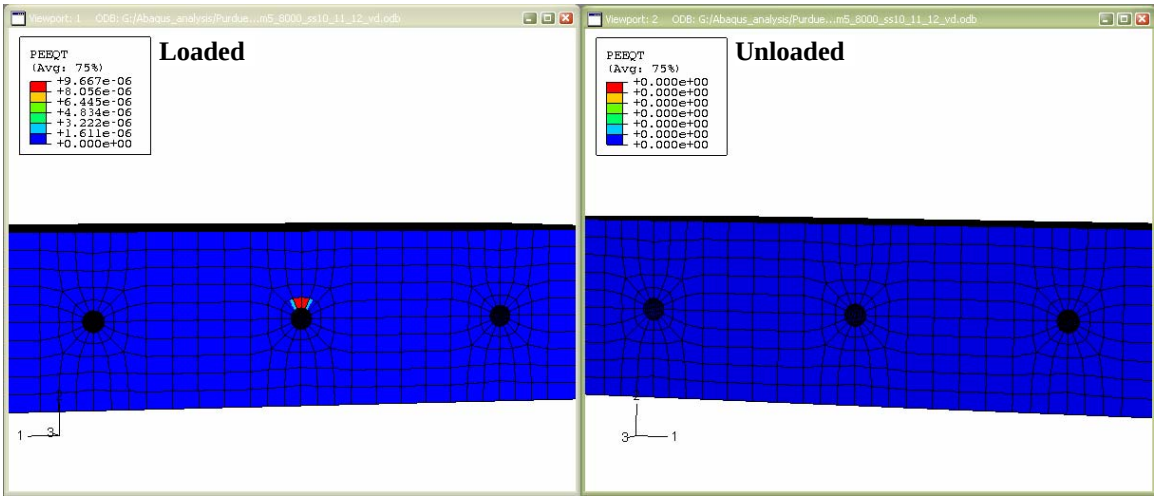

(d) Inelastic Tensile Strains at end of load application

Figure B8: Stresses and Strains for three dowel bars calibrated using the average bond – displacement behavior of specimens 10, 11 and 12 at end of load application

BEHAVIOR OF ZINC CLAD DOWEL SPECIMENS

Table B5: Summary of Results for single dowel bar with average bond – pullout behavior of Zinc Clad dowel specimens 13, 14 and 15

ss13_14_15	At Joint Opening		After Loading	
	Loaded side	Unloaded side	Loaded side	Unloaded side
Smax	194.10	193.60	219.50	235.80
Smin	303.70	296.50	2123.00	1261.00
PEEQ	0.00	0.00	4.01E-04	9.40E-05
PEEQT	0.00	0.00	6.13E-05	1.74E-04

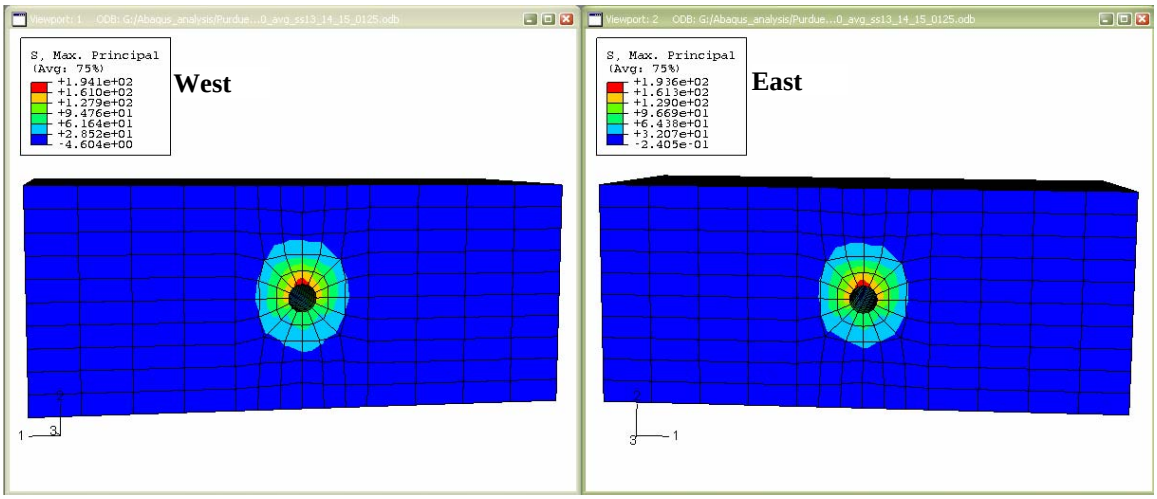

(a) Maximum Tensile Stress at Joint Opening (1/8 in.)

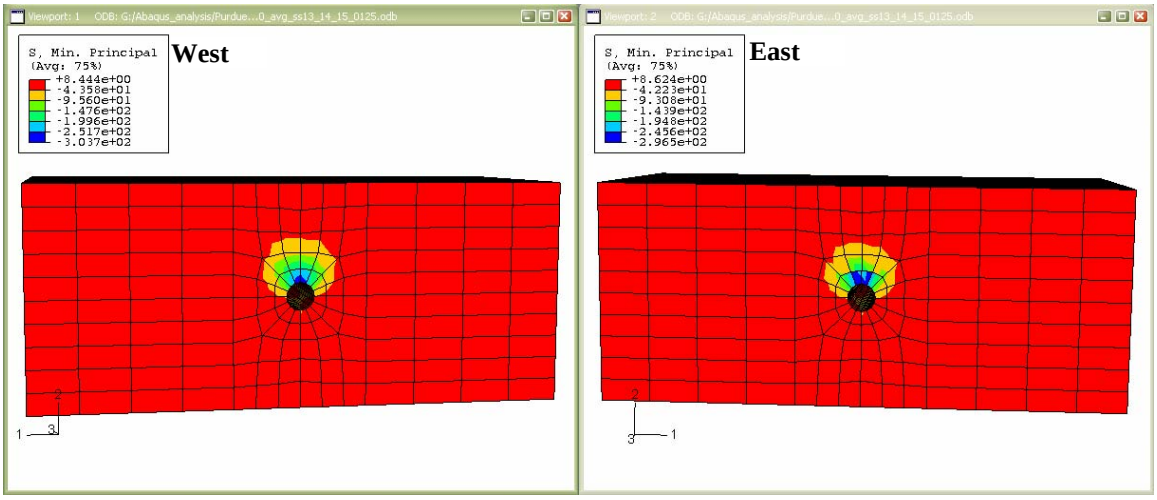

(b) Maximum Compressive Stress at Joint Opening (1/8 in.)

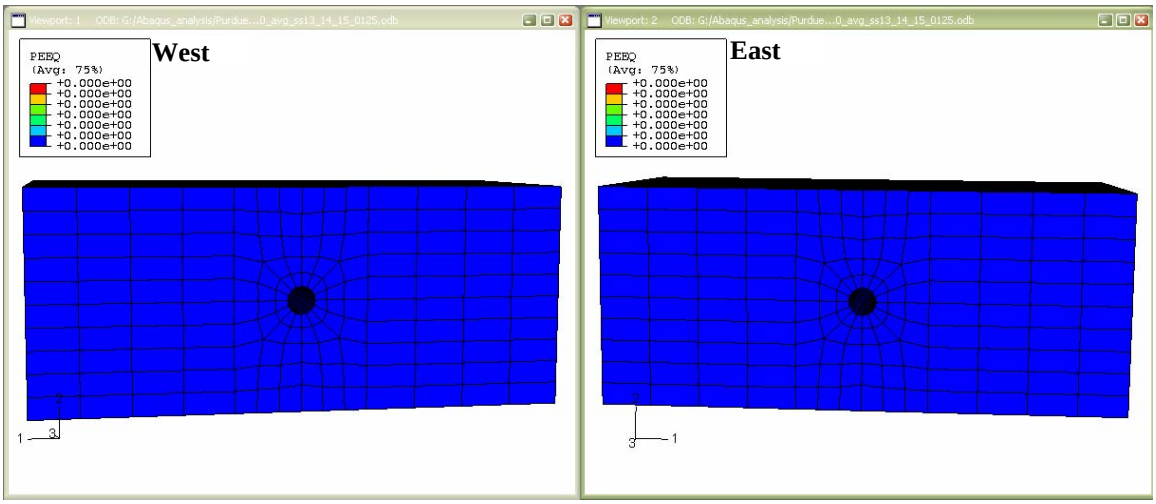

(c) Inelastic Compressive Strains at Joint Opening (1/8 in.)

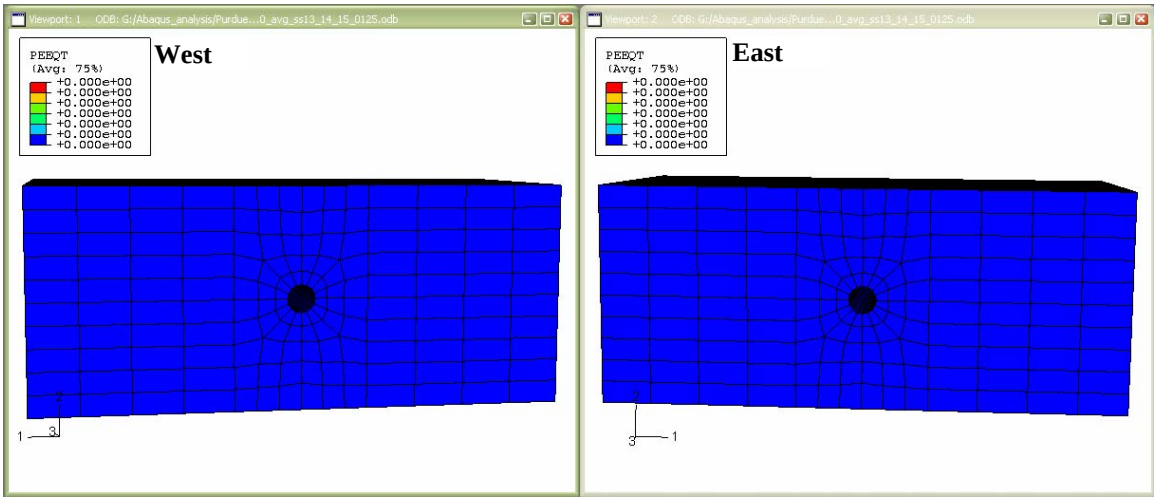

(d) Inelastic Tensile Strains at Joint Opening (1/8 in.)

Figure B9: Stresses and Strains for three aligned dowel bars calibrated using the average bond – displacement behavior of specimens 13, 14 and 15 at 1/8 in joint opening

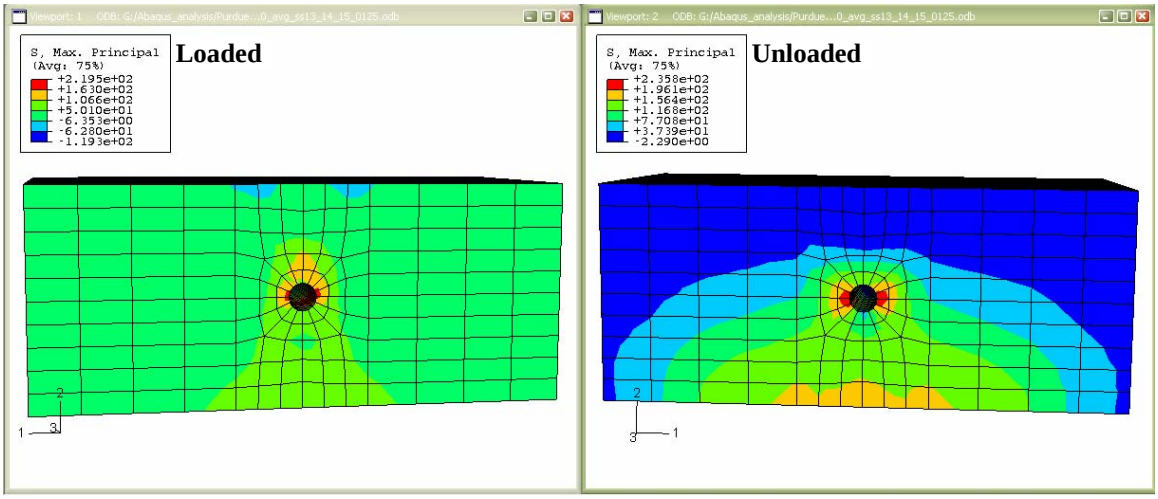

(a) Maximum Tensile Stresses at end of load application

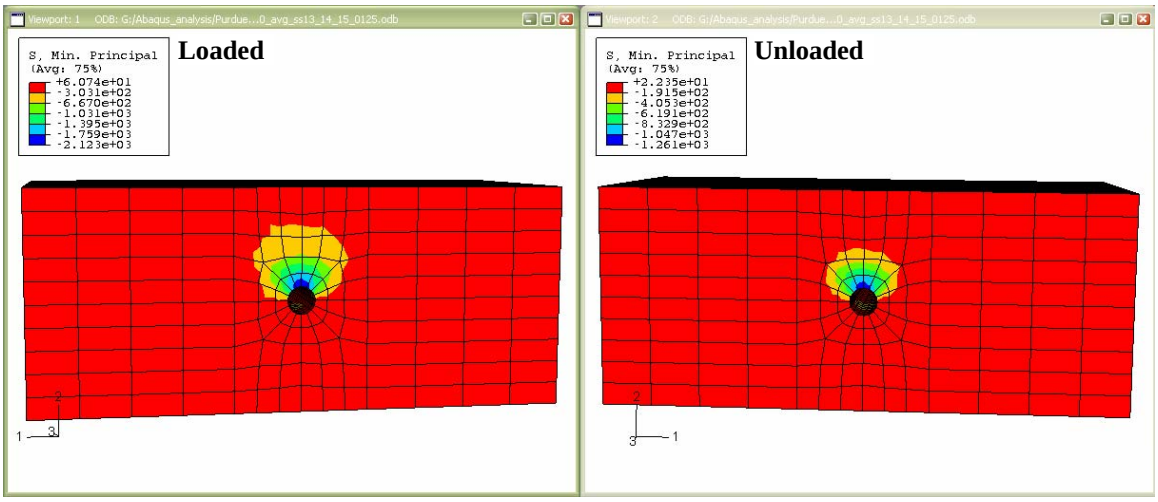

(b) Maximum Compressive Stresses at end of load application

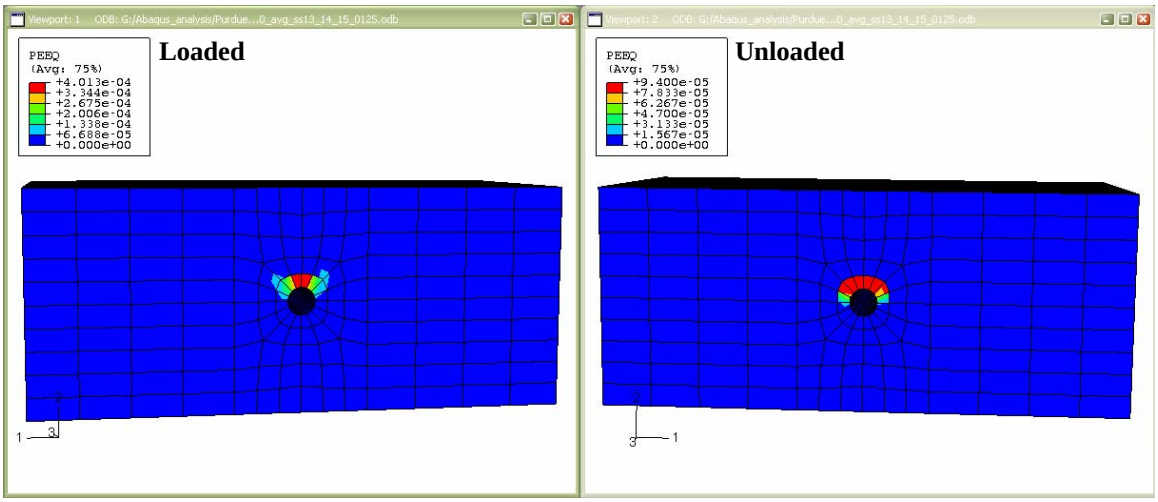

(c) Inelastic Compressive Strains at end of load application

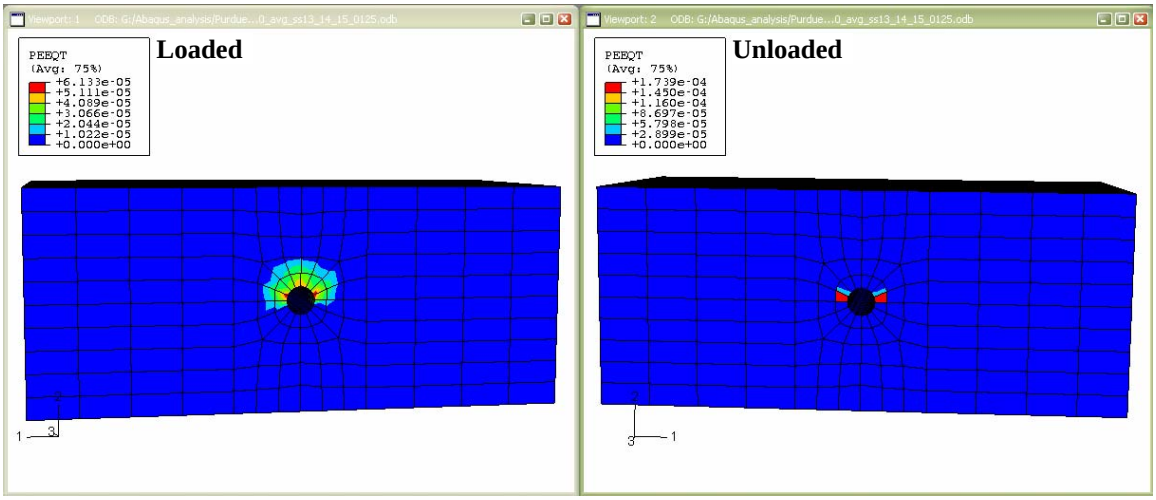

(d) Inelastic Tensile Strains at end of load application

Figure B10: Stresses and Strains for a single dowel bar calibrated using the average bond – displacement behavior of specimens 13, 14 and 15 at end of load application

Table B6: Summary of Results for three aligned dowel bar with average bond – pullout behavior of zinc clad specimens 13, 14 and 15

ss13_14_15	At Joint Opening		After Loading	
	Loaded side	Unloaded side	Loaded side	Unloaded side
Smax	195.1	191.9	176.6	140.3
Smin	242.6	242.2	883.2	274.1
PEEQ	0.00	0.00	5.23E-05	0.00E+00
PEEQT	0.00	0.00	9.65E-06	0.00E+00

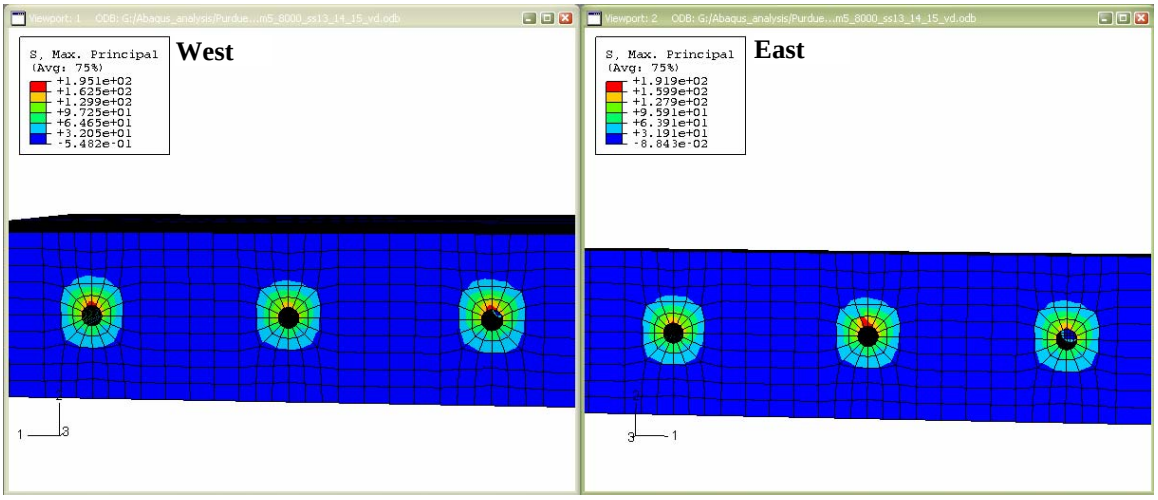

(a) Maximum Tensile Stress at Joint Opening (1/8 in.)

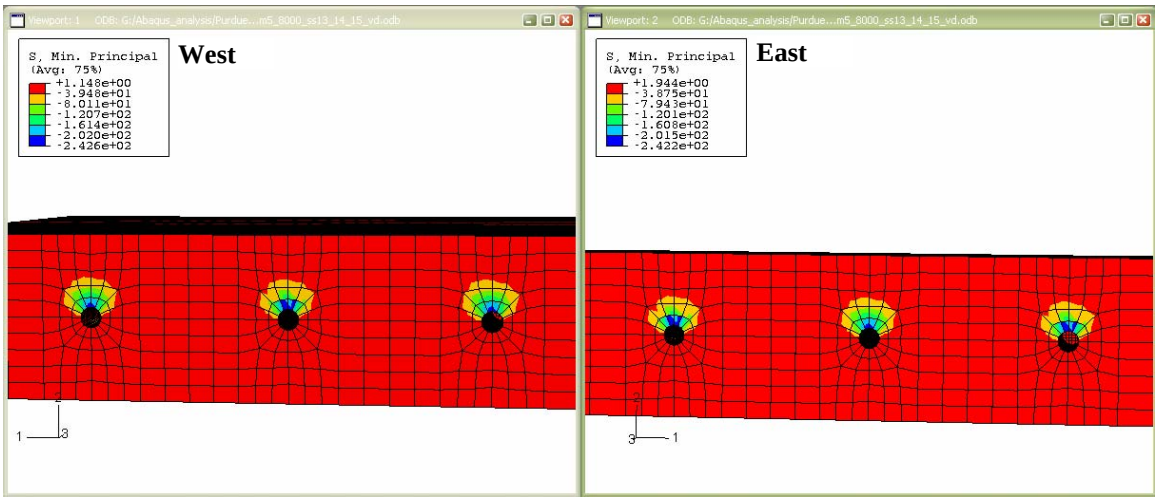

(b) Maximum Compressive Stress at Joint Opening (1/8 in.)

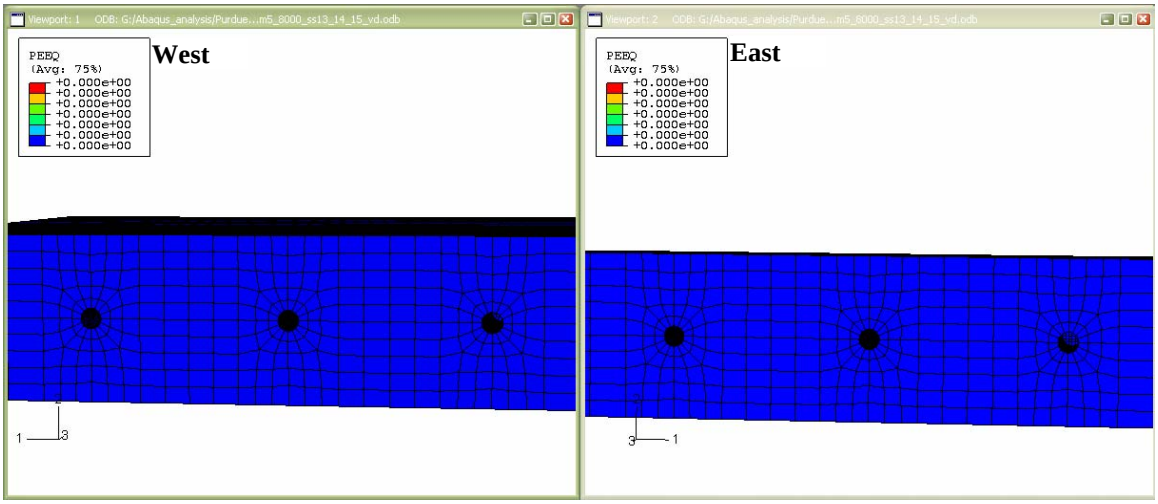

(c) Inelastic Compressive Strains at Joint Opening (1/8 in.)

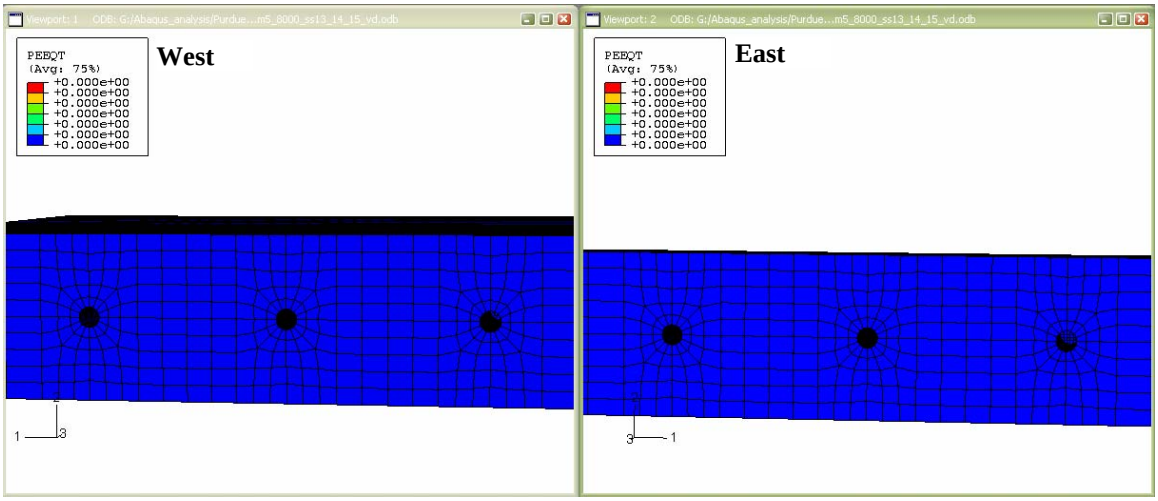

(d) Inelastic Tensile Strains at Joint Opening (1/8 in.)

Figure B11: Stresses and Strains for three aligned dowel bars calibrated using the average bond – displacement behavior of specimens 13, 14 and 15 at 1/8 in joint opening

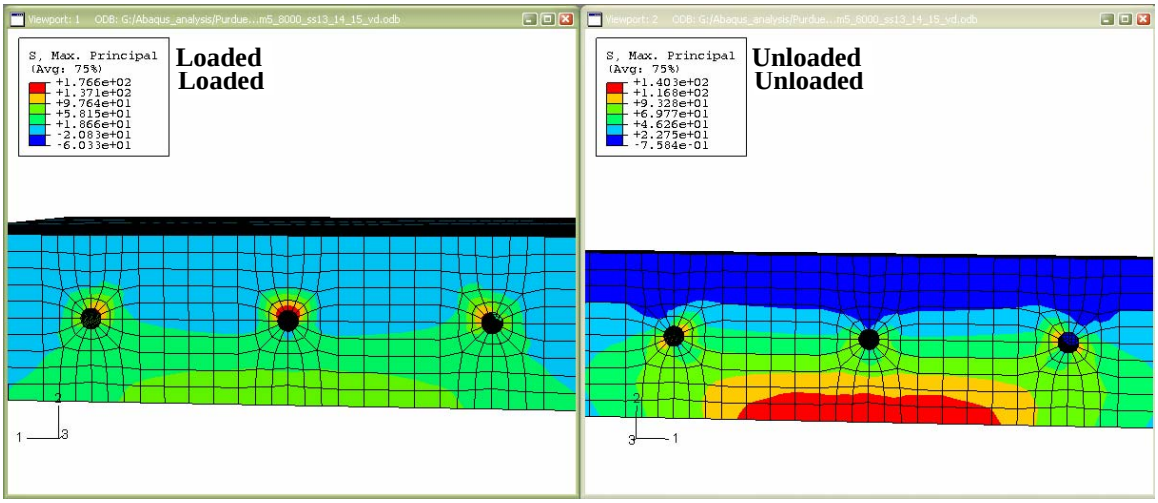

(a) Maximum Tensile Stresses at end of load application

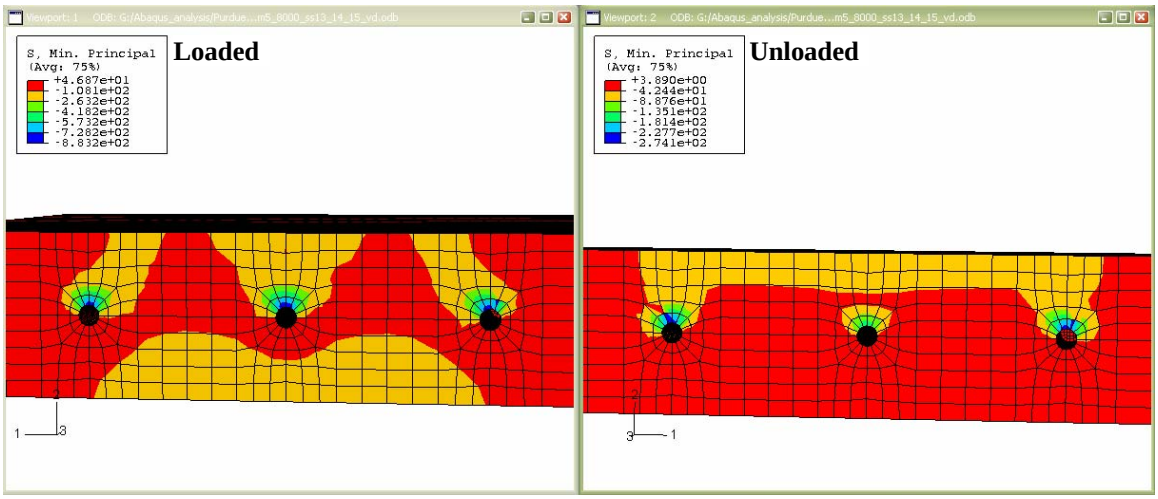

(b) Maximum Compressive Stresses at end of load application

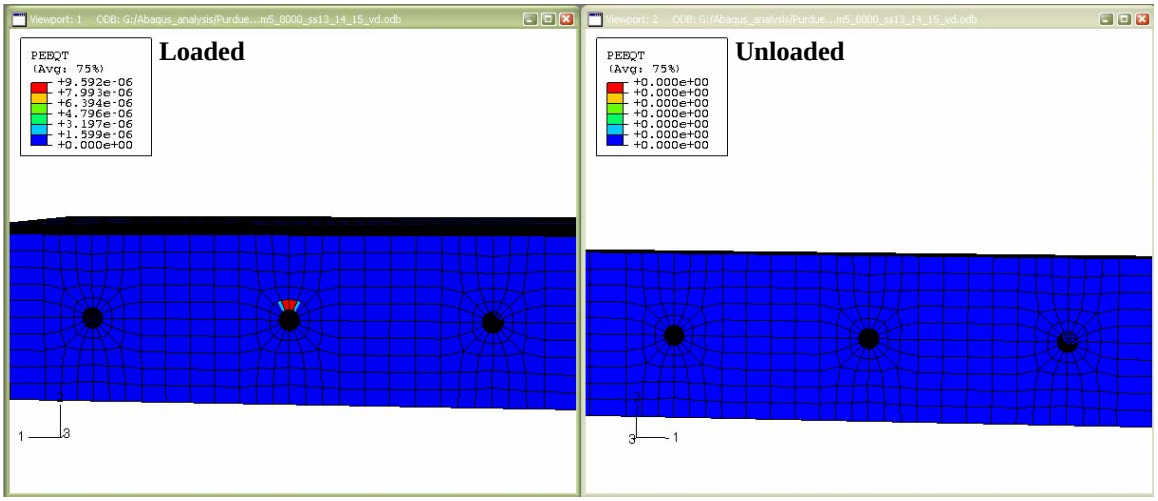

(c) Inelastic Compressive Strains at end of load application

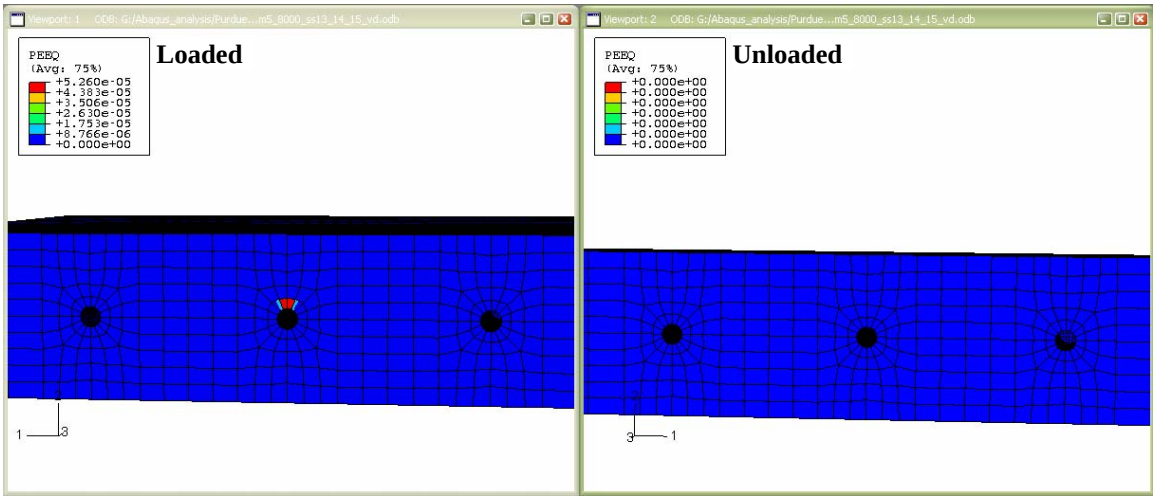

(d) Inelastic Tensile Strains at end of load application

Figure B12: Stresses and Strains for three dowel bars calibrated using the average bond – displacement behavior of specimens 13, 14 and 15 at end of load application